

UNIVERSITY OF NAPOLI FEDERICO II



Doctorate School in Biotechnology

Doctorate Program in
Insect Science and Biotechnology
Coordinator: Prof. Francesco Pennacchio
XXVII Cycle

“The role of the *mfl/Nop60b* *Drosophila* gene in tissue homeostasis and cell-proliferation”

CANDIDATE: Dr. Di Giovanni Annamaria
MENTOR: Prof. Maria Furia

Napoli 2015

CONTENTS

LIST OF PUBLICATIONS RELATED TO THE THESIS	3
ABSTRACT	4
AIMS OF THE STUDY	6
INTRODUCTION	
• The genetic and molecular organization of <i>Drosophila melanogaster</i> <i>minifly (mfl)</i> gene	9
• The H/ACA snoRNPs complexes and their functions	13
• Dyscheratosis congenita: ribosomopathy or telomere disease?	15
• <i>Drosophila</i> wing disc: a useful system to investigate growth proliferation and differentiation	18
• Determination of Anterior/Posterior and Dorsal/Ventral axis of imaginal wing disc	20
• <i>Drosophila</i> adult wing: structure and organization	23
• Induction of <i>mfl</i> gene silencing by the Gal4/UAS system	24
• The role of JNK pathway	27
• The JAK/STAT Pathway	28
MATERIALS AND METHODS	31
RESULTS	
• Effects of Mfl depletion on wing disc homeostasis	35
• Wingless ectopic secretion is essential for the occurrence of regenerative growth in <i>mfl</i> silenced discs	36
• Upon p35 expression, Mfl-depleted undead cells are formed along the A/P border	40
• <i>mfl</i> silencing causes “apoptosis induced proliferation”	43
• The “apoptosis induced proliferation” that occurs in Mfl depleted discs correlates with ectopic activation of the JAK/STAT pathway	46
• Mfl depletion promotes EMT in a cell non autonomous manner	48
• JNK activation may act to prevent overgrowth in Mfl depleted cells	51
• <i>mfl</i> acts as Tumor Suppressor Gene (TGS)	55
• <i>mfl</i> gene silencing and its interplays with the Hippo pathway	59
DISCUSSION	63
BIBLIOGRAPHY	66
ORIGINAL PAPER	73

LIST OF PUBLICATIONS RELATED TO THE THESIS

Rosario Vicidomini¹, Annamaria Di Giovanni¹, Arianna Petrizzo, Liliana Felicia Iannucci, Giovanna Benvenuto, Anja C. Nagel, Anette Preiss and Maria Furia. Loss of *Drosophila* pseudouridine synthase triggers apoptosis-induced proliferation and promotes cell-nonautonomous EMT. *Cell Death Dis.* In press

¹These authors contributed equally to this work

ABSTRACT

The *Drosophila mfl/Nop60b* gene belongs to a highly conserved family whose members encode the ubiquitous pseudouridine synthase component of H/ACA snoRNPs. These nucleolar complexes are involved in essential cellular processes, such as ribosome biogenesis and RNA pseudouridylation. Loss of function mutations of the *mfl/Nop60b* human orthologue cause X-linked Dyskeratosis Congenita, a multisystemic syndrome accompanied by telomerase defects, premature aging, stem cell dysfunction and increased cancer susceptibility. The striking conservation of snoRNP functions, coupled with a highly divergent mechanism of telomere elongation, makes *Drosophila* an ideal animal model in which to assess non-telomeric functions of eukaryotic pseudouridine synthases.

Since *Drosophila* imaginal wing discs represent an ideal system to investigate cell death, proliferation and patterning, I focused on the effects triggered by *mfl*-silencing in this tissue. Here, I show that localized depletion of Mfl protein in the *Drosophila* wing discs not only triggers apoptosis, but induces Wingless (Wg) secretion, promoting the occurrence of regenerative phenomena. I demonstrate that loss of Mfl can induce apoptosis-induced proliferation mediated by Wg and correlated with JAK/STAT pathway activation. Intriguingly, I show that Mfl depletion can also stimulate cell non- autonomous events of cell fate changes that result in Epithelial Mesenchymal Transition (EMT).

Furthermore, my experiments reveal that, upon *mfl* silencing, Caspase3-mediated cell death is induced by JNK activation, while *mfl* and *jnk* simultaneous silencing causes a dramatic overgrowth. These results suggest that *mfl* acts as a tumor suppressor and that JNK activation may represent a mechanism able to prevent the overgrowth of Mfl-depleted cells. The possibility that the interplay between pseudouridine synthase and the JNK pathway may be evolutionarily conserved could gain further insight into the so far unexplained high susceptibility to malignancy exhibited by X-DC patients.

AIMS OF THE STUDY

In eukaryotic cells, conversion of selected uridines to pseudouridines is one of the most common modifications of cellular RNAs (Kiss et al., 2006; Schwartz et al., 2014). RNA site-specific pseudouridylation is performed by box H/ACA snoRNPs, that are composed of a molecule of a box H/ACA snoRNA (small nucleolar RNA), which select by base-pairing the specific site to be modified, and a set of four highly conserved associated proteins, one of which acts as catalytic pseudouridine synthase (reviewed by Kiss et al., 2006). snoRNP pseudouridine synthases are highly conserved from Archaea to man, and include the *Drosophila* Mfl/NOP60B (Giordano et al., 1999) protein and human dyskerin, encoded by the *DKC1* gene (Heiss et al., 1998).

Reduced levels or hypomorphic mutations in the *DKC1* gene cause the X-linked Dyskeratosis (X-DC) multisystemic disorder (Heiss et al., 1998). X-DC is characterized by abnormal pigmentation of the skin, nail dystrophy and oral leukoplakia. Other symptoms include chronic bone marrow failure (which represents the main cause of death), stem cell dysfunction, testicular atrophy, premature aging, pulmonary fibrosis, increased susceptibility to cancer (which is the second leading cause of death), and a series of additional defects (reviewed by Angrisani et al., 2014). The broad spectrum of X-DC symptoms reflects the multiple roles played by dyskerin. Indeed, dyskerin is not only a H/ACA snoRNPs core

component, but participates also in the formation of active telomerase complex. This protein is thus involved in at least two essential but distinct nuclear functional complexes, one involved in ribosome biogenesis and snoRNA stability, and the other in telomere maintenance. Therefore, the distinction between the effects caused by telomere shortening and those related to impaired snoRNP functions is one of the main challenges posed by the pathogenesis of the X-DC disease.

Considering the availability of sophisticated genetic tools, *Drosophila melanogaster* can represent an advantageous model organism to dissect the multiple roles played by pseudouridine synthases. *Drosophila* dyskerin is 66% identical and 79% similar to human dyskerin, and is equally involved in rRNA processing and pseudouridylation (Giordano et al., 1999); however, it has no role in the maintenance of telomere integrity, since fly telomeres are maintained by insertion of specific retrotransposons at chromosome ends (Pardue et al., 2005). This divergent procedure of telomere maintenance makes *Drosophila* an ideal organism to delineate the range of biological effects specifically triggered by loss of H/ACA snoRNP activity. In particular, the *Drosophila* imaginal wing disc represents an ideal system to investigate growth, proliferation, patterning and cell death.

Previous studies showed that localized depletion of *Drosophila* dyskerin in the wing discs not only causes cell death, but additionally triggers a

variety of developmental defects (Tortoriello et al., 2010). More recently, these defects were studied in further detail. It was demonstrated that Mfl depletion induces simultaneous Caspase3 (Cas3) activation and Wingless (Wg) secretion in the wing disc, suggesting the occurrence of regenerative phenomena (Vicidomini et al., 2015). Loss of Mfl can in fact induce apoptosis-induced proliferation mediated by Wg and JAK/STAT pathway; moreover, it can also stimulate cell non autonomous events of cell fate changes that result in Epithelial Mesenchymal Transition (EMT). On the basis of these results (Vicidomini et al., 2015), I further investigated the effects triggered by Mfl depletion and deeply analysed the Mfl/JNK functional interplay. Interestingly, the genetic dissection of the regenerative process revealed that Caspase3 activation is mediated by JNK, and that simultaneous silencing of *mfl* and *jnk* genes causes an unexpected overgrowth of the wing disc. These results show that *mfl* acts as a tumor suppressor, and that JNK activation can prevent overproliferation of *Drosophila* Mfl-depleted cells. Worth noting, the *mfl* tumor suppressor function may be evolutionarily conserved and possibly account for the high susceptibility to malignancy showed by X-DC patients.

INTRODUCTION

The genetic and molecular organization of *Drosophila melanogaster* *minifly* (*mfl*) gene

Drosophila melanogaster minifly gene is a member of the highly conserved protein family encoding for eukaryotic pseudouridine synthases. These ubiquitous nucleolar proteins play a central role in ribosomal RNA processing and pseudouridylation (reviewed by Angrisani et al., 2014). The *Drosophila minifly* gene maps on the chromosome arm 2R, at the 60B-60C polytene subdivisions boundary, and proved to be essential for *Drosophila* viability and female fertility (Giordano et al., 1999).

The first *minifly* allele, *mfl*¹, was isolated in the course of a PZ-element mutagenesis screen on the second chromosome as a viable, recessive mutation causing a variety of phenotypic abnormalities. The *mfl*¹ pleiotropic phenotype included an extreme reduction of body size, developmental delay, defects in the abdominal cuticle, strong reduction in the length and thickness of abdominal bristles (Fig. 1) and reduced female (Giordano et al., 1999) and male fertility (Kauffman et al., 2003). Most traits of the *mfl*¹ phenotype largely overlapped those caused by the *Drosophila Minute* (Kay and Jacobs-Lorena, 1985), *mini* (Procunier and Tartof, 1975) or *bobbed* mutations (Boncinelli et al., 1972) that affect, respectively, the synthesis of ribosomal proteins, 5S, 18S and 28S

rRNAs.

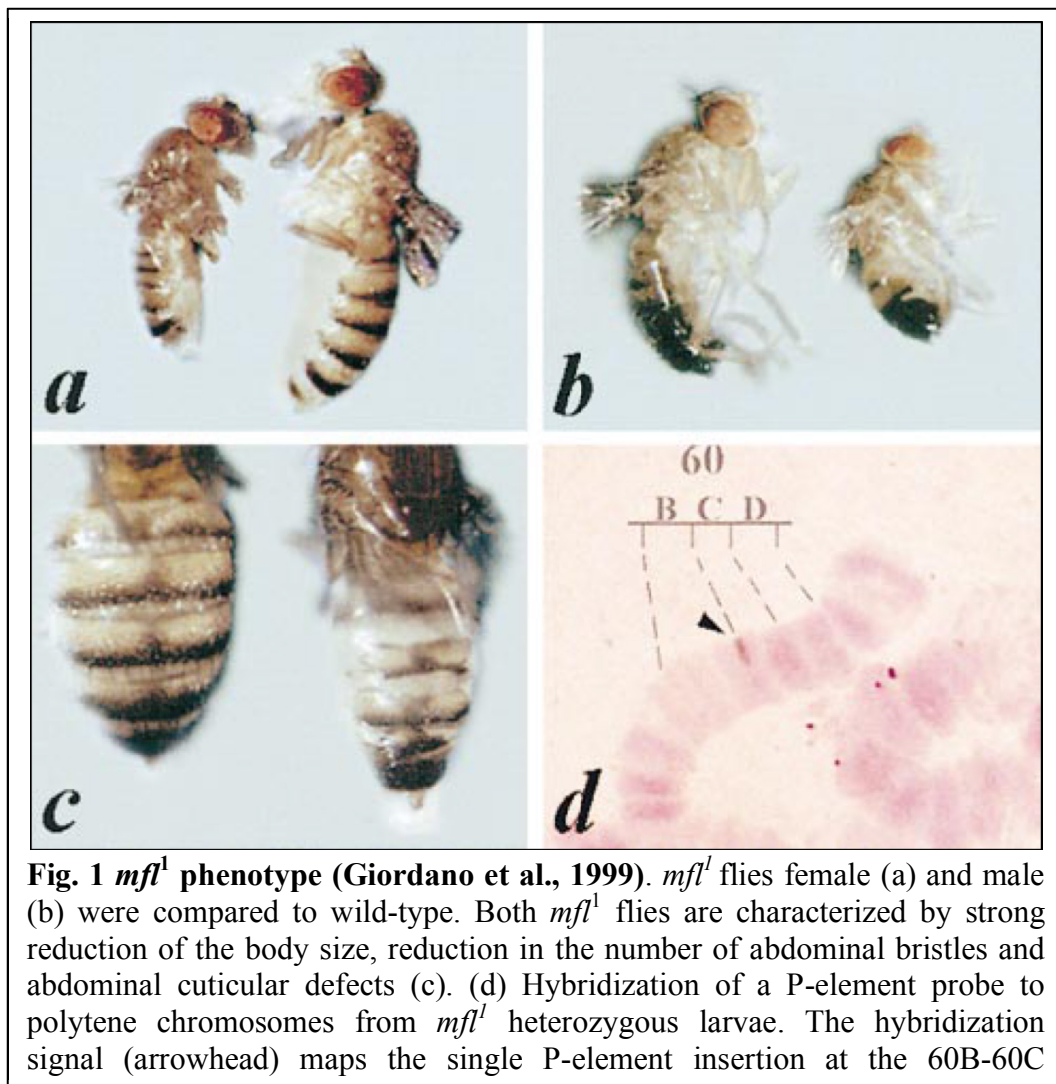


Fig. 1 *mfl*¹ phenotype (Giordano et al., 1999). *mfl*¹ flies female (a) and male (b) were compared to wild-type. Both *mfl*¹ flies are characterized by strong reduction of the body size, reduction in the number of abdominal bristles and abdominal cuticular defects (c). (d) Hybridization of a P-element probe to polytene chromosomes from *mfl*¹ heterozygous larvae. The hybridization signal (arrowhead) maps the single P-element insertion at the 60B-60C

Other two *mfl* alleles, *mfl*⁰⁵ and *mfl*⁰⁶, were obtained by P-element insertion on the coding region. These two alleles showed a strong reduction of *mfl* expression, causing larval lethality (Giordano et al., 1999). Since the viable hypomorphic *mfl*¹ allele showed only a modest reduction of *mfl* expression, these data indicated that gene expression level may be critical for *Drosophila* viability.

mfl encodes for two main transcripts, respectively of 1.8 and 2.0 kb in length (Fig. 2). These two species have different expression profiles: the

1.8 kb mRNA is constitutively expressed in both sexes throughout the life cycle, while the 2.0 kb species is mainly expressed in females and is maternally transmitted to the developing embryos (Giordano et al., 1999). The 1.8 and 2.0-kb *mfl* mRNA isoforms share a common coding region and differ from each other only at their alternatively spliced 3' untranslated region, where two additional exons (7 and 8) are specifically included in the 2.0-kb mRNA.

In addition, *mfl* produces two minor coding transcripts (Fig. 2; Riccardo et al., 2007). One of these less abundant transcript is about 2.2 kb length and is characterized by an extended 3'UTR, while a second is about 1 kb, accumulates mainly in females and is characterized by the skipping of five internal exons and by the absence of any internal stop codon, indicating that it encodes a rare variant spliced protein isoform, called Mfl α (Riccardo et al., 2007).

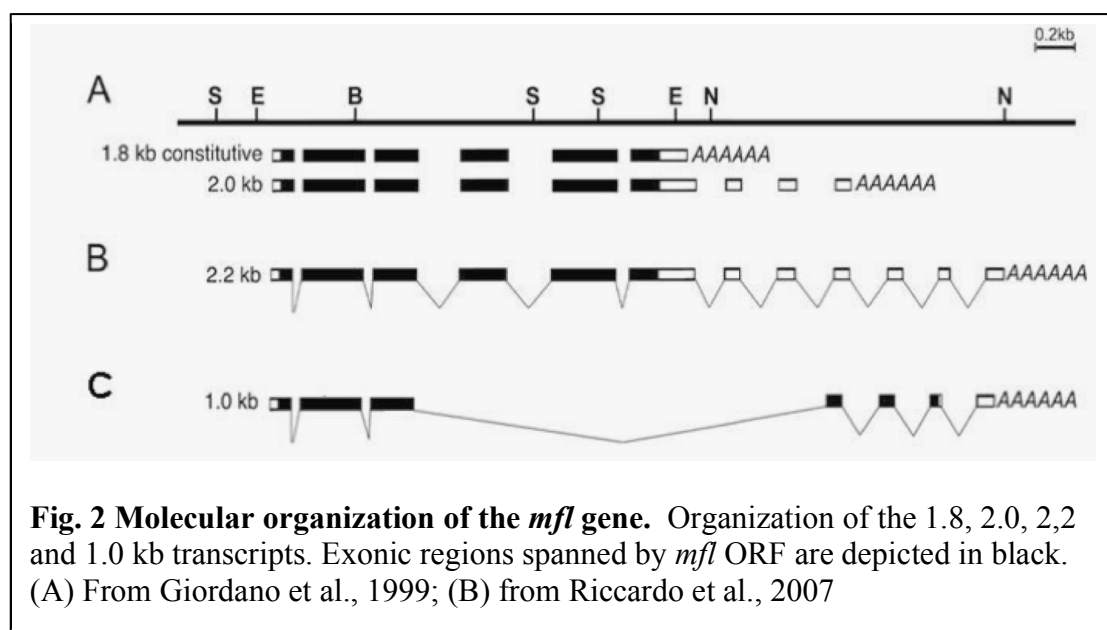


Fig. 2 Molecular organization of the *mfl* gene. Organization of the 1.8, 2.0, 2.2 and 1.0 kb transcripts. Exonic regions spanned by *mfl* ORF are depicted in black. (A) From Giordano et al., 1999; (B) from Riccardo et al., 2007

The *mfl* open reading frame (ORF), identically present in 1.8, 2.0 and 2.2-kb subforms, encodes a predicted protein of 508 amino acids (called Mfl), with a calculated molecular mass of 56 kD. This protein belongs to the Cbf5p/NAP57/dyskerin family. The *Cbf5* yeast gene was the first member of this gene family to be identified (Jiang et al., 1993). Immediately after, a mammalian orthologue, named Nap57, was recognized in rats, and postulated to be involved in nucleo-cytoplasmic shuttling of pre-ribosomal structures (Meier and Blobel 1994). Later on, yeast *Cbf5* inactivation was shown to be lethal, and the lethality was attributed to defective processing and pseudouridylation of rRNAs precursors (Cadwell et al., 1997; Zebarjadian et al., 1999). In the same period, a *Drosophila* orthologue, named *Nop60B/minifly*, was recognized (Phillips et al., 1998) and shown necessary for proper maturation and pseudouridylation of rRNAs precursors (Giordano et al., 1999). Furthermore, the human orthologue, named *DKC1* gene, was identified on 1998 (Heiss et al., 1998) and it was found to be causative of the X-linked dyskeratosis congenita disease (reviewed by Angrisani et al; 2014).

The *Drosophila* Mfl polypeptide is highly related with other members of the family, particularly with human dyskerin, sharing with it 66% identity and 79% similarity (Fig. 3). The conservation increases remarkably within functional domains, indicating that their function has been

preserved during evolution.

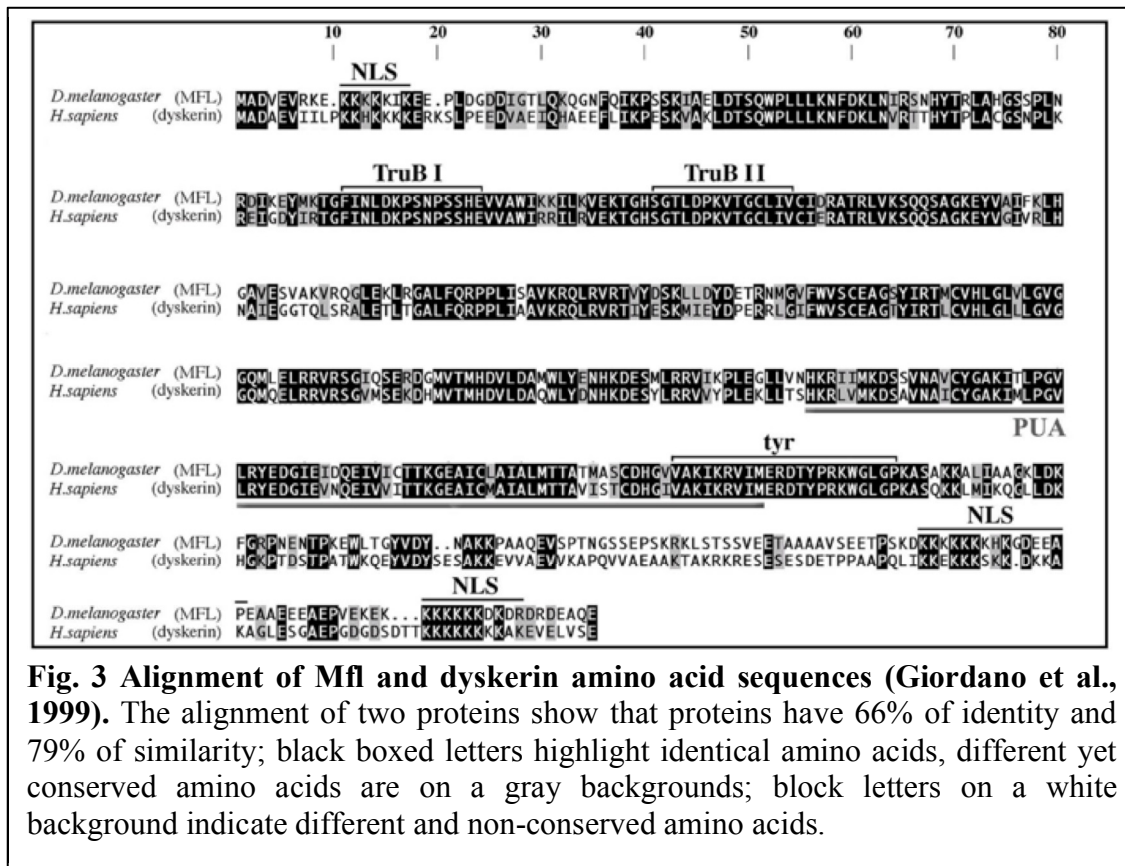


Fig. 3 Alignment of Mfl and dyskerin amino acid sequences (Giordano et al., 1999). The alignment of two proteins show that proteins have 66% of identity and 79% of similarity; black boxed letters highlight identical amino acids, different yet conserved amino acids are on a gray backgrounds; block letters on a white background indicate different and non-conserved amino acids.

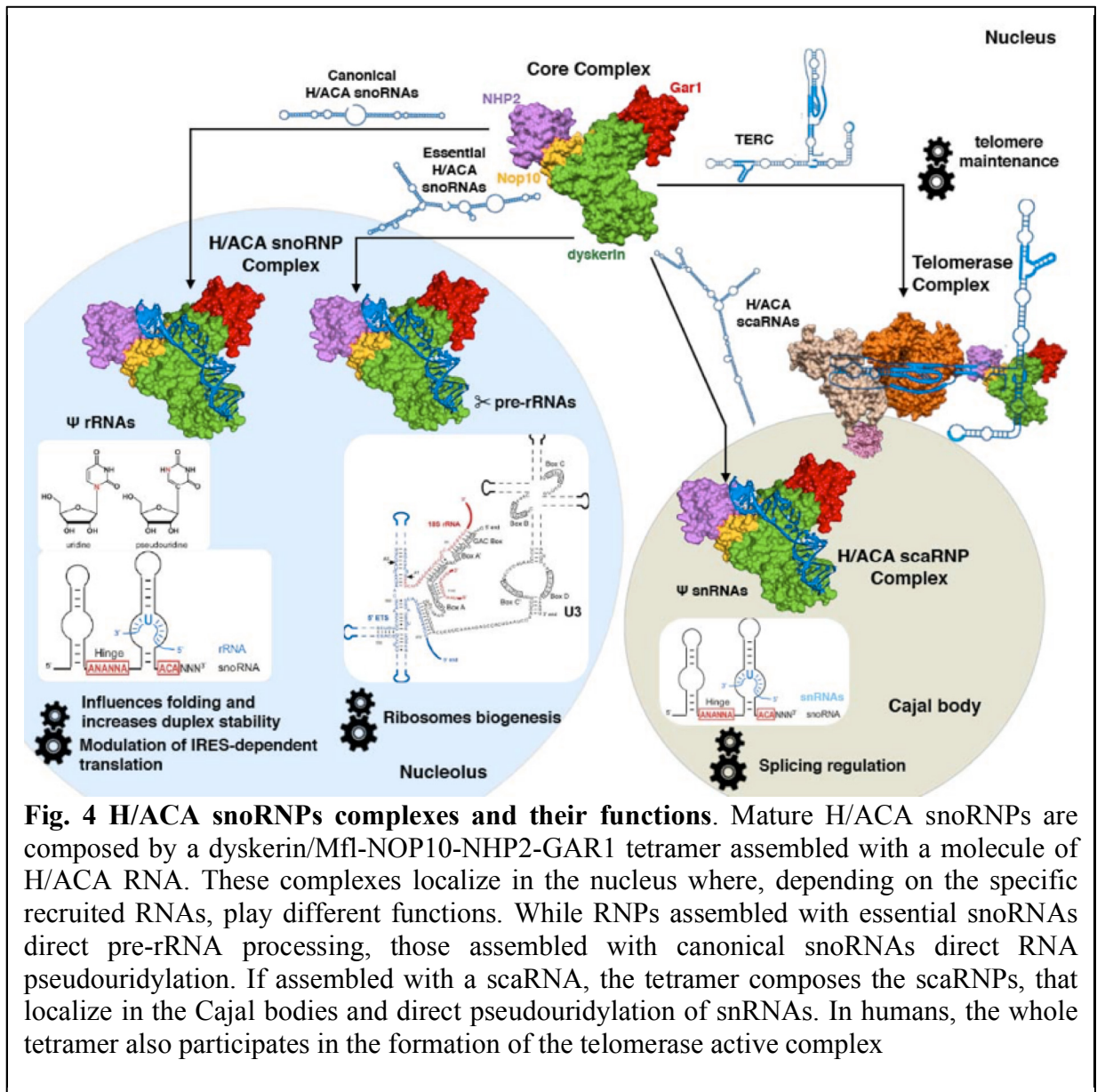
The H/ACA snoRNPs complexes and their functions

Mfl protein, as all members of Cbf5p/NAP57/dyskerin family, has a prevalent nucleolar localization. Within the nucleolus, this protein participates to the formation of the H/ACA small nucleolar ribonucleoparticles (snoRNPs) complexes (Kiss et al., 2006), whose activity is known to be involved in rRNA processing and site-specific pseudouridylation of rRNA and snRNAs (reviewed by Angrisani et al., 2014), as well as of mRNAs and of additional classes of ncRNAs (Schwartz et al., 2014).

H/ACA snoRNPs are hetero-pentameric complexes in which Mfl associates with one molecule of small nucleolar RNA (snoRNA) of the H/ACA class and three highly conserved proteins: NOP10, NHP2 and GAR1 (Kiss et al., 2006). The specific snoRNA that is recruited by the complex determines both the target recognition and the biological role of snoRNP complexes (Fig. 4; reviewed by Angrisani et al., 2014). By acting as guide, each assembled snoRNA selects by base complementarity the target RNA and the specific site to be pseudouridylated (Lafontaine and Tollervey, 1998). In the pseudouridylation process, Mfl directs the isomerisation of specific uridines to pseudouridines, acting as catalytic pseudouridine synthase. Most common targets are rRNAs and are modified in the nucleoli, while snRNAs of the U1 spliceosome are modified in the Cajal bodies, and thus have been named Cajal body-specific RNAs (scaRNAs; Richard et al., 2003).

Furthermore, H/ACA snoRNPs also direct the endonucleolytic cleavages required for rRNA processing, under the guide of U17, E2 and E3 H/ACA snoRNAs, all essential for cell growth (reviewed by Angrisani et al., 2014). Worth nothing, beside H/ACA snoRNPs, mammalian dyskerin is also a component of the active telomerase complex. The involvement of dyskerin in maintenance of the telomere ends was established by Cohen et al. (2007), that identified dyskerin as a component of the

telomerase active holoenzyme (Fig. 4).



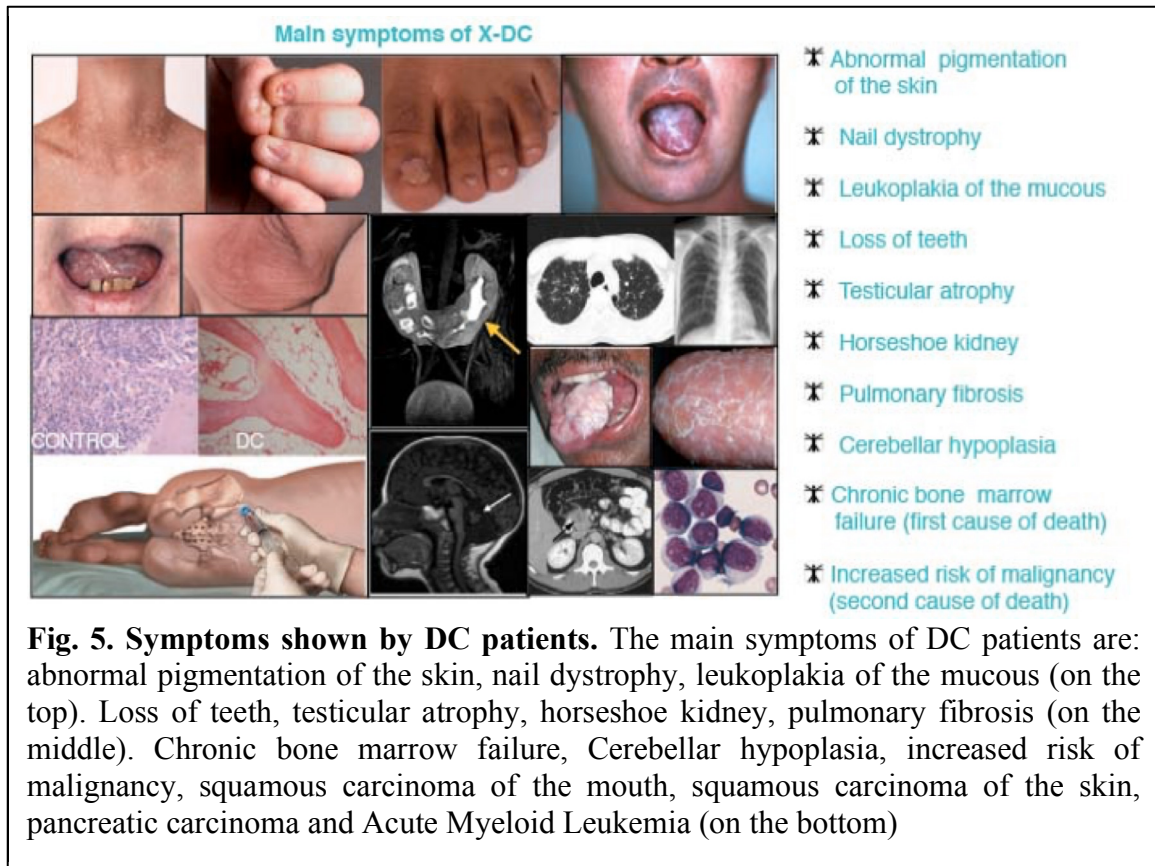
Dyscheratosis congenita: ribosomopathy or telomere disease?

Mutations in factors that allow synthesis, processing and modification of rRNA, assembly and nuclear export of pre-ribosomal particles or ribosome translational efficiency cause tissue- or cell-specific phenotypes and produce a variety of diseases, collectively known as ribosomopathies

(McCann and Baserga, 2013). Eukaryotic rRNA pseudouridine synthases are among these factors. The high biological relevance of rRNA pseudouridine synthases is testified by the fact that reduced levels or hypomorphic mutations in the human coding gene cause the human X-linked dyskeratosis (X-DC) multisystemic disorder.

Dyskeratosis Congenita (DC) is a disease characterized by a classic triad, made up of abnormal pigmentation of the skin, nail dystrophy and oral leukoplakia. Other symptoms include testicular atrophy, stem cell deficiency, chronic bone marrow failure (which represent the main cause of death), premature loss of teeth, premature graying and/or loss of hair, pulmonary fibrosis, increased susceptibility to cancer (which is the second cause of death), and a series of other defects (Fig. 5).

X-DC is caused by mutations in the dyskerin-encoding *DKC1* gene. Dyskerin contains at least three preserved functional domains: the dyskerin-like domain (DKLD; 48-106 aa) so far with unknown function, but typical of this protein family; the TruB_N pseudouridine synthase catalytic domain, that includes the active site (110-226 aa) directly involved in the pseudouridylation process, and the PUA RNA binding domain (297-370 aa), involved in recognition of snoRNAs of the H/ACA family.



As mentioned above, human dyskerin is an essential and evolutionarily conserved multifunctional protein that associates with two nuclear complexes: the H/ACA snoRNPs, that control ribosome biogenesis, RNA pseudouridylation, and stability of H/ACA snoRNAs, and the telomerase active holoenzyme, that safeguards telomere integrity. This dual role makes it difficult to distinguish between the effects related to loss of snoRNP functions and those caused by telomere attrition. As a consequence, whether X-DC must be regarded primarily as a ribosomopathy or as a telomere disease is still on debate.

Considering the availability of sophisticated genetic tools, *Drosophila melanogaster* can represent an advantageous model organism to dissect

the multiple roles played by pseudouridine synthases. Indeed, *Drosophila* pseudouridine synthase is 66% identical and 79% similar to human dyskerin (see Fig. 3), and is equally involved in rRNA processing and pseudouridylation (Giordano et al., 1999); however, it has no role in the maintenance of telomere integrity, since fly telomeres are maintained by insertion of specific retrotransposons at chromosome ends (Pardue et al., 2005). This divergent procedure of telomere maintenance makes *Drosophila* an ideal organism to delineate the range of biological effects specifically triggered by loss of H/ACA snoRNP activity. In particular one anatomical structure of the *Drosophila* can furnish an excellent and well studied model to investigate developmental events: the imaginal disc/adult wing system. This system will be described in next sections.

***Drosophila* wing disc: a useful system to investigate growth proliferation and differentiation**

Drosophila imaginal wing disc represents an ideal system to investigate cell growth, proliferation and patterning. *Drosophila* imaginal discs are larval epithelial organs from which, following metamorphosis, the adult body structures and appendages originate. The imaginal wing disc, precursor of the adult wing, appears formed by two cell types: the upper squamous peripodial cells and the pseudostratified columnar epithelium made of undifferentiated, proliferating cells that represent the actual

imaginal disc (Fig. 6). The first will originate the epithelial veil that welds the structures, the second will originate the integument and the wing (Bate and Martinez-Arias, 1993).

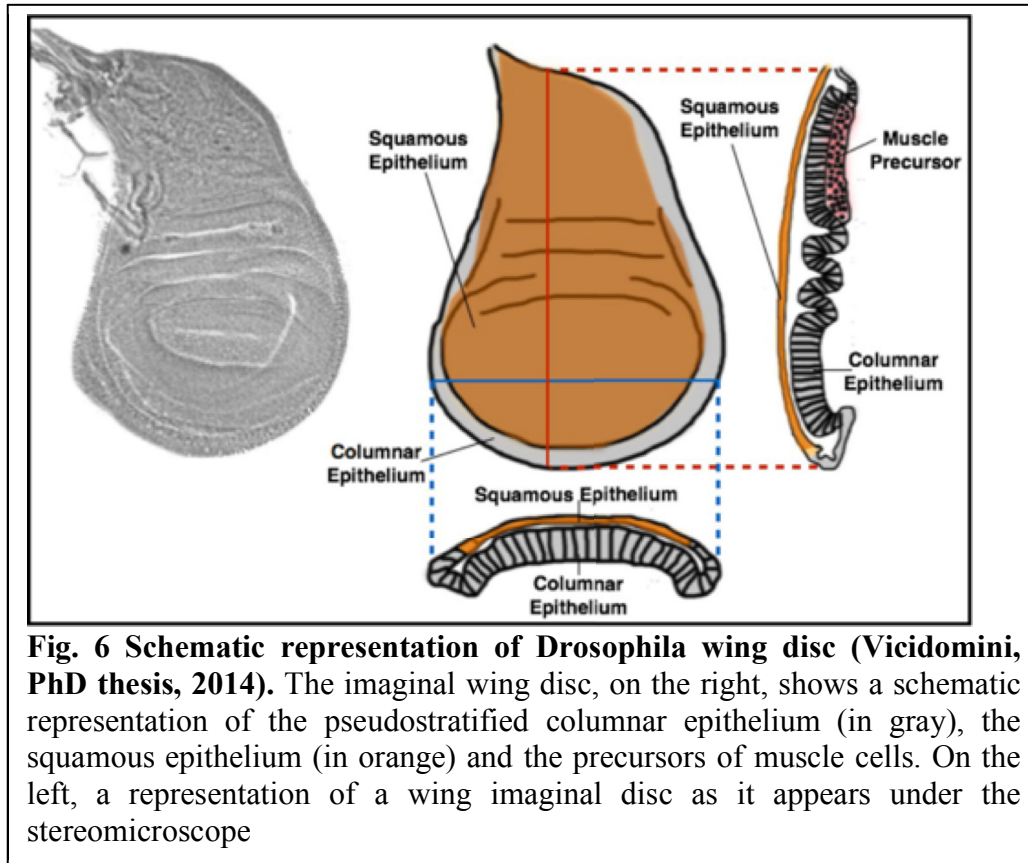
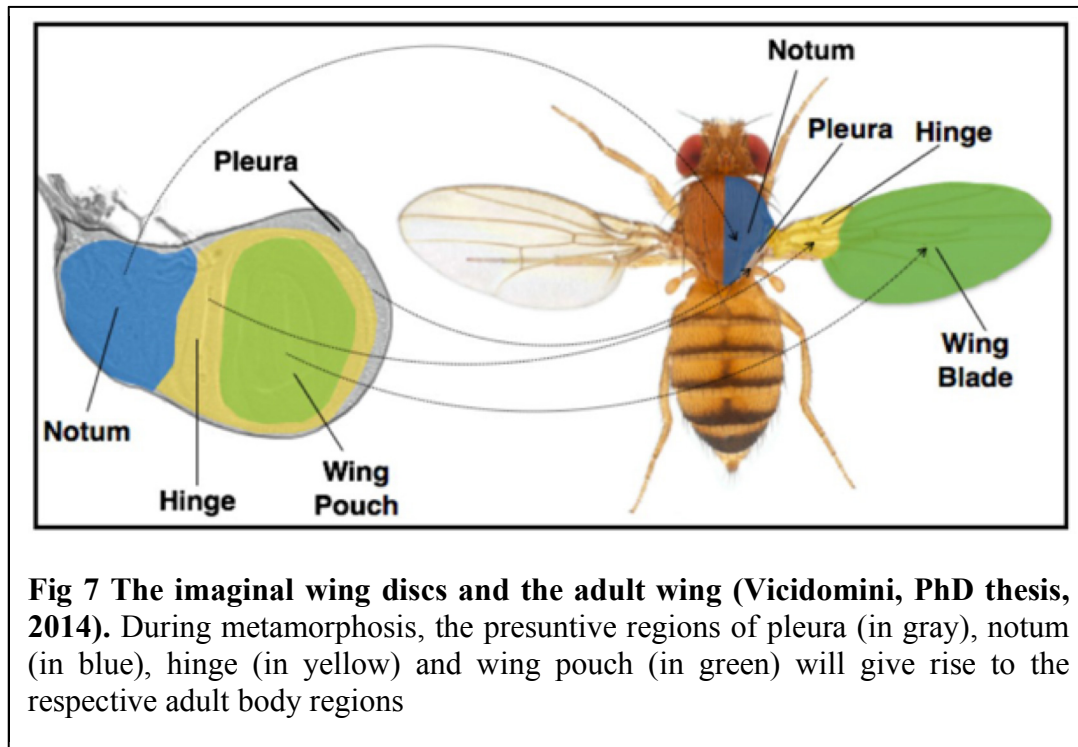


Fig. 6 Schematic representation of *Drosophila* wing disc (Vidomini, PhD thesis, 2014). The imaginal wing disc, on the right, shows a schematic representation of the pseudostratified columnar epithelium (in gray), the squamous epithelium (in orange) and the precursors of muscle cells. On the left, a representation of a wing imaginal disc as it appears under the stereomicroscope

When it is formed during embryonic development, the wing imaginal disc comprises around 20 cells (Bate and Martinez-Arias, 1993). These cells intensely proliferate during second and third larval instars to generate a disc of around 50,000 cells in the late third instar. By this stage, the wing primordium is established and its major elements can be identified. The centrifugal regions of the imaginal disc will give rise to the thorax structures, the notum and the pleura. The middle region will give rise to the hinge region, while the central region, the wing pouch, is the

presumptive territory that will form the wing lamina (Fig. 7).



Since the imaginal wing disc is morphologically and biochemically very similar to mammalian epithelia and encounters a dramatic increase in cell number in a relatively short length of time (Garcia-Bellido and Merriam, 1971), it represents a useful model for studying how growth and proliferation are regulated in epithelial tissues.

Determination of Anterior/Posterior and Dorsal/Ventral axis of imaginal wing disc

As mentioned above, the imaginal wing disc provides an ideal system in which to investigate how growth, proliferation and differentiation are coordinated in the context of a developing organ. Indeed, cell

proliferation is essentially uniform across the whole disc (Potter and Xu, 2001) and is controlled by the same morphogens that govern wing patterning. Gradients of two morphogens, Decapentaplegic (Dpp), a member of the TGF- β family, and Wingless (Wg), a member of the Wnt family, establish a link between cell proliferation and developmental programs. During disc development, a gradient of Dpp determines the Anterior/Posterior (A/P) axis, while a gradient of Wg subsequently defines the Dorsal/Ventral (D/V) axis, giving rise to the A/P and D/V compartments (Dahmann et al., 2011).

More in detail, in the developing imaginal discs of *Drosophila*, a small number of lineage restrictions prevent the mixing of cells in adjacent compartments. The A/P boundary is established during early embryogenesis. In fact early evidence from García-Bellido et al. showed that this restriction occurs no later than the first blastoderm division (García-Bellido et al., 1973). Anterior/Posterior axis is triggered by the activation of the *engrailed* (*en*) gene (Fig. 8). *en* is specifically expressed within the Posterior compartment and induces the expression of *hedgehog* (*hh*) in this compartment (Tabata and Kornberg 1994; Zecca et al. 1995). Hh protein is a morphogen that spreads in a line of cells along the Anterior/Posterior border, where it induces the expression of another morphogen, Decapentaplegic (Dpp) (Tabata and Kornberg 1994; Zecca et al. 1995). This process leads to the activation and the repression of a large

number of regulatory genes that finally will result in the definition of the Anterior/Posterior axis.

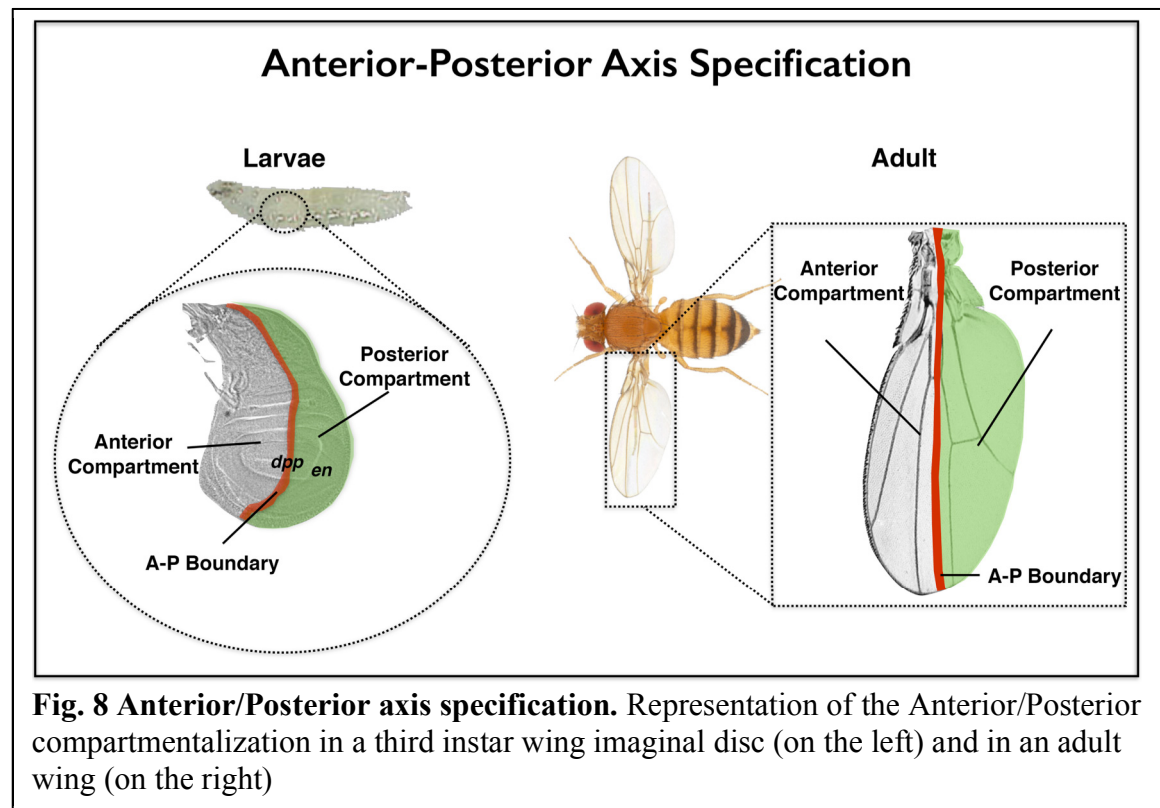
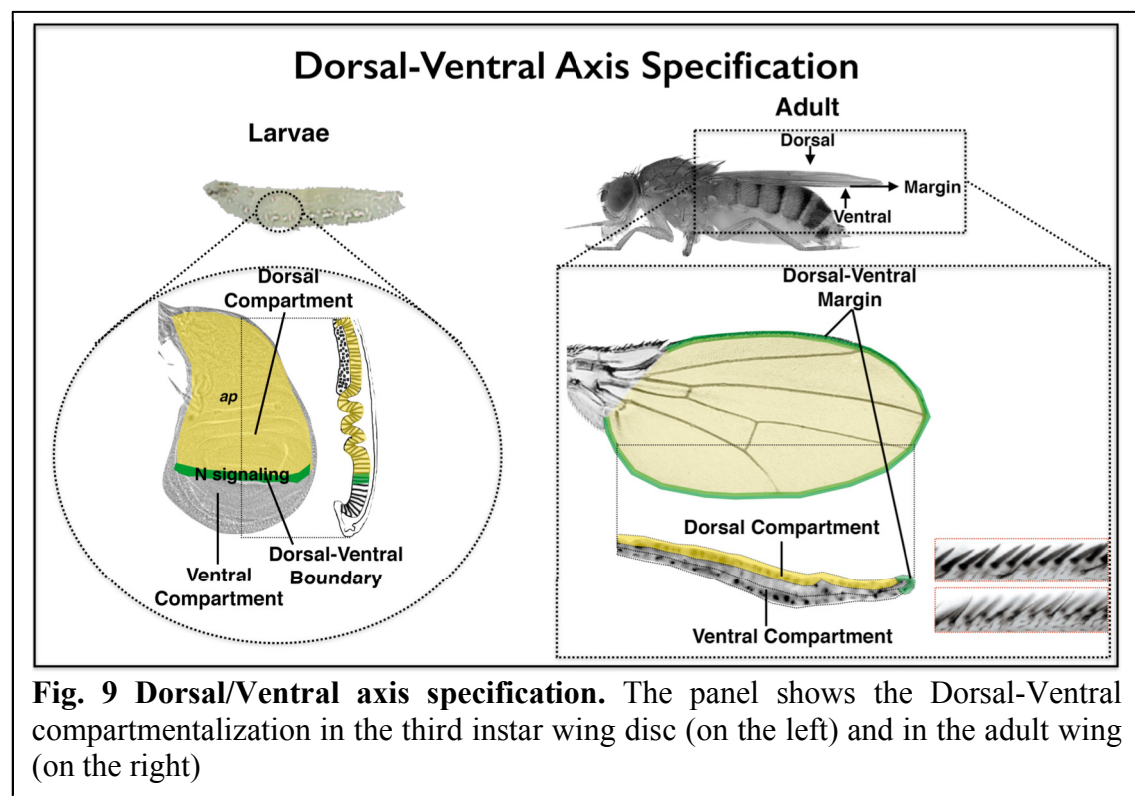


Fig. 8 Anterior/Posterior axis specification. Representation of the Anterior/Posterior compartmentalization in a third instar wing imaginal disc (on the left) and in an adult wing (on the right)

Unlike the A/P boundary, the D/V boundary is established only in the middle stages of larval development. The Dorsal/Ventral restriction border is triggered by the transcription factor encoded by *apterous* (*ap*) gene (Fig. 9). *ap* is expressed in what appears to be the Dorsal region of the wing disc beginning in the middle of the second instar (Williams et al., 1993). The Ap protein induces Fringe (Fng; Irvine and Wieschaus 1994) and Serrate (Ser; Kim et al., 1995) expression in the Dorsal cells, while restricts Delta (Dl) expression to Ventral cells. Delta and Serrate are two Notch (N) ligands (Milán and Cohen 2000), while Fringe is a

secreted glycosyl transferase that modifies Notch receptor affinity for ligands. Delta and Serrate are able to activate Notch only in two cell stripes at the Dorsal/Ventral boundary (de Celis et al. 1996). At this region, Notch activates the expression of *wingless* (*wg*), *cut* (*ct*) and *vestigial* (*vg*) and, as a consequence, the D/V restriction boundary is formed and the wing blade presumptive territory begins to be defined.



Drosophila adult wing: structure and organization

The imaginal wing disc is the precursor of the adult wing. During prepupal and initial pupal stages, the wing disc everts and the centrifugal regions of wing disc originate the Dorsal and Ventral body wall thorax structures: notum and pleura. The middle region of wing disc gives rise to

the hinge, while from the central region, called wing pouch, the wing lamina differentiates (see Fig. 7).

For this reason, the wing pouch is defined as the distal region of the wing disc, while hinge and pleura are considered proximal. The hinge connects the wing to the Dorsal (notum) and Ventral (pleura) thorax. The wing lamina, called wing blade, in the Anterior border presents three series of sensorial bristles and two types of cells that form vein and intervein territories. In each wing blade are present five veins (Fig. 10) formed by live epithelial cells composing tubular structures. These structures give

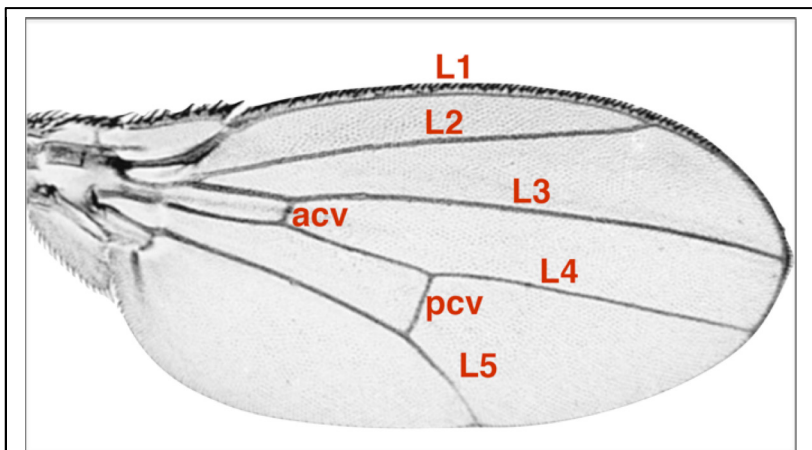


Fig. 10 Organization of Drosophila adult wing. Drosophila adult wing is composed by five longitudinal veins (L1, L2, L3, L4, L5 in the figure) and by anterior cross vein and posterior cross vein (acv and pcv respectively in the figure)

stiffness to the wing and accommodate the tracheas and the neuronal sheafs. Intervein cells are instead dead and chitinized, and are

characterized by the differentiation of a single trichome per cell.

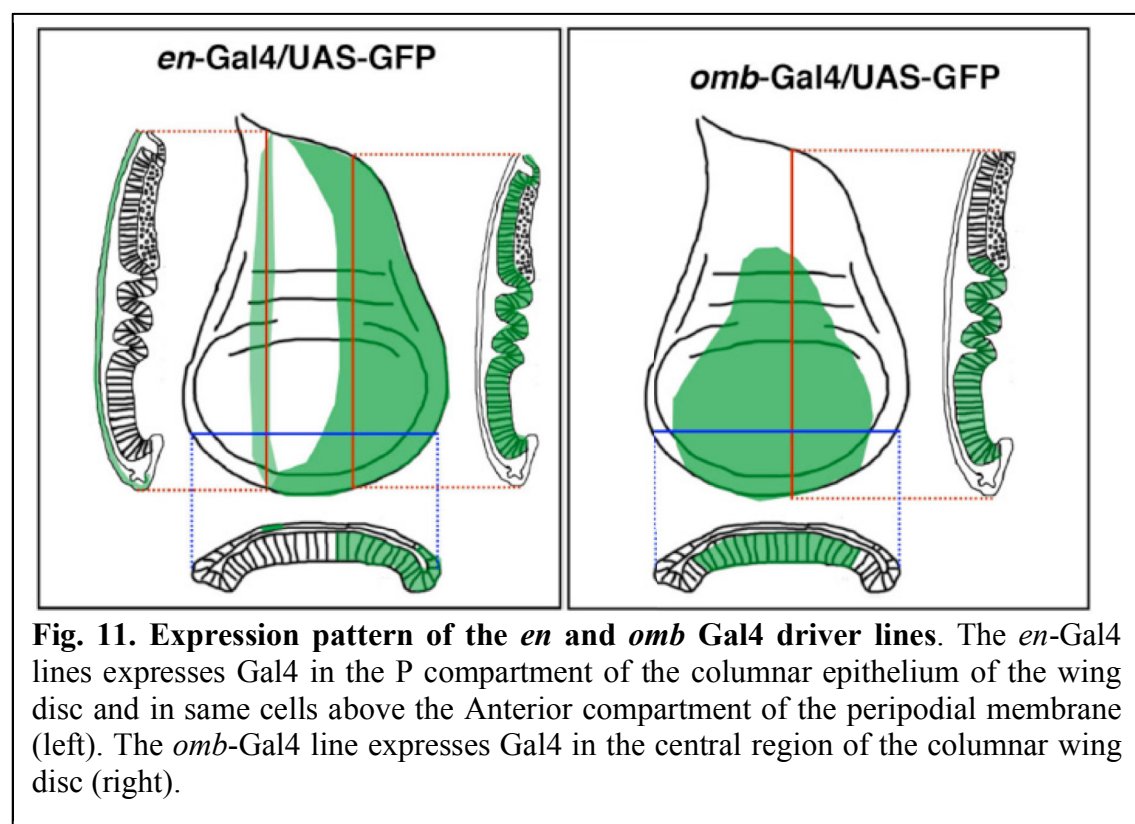
Induction of *mfl* gene silencing by the Gal4/UAS system

As mentioned above, Drosophila is a useful model system to evaluate the

telomerase-independent roles played by pseudouridine synthases. Hypomorphic mutations in *mfl* gene causes developmental delay, defective maturation of rRNA, small body size, alterations of the abdominal cuticle and reduced fertility, while null mutations causes larval lethality. All these phenotypes make difficult to use the mutants to perform a detailed analysis of the molecular mechanisms that underlie X-DC. This problem could be overcome by triggering gene silencing by using the Gal4/UAS system to trigger the RNA interference (RNAi) process *in vivo*. In *Drosophila*, the Gal4-UAS system (Fischer et al., 1988; Brand and Perrimon, 1993) is routinely used to analyze the function of developmental genes. This technique is based on two different kinds of transgenic strains, called “driver” and “responder” lines. In a driver line the gene for the yeast transcriptional activator Gal4 is placed under the control of a specific promoter, while in the responder line the gene of interest is fused to the UAS (Upstream Activating Sequence) DNA-binding motif of Gal4. The effector gene will be transcriptionally silent unless animals carrying it are crossed to those of a driver line. In the progeny of this cross, expression of the effector gene will reflect the pattern of expression of Gal4 in the driver, which is ultimately dependent on the promoter that has been used to control it. Thus system allows to target gene expression in a temporal and spatial fashion. In our experiments, we silenced *mfl* gene by using the Gal4–UAS system to

trigger the UAS-dependent expression of a *mfl*-RNAi effector line. In particular, in my experiments I used the *en*-Gal4 and the *omb*-Gal4 driver lines that will be active only within specific anatomical regions (Fig. 11) and at specific developmental times.

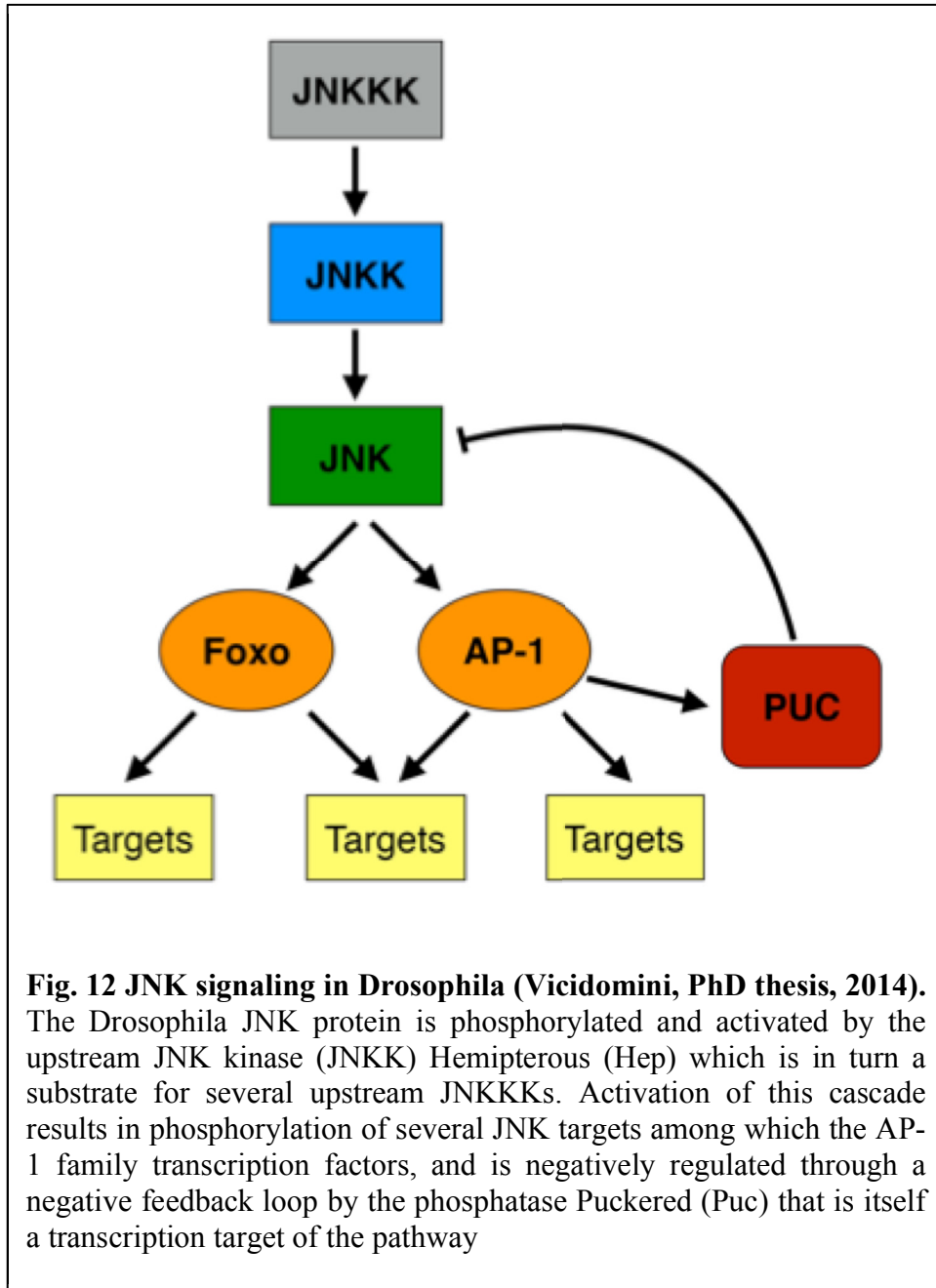
In previous experiments, it was demonstrated that localized depletion of *Drosophila* Mfl causes apoptosis and triggers a variety of developmental



defects in the wing discs (Tortoriello et al., 2010). In my work, using the *en*-Gal4 and *omb*-Gal4 driver lines, these defects were studied in more detail. In particular, I analysed the Mfl/JNK functional interplay and I demonstrated that loss of Mfl can induce apoptosis-induced proliferation mediated by Wg and JAK/STAT pathway. A brief summary of these pathways is shown in the next two sections.

The role of JNK pathway

The JNK signal transduction pathway has been implicated in several aspects of tumour development and is an evolutionarily conserved stress-induced MAPK cascade involved in multiple cellular processes, including proliferation, differentiation, morphogenesis and apoptosis. The mitogen-activated protein kinase (MAPK) pathway is one of the major systems that transduces extracellular signals into cells. MAPK cascades includes at least 3 protein kinases in series: MAPK kinase kinases (also known as MEKK) and MAPK kinases (also known as MEK and MAPK). MAPK kinase kinases phosphorylate and activate the downstream MAPK kinases, which in turn phosphorylate and activate MAPK. These kinases are activated by dual phosphorylation. In *Drosophila*, only the JNK protein Basket (Bsk) is phosphorylated and activated by the upstream JNK kinase (JNKK) Hemipterous (Hep), which is in turn a substrate for several upstream JNKKs that respond to a variety of internal and environmental stimuli. Activation of this cascade results in phosphorylation of several JNK targets, among which the AP-1 family transcription factors Jun and Fos. The cascade is negatively regulated through a negative feedback loop by the phosphatase Puckered, that is itself a Jun/Fos transcription target (Fig. 12).

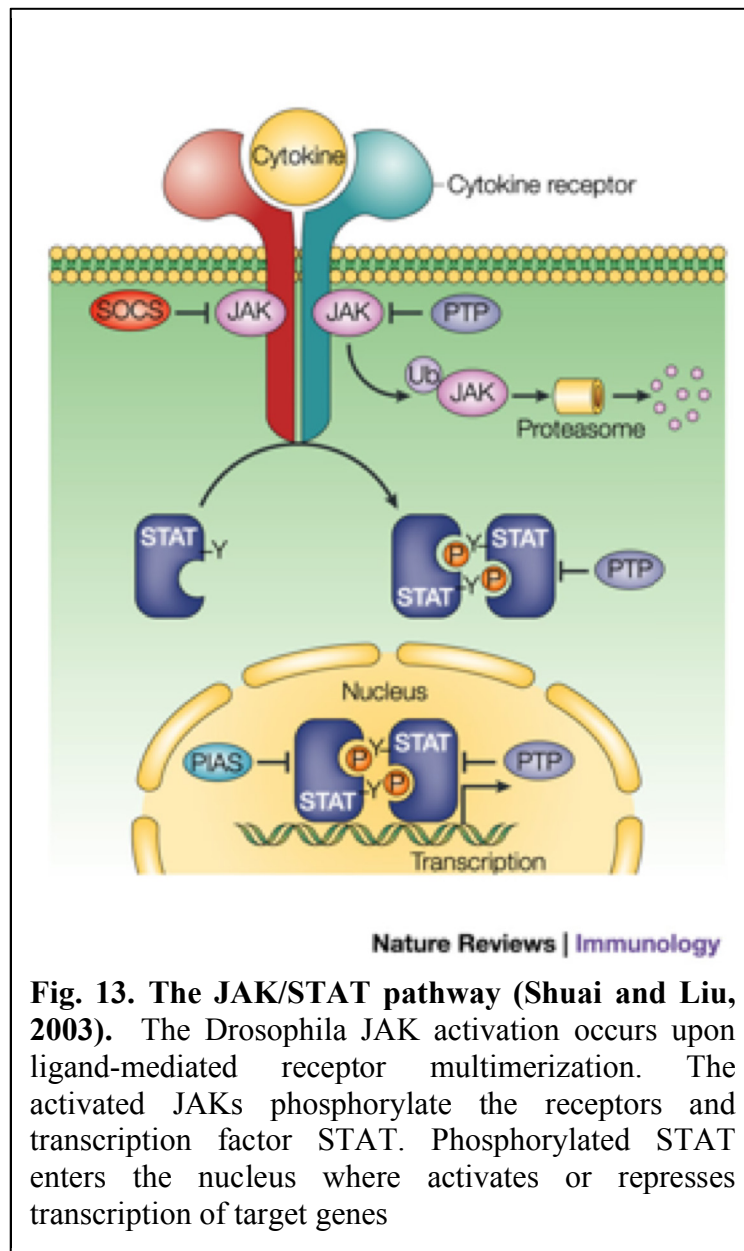


The JAK/STAT Pathway

Janus kinase/signal transducers and activators of transcription (JAK/STAT) pathway is a pleiotropic cascade used to transduce a multitude of signals regulating development and homeostasis from humans to flies. In mammals, the JAK/STAT pathway is the principal

signaling mechanism for a wide array of cytokines and growth factors. JAK activation stimulates cell proliferation, differentiation, cell migration and apoptosis. These cellular events are critical to hematopoiesis, immune development and other processes (reviewed by Rawlings et al., 2004). JAK/STAT signaling is relatively simple, with only a few principal components (Heinrich et al., 2003), and its intracellular activation occurs when ligand binding induces the multimerization of receptor subunits. The cytoplasmic domains of two receptor subunits must be associated with JAK tyrosine kinases. In mammals, the JAK family comprises four members: JAK1, JAK2, JAK 3 and Tyk2. JAKs activation occurs upon ligand-mediated receptor multimerization. The activated JAKs subsequently phosphorylate additional targets, including both the receptors and the major substrates, STATs. STATs are latent transcription factors that reside in the cytoplasm until activated. The seven mammalian STATs bear a conserved tyrosine residue near the C-terminus that is phosphorylated by JAKs. Phosphorylated STATs enter the nucleus where bind specific regulatory sequences to activate or repress transcription of target genes. JAK/STAT pathway has three major classes of negative regulator: SOCS (suppressors of cytokine signaling), PIAS (protein inhibitors of activated stats) and PTPs (protein tyrosine phosphatases; see Fig. 13). SOCS proteins are a family of at least eight members containing an SH2 domain and a SOCS box at the C-terminus

(Alexander, 2002). The SOCS complete a simple negative feedback loop in the JAK/STAT circuitry: activated STATs stimulate transcription of



the SOCS genes and the resulting SOCS proteins bind phosphorylated JAKs and their receptors to turn off the pathway. The JAK/STAT pathway is ubiquitous from humans to flies (reviewed by Rawlings et al., 2004), and a complete but simplified JAK/STAT signaling pathway is found in

Drosophila (Hombria and Brown, 2002). There are single homologues for JAK and STAT, as well as three SOCS homologues. Furthermore, there is a single JAK/STAT pathway receptor, Domeless. Each of these components acts in the same fashion as its mammalian counterpart.

MATERIALS AND METHODS

Drosophila strains

Flies were raised on standard *Drosophila* medium at 25°C. The *en-Gal4*, *omb-Gal4/FM7*, UAS-GFP/CyO, 10XSTAT92E-dGFP/TM6C, UAS-RedStinger, UAS-FLP, Ubi-p63E(FRT.STOP)Stinger, UAS-IR*mfl* (#36595), strains were obtained from the Bloomington *Drosophila* Stock Center at Indiana University (BDSC, USA); UAS-IR*mfl* (v46282) and UAS-IR*bsk* (#104569) strains were obtained from the Vienna *Drosophila* RNAi Center (VDRC, Austria). *wg-lacZ/CyO* and UAS-p35/TM3Sb stocks were kindly provided by L. Johnston (Columbia University, USA). M-,*en-Gal4*,UAS-GFP/In(2LR)Gla,Bc strain was kindly provided by D. Grifoni (Bologna University, IT).

Mounting adult wings

Wings were removed from adult flies and dehydrated in 100% ethanol for 5 min. The wings were placed on a microscope slide, and ethanol allowed to evaporate. A small drop of Euparal Mounting Medium (Roth, Karlsruhe, Germany) was dropped onto the wing and a glass coverslip placed on top. Images were captured with a Spot digital camera and a Nikon E1000 microscope.

Immunofluorescence stainings

Drosophila Larvae were dissected in PBS (Phosphate Buffer Saline, pH 7.5) and fixed in 3,7% formaldehyde (Sigma) in PBS. Tissues were permeabilised in PBS-Triton 0,3% for 45' at room temperature, blocked for 1 hour in PBS-Triton 0,3%, 2% BSA (Bovine Serum Albumine, Sigma) and incubated overnight at 4°C in PBS-Triton 0,3%, 2% BSA with primary antibody. Tissues were then incubated with secondary antibody for 1 hour at room temperature. Accurate washes in PBS- Triton 0,3% were performed following each step. Wing discs were then mounted on microscopy slides using anti-bleaching slide mounting medium Fluoromount (Beck- man Coulter). The following antibodies and dilutions were used: customer rabbit polyclonal antibody against Mfl (Sigma-Aldrich Inc., St. Louis, MO, USA; dilution 1: 100); mouse monoclonal antibodies against Wingless, Cut, β -Galactosidase, Ultrabithorax (Hybridoma Bank, University of Iowa, Iowa City, IA, USA; dilution 1:50 anti-Wg, 1:100 anti-Cut; 1:250 anti- β -Gal and 1:50 anti-Ubx); rabbit polyclonal antibody against Twist (dilution 1:50; gift from M. Frasch); rabbit polyclonal antibody against cleaved Caspase-3 (Cas3) (Cell Signaling Tech., Danvers, MA, USA; dilutions 1:500 anti-Cas3); rabbit polyclonal antibody against aPKC (Santa Cruz Biotechnology, dilution 1:200); Rabbit polyclonal antibody against d-Myc (dilution 1:5; gift from D. Grifoni). Rabbit polyclonal antibody

against Yorkie (dilution 1:400; gift from K. Irvine). Fluorescent secondary antibodies were from Jackson ImmunoResearch (Dianova, Hamburg, Germany) and used at a final dilution of 1:200. Rhodamine Phalloidin Conjugate for actin cytoskeleton staining was obtained from Molecular Probes (Eugene, OR, USA; dilution 1:250). Confocal images were obtained with a Zeiss LSM510 confocal microscope.

S-Phase Marker

For EdU immunohistochemistry, we used the Click-iT EdU imaging kit (Invitrogen, Carlsbad, CA, USA). Discs were dissected and incubated in 10 μ M EdU in Ringer's for 20 min or 2h. Following EdU labeling, discs were fixed in 3,7% formaldehyde (Sigma) in PBS. Tissues were permeabilised in PBS-Triton 0,3% for 45' at room temperature, blocked for 1 hour in PBS-Triton 0,3%, 2% BSA (Bovine Serum Albumine, Sigma) and incubated overnight at 4°C in PBS-Triton 0,3%, 2% BSA with primary antibody. Tissues were then incubated with secondary antibody for 1 hour at room temperature. Accurate washes in PBS were performed following each step. The discs were then incubated in 1x Click-iT reaction cocktail for 30' and mounted.

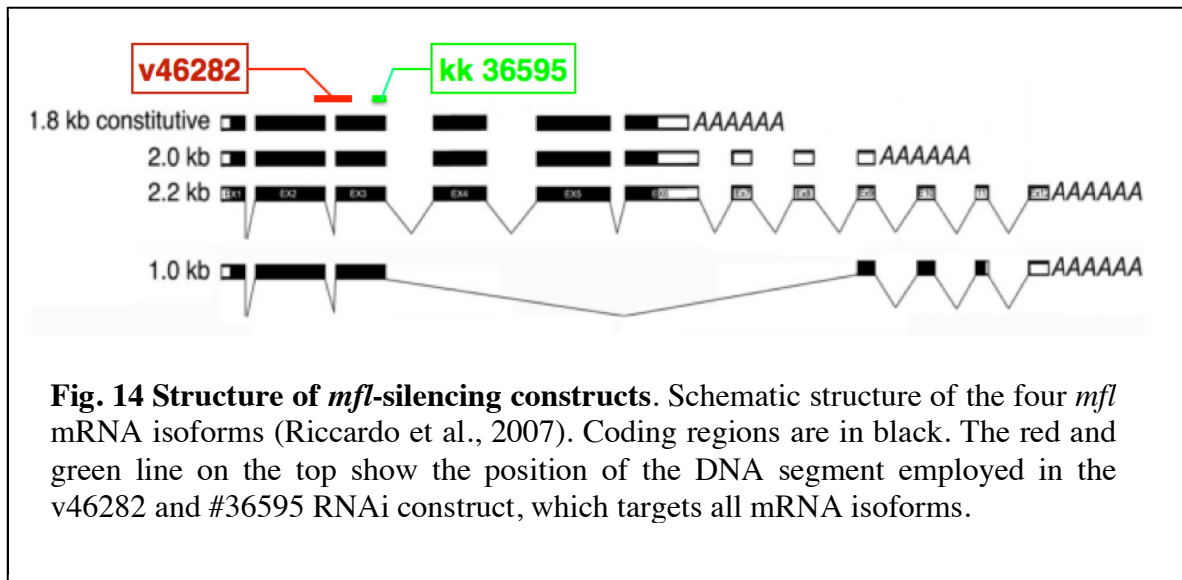
Z-stack analysis

All captured pictures (in RAW format) have been analyzed and processed with ImageJ v1.440 software. Z-stack analysis was performed by using STACK>ZProjection and STACK>Orthogonal views ImageJ plug-in.

RESULTS

Effects of Mfl depletion on wing disc homeostasis

In previous experiments, it was demonstrated that Mfl depletion in *Drosophila* wing disc causes two opposite effects in the silenced domain: while patches of cells around the A/P margin undergo apoptosis, those surrounding - located more distally respect to the A/P boundary - secrete the Wg morphogen, as a sort of homeostatic compensatory mechanism (Vicidomini et al., 2015). Since these coupled phenomena typically occur in regenerative processes (Ryoo et al., 2004), I decided to further dissect the events occurring in the silenced disc. In order to define in more detail how Mfl loss can affect growth and development, I used the Gal4/UAS system (Brand and Perrimon, 1993) to silence Mfl activity in a restricted area of wing disc. To this aim, I used the *optomotor-blind*-Gal4 (*omb*-Gal4) and *engrailed*-Gal4 (*en*-Gal4) driver lines. The *engrailed* driver is expressed only in the posterior compartment of discs, while the *optomotor-blind* is expressed in a central domain that broadly spans from presumptive veins 1 and 2 in the anterior compartment to the presumptive veins 4 to 5 in the posterior compartment (Grimm and Pflugfelder, 1996). I used two different UAS-IR*mfl* lines (v46282 and #36595) both giving identical results and proving to knock-down efficiently all *mfl* mRNAs (Fig. 14).



Wingless ectopic secretion is essential for the occurrence of regenerative growth in *mfl* silenced discs

As mentioned above, *mfl* silencing induces apoptosis in the central part of the wing disc (Vicidomini et al., 2015; see Fig. 15). I confirmed that cell death is a major consequence of *mfl* down-regulation by detecting the presence of pyknotic nuclei located basally in the pseudostratified epithelium. As show in Fig. 16, the intense staining of DAPI marks in fact a degenerative state of cell nuclei. Beyond the high level of activated Cas3, high levels of Wg protein were detected along the entire A/P boundary and in both dorsal and ventral compartments of the inner ring (Vicidomini et al., 2015; see Fig. 15). The activity of Wg signaling is known to be required for the specification, growth and morphogenesis of

the wing pouch (Gonsalves and DasGupta, 2008). Moreover, several

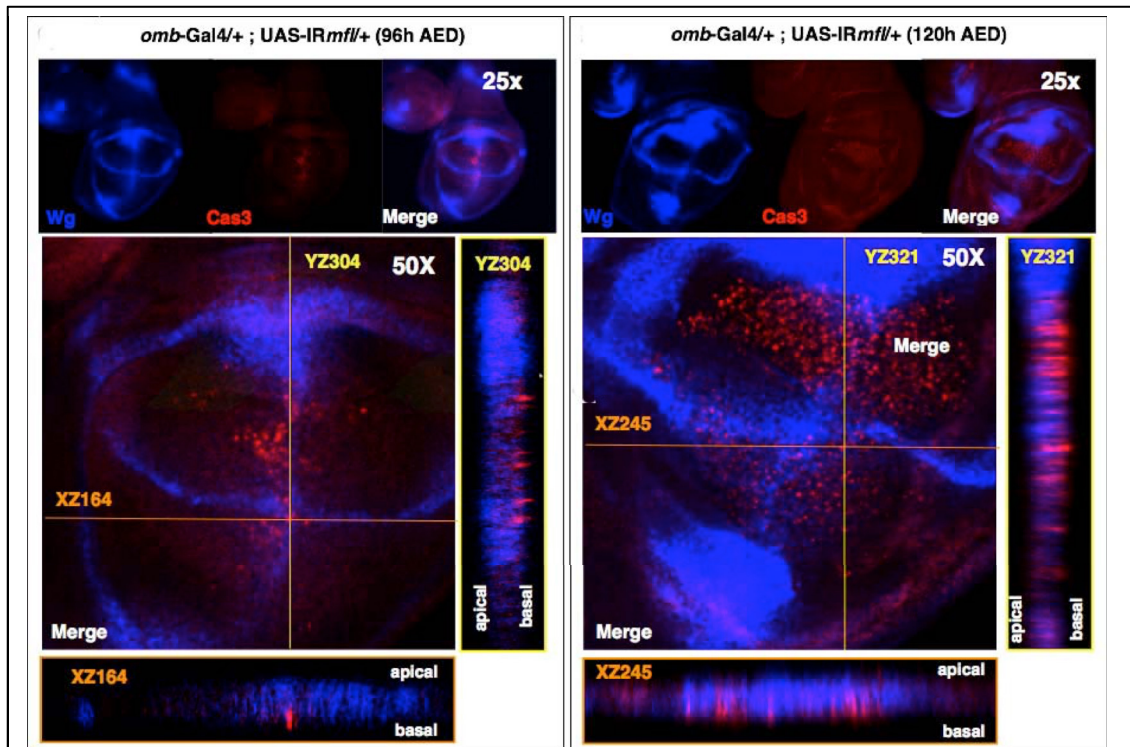


Fig. 15 Mfl depletion induces both Cas3 and Wg activation in the wing discs (Vicidomini et al., 2015). *omb>IRmfl* silenced discs collected at two developmental times: 96 h (left) and 120 h (right) After Egg Deposition (AED). At 96h AED, clusters of Cas3-positive spots mark the A/P boundary, flanked by Wg ectopic induction. At 120h AED, the number of Cas3-positive spots increase, together with Wg ectopic induction. Cas 3 is in red; Wg in blue

authors showed that ectopic secretion of Wg at the edge of the dying

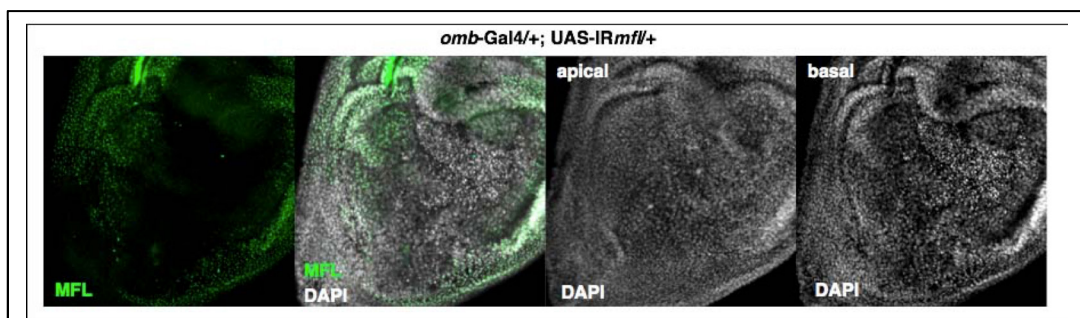
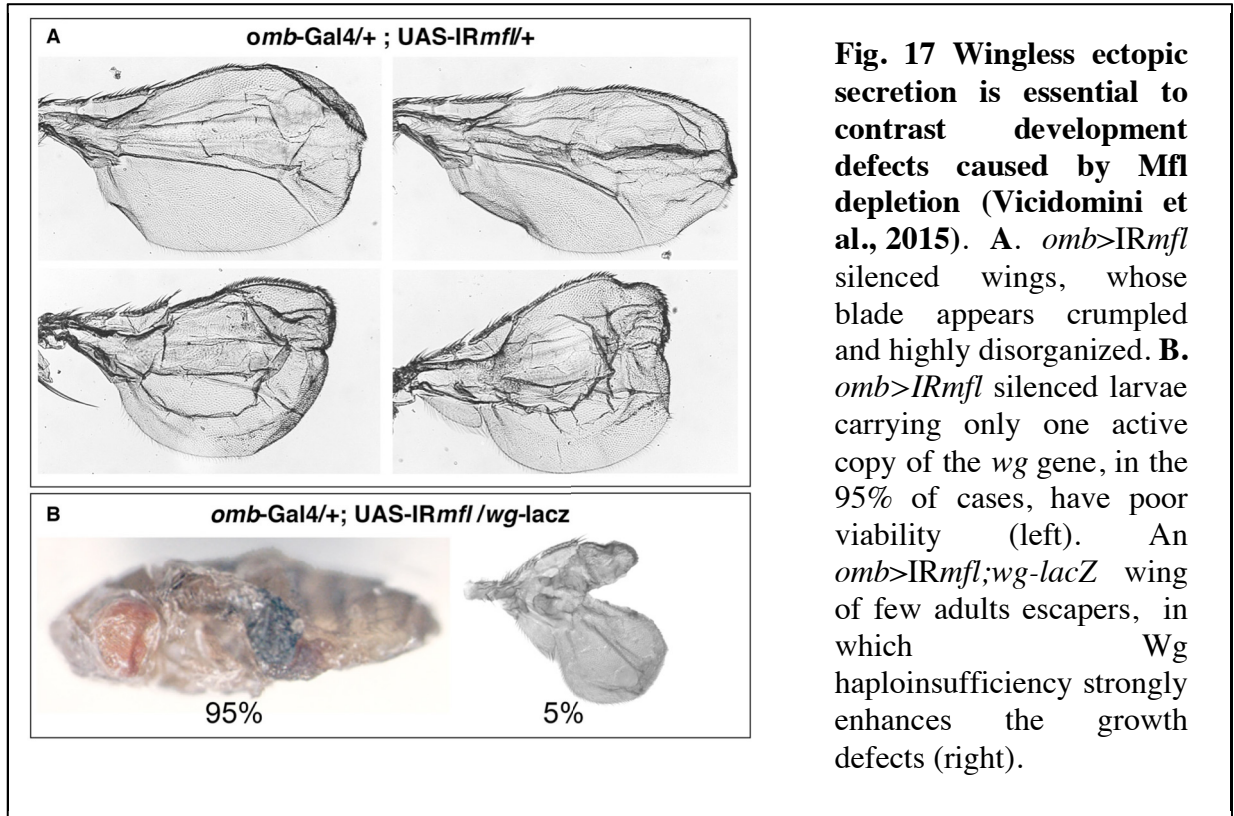


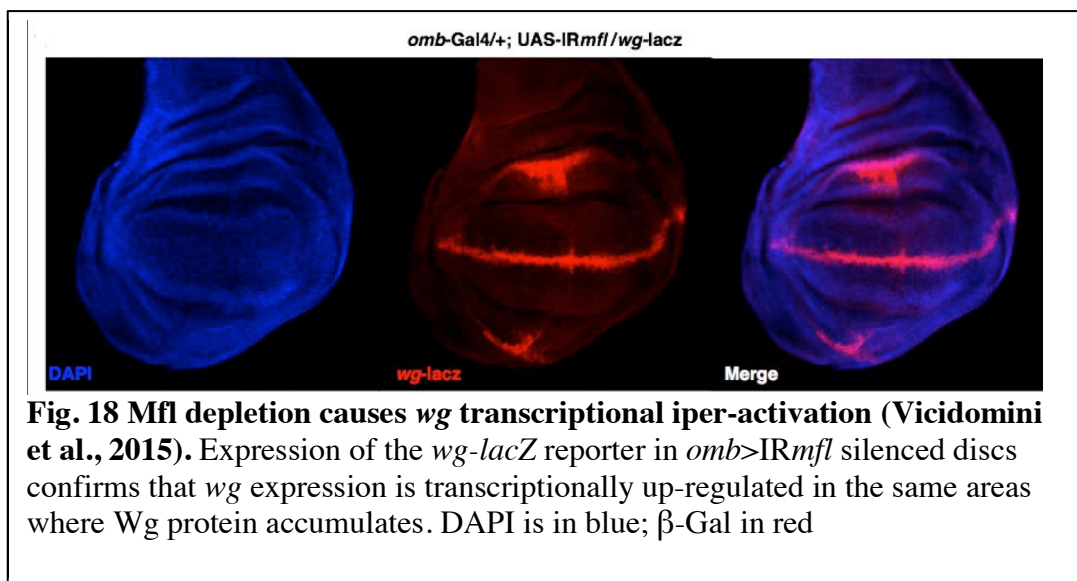
Fig. 16 Mfl depletion induces apoptosis in the wing discs (Vicidomini et al., 2015). DAPI staining of *omb>IRmfl* discs shows basal clusters of pyknotic nuclei within the silenced domain. Note that the basal focal plans are separated by apical focal plans and pyknotic nuclei are detected only basally. DAPI is in gray; Mfl in green

tissue is essential for regenerative growth (Pérez-Garijo et al., 2004; Smith-Bolton et al., 2009). In order to define whether Wg over-expression is essential for the occurrence of the regenerative processes observed in the silenced discs, I utilized the *wg-lacZ* insertion, a *wg* loss-of-function allele that also acts as *wg* transcriptional reporter. Since the *wg* gene is mutant due to the *lacZ* insertion (Oh et al., 2003), these *IRmfl* silenced larvae have only one active copy of the *wg* gene. I noticed that these larvae, in the 95% of cases, had poor viability; moreover, a few adult escapers (5% of total) all developed highly deformed wings with dramatic growth defects and the central *omb* domain often missing (Fig. 17B).

Thus, with respect to *mfl* silencing alone, that led to disturbed wing morphology typified by a detachment of the two wing layers and blistered wings (Fig. 17A), the heterozygous *wg* background markedly worsened the wing phenotype. This enhancement is consistent with a dose-effect, and suggests that high-level of Wg is required to contrast the developmental defects caused by Mfl depletion



I then took advantage of the *wg-lacZ* as transcriptional reporter to visualize *wg* transcriptional activity in these silenced discs. As shown in Fig. 18, beta-Galactosidase staining revealed that *wg* expression fully



overlaps the areas previously marked by Wg protein accumulation, confirming that cells surrounding the apoptotic foci are involved in producing high-level of Wg.

Upon p35 expression, Mfl-depleted undead cells are formed along the A/P border

In *Drosophila* wing discs, regenerative processes based on apoptosis-induced proliferation are usually visualized in conditions of apoptotic block. These conditions, obtained upon over-expression of the baculovirus p35 protein, known to inhibit the function of Cas3 but not its activation (Hay et al., 1994; Callus and Vaux, 2007), lead to formation of large “undead cells” that produce large amount of Wg (Martín et al., 2009). To this aim, I over-expressed the baculovirus p35 protein into Mfl depleted discs. In these experiments, the *omb*-Gal4 driver line directed simultaneous expression of UAS-IR*mfl* and UAS-p35 transgenes, and the morphology of the epithelium was monitored by following the formation of F-actin with phalloidin staining. As shown in Fig. 19, in the silenced discs the tissue appears wrinkled and folded with fractures along the A/P border, where clusters of Cas3-positive cells were previously observed (Fig. 19B).

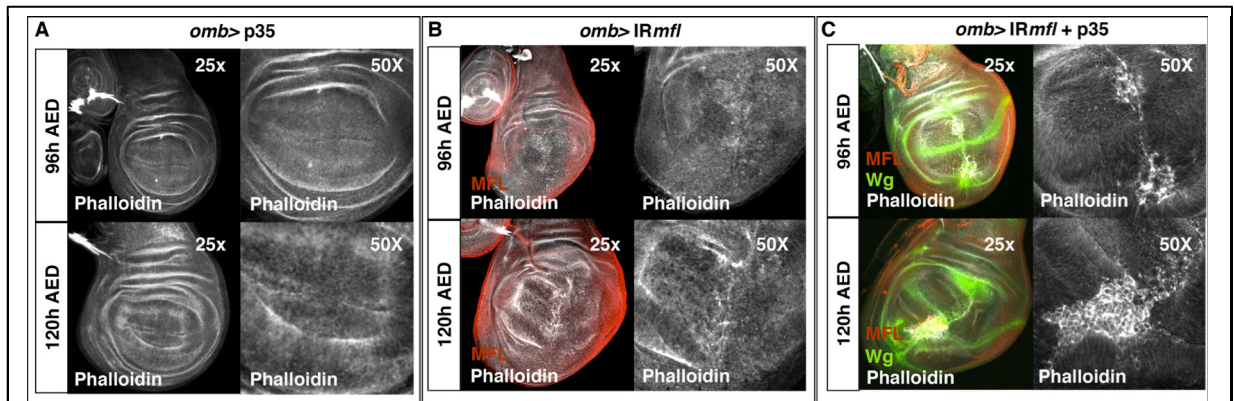


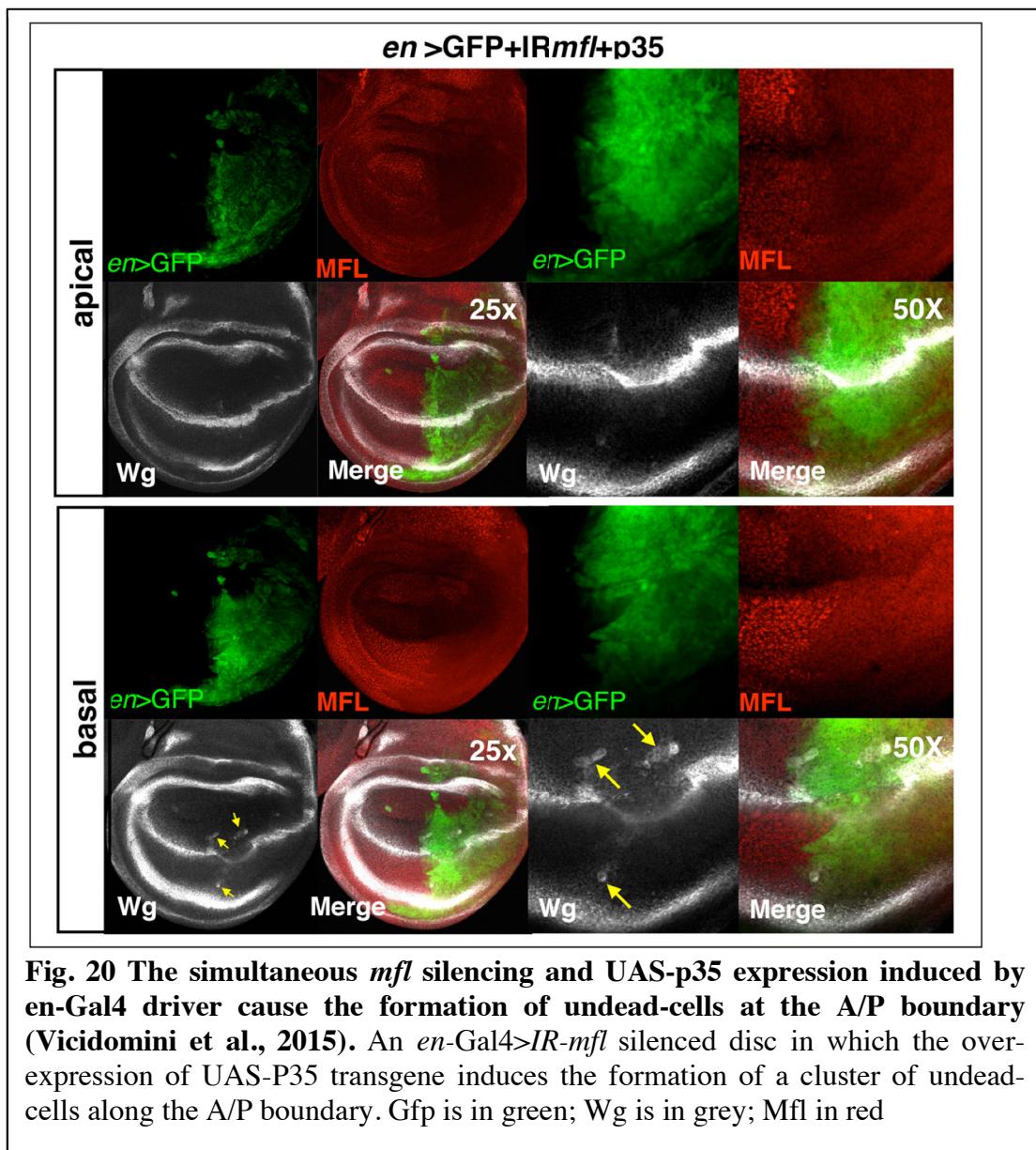
Fig. 19 In the *mfl* silenced discs, UAS-p35 expression generates patches of large “undead cells” (Vicidomini et al., 2015). *omb>p35* control disc were collected at 96h AED (up panel) and 120 h AED (bottom panel) and stained with phalloidin. **B.** Phalloidin staining of *omb>IRmfl* silenced disc collected at 96h AED (up panel) and 120 h AED (bottom panel) shows a strong tissue disorganization. **C.** In the presence of p35, phalloidin staining reveals the formation of undead cells (secreting high level of Wg) along the A/P border of the silenced disc. Phalloidin is in grey; Wg in green; Mfl in red

These local fractures were strongly enhanced in presence of the UAS transgene that expresses the baculovirus p35 protein. As expected, in the silenced discs UAS-p35 expression generates in fact patches of large “undead cells” all clustered at the A/P boundary (Fig. 19C), while in a wild type background it has no effect on the epithelium structure (Fig. 19A).

Similar results were obtained when simultaneous expression of UAS-*IRmfl* and UAS-p35 transgenes was directed by the *en*-Gal4 driver in the posterior compartment of wing disc. As shown in Fig. 20, also in this case undead cells were found along the A/P boundary. However, the apoptosis was scarcely induced, and the number and the size of clusters of undead cells were consequently reduced. This difference cannot be

related to the driver strength or a more precocious activation, since *omb-Gal4* is known to be almost as strong as *en-Gal4*, and its activation occurs at later developmental time. Therefore, I suggest that it can be related to the different silenced domain. Indeed, *en* expression is restricted to the posterior compartment, while *omb* spans the central part of wing disc and includes the A/P boundary cells, that are likely more sensitive to depletion of Mfl protein and thus proner to apoptosis.

Finally, although the undead cells secreted high-levels of Wg (Martín et al., 2009; see Fig 19, 20), no phenotypic rescue was reached, indicating that Wg overproduction, although required, is not sufficient to recover Mfl depletion.

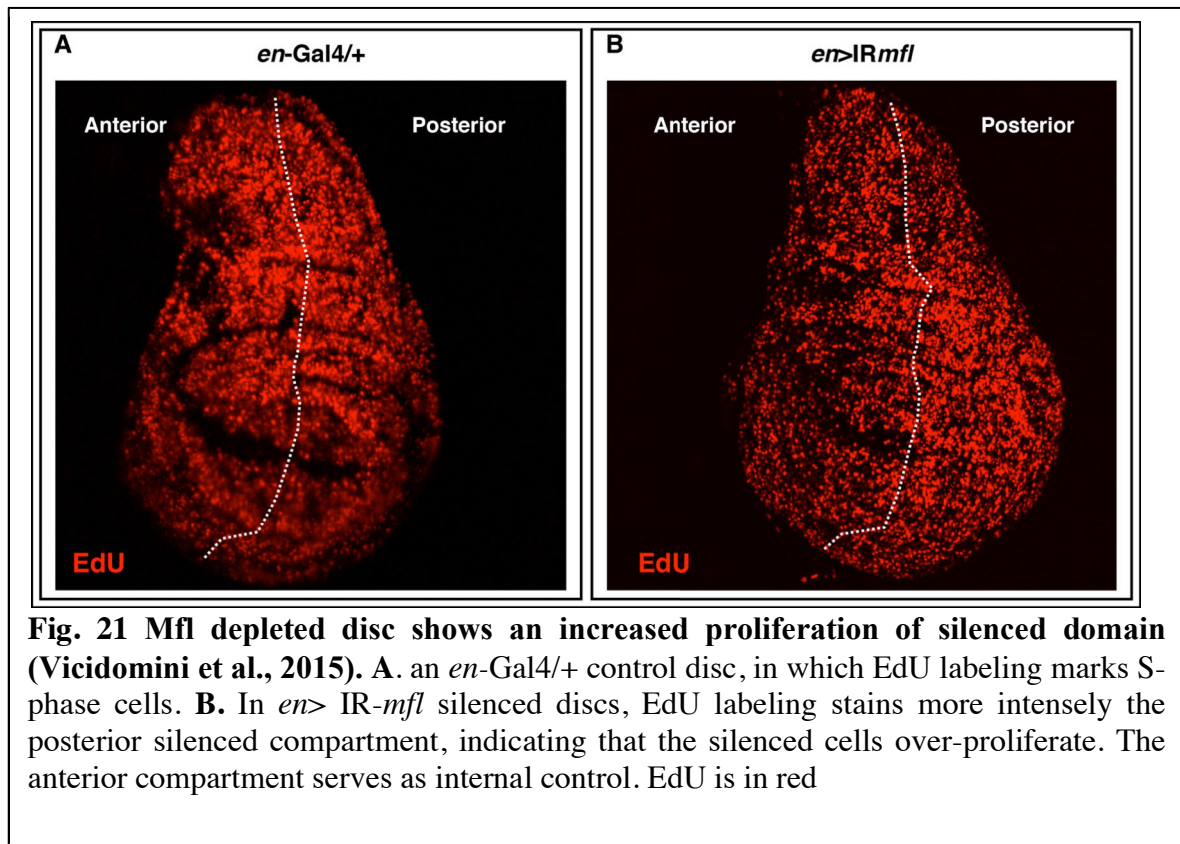


***mfl* silencing causes “apoptosis induced proliferation”**

Considering the high-level Wg expression, I checked the effect triggered by *mfl* silencing on cell growth. To determine the effects of Mfl depletion on cell proliferation, I stained the *en*-Gal4 silenced discs by EdU incorporation to specifically mark DNA synthesis and label S-phase cells.

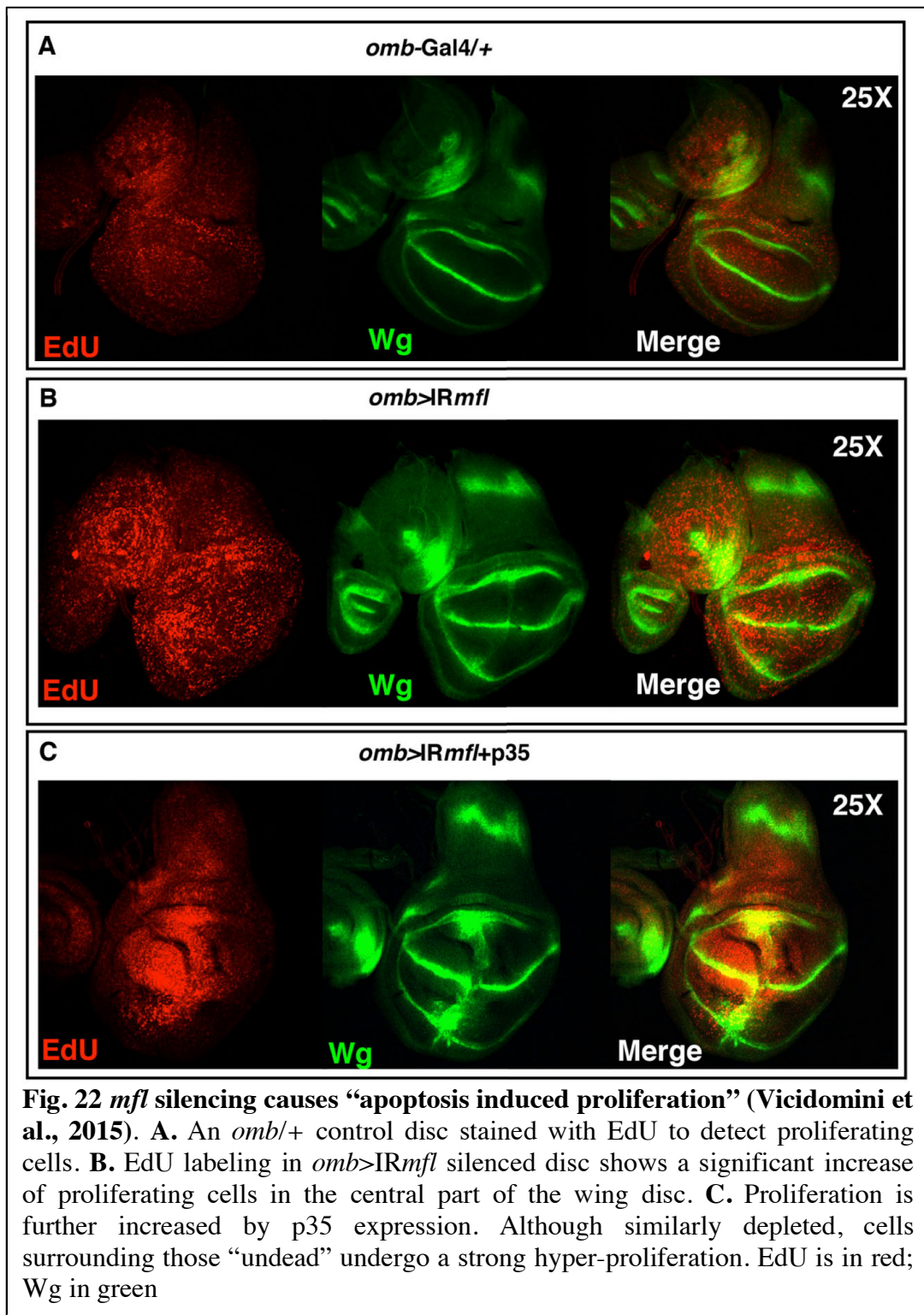
As shown in Fig. 21, this approach enabled to reveal a significant

enhancement of the proliferative activity in the silenced posterior compartment.

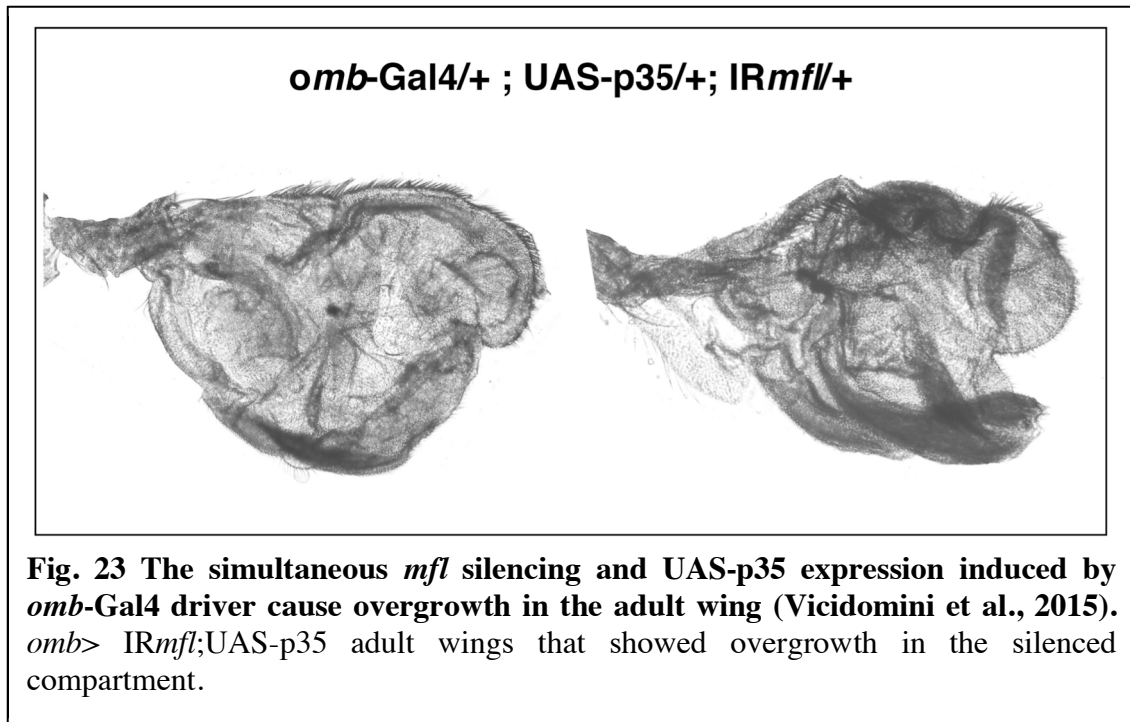


Identical results were obtained when *mfl* silencing is directed by the *omb-Gal4* driver. In fact, despite the massive apoptosis observed in the silenced areas (see Fig 15,16), the overall proliferation rate was enhanced with respect to controls (Fig. 22A,B), and even further in presence of p35 expression (Fig. 22C).

Occurrence of over-proliferation was further confirmed by the wing phenotype of rare *omb>IR-mfl;UAS-p35* adult escapers, that developed highly deformed wings characterized by a dramatic overgrowth. As



shown in Fig. 23, these wings presented a detachment of dorsal/ventral that typically occurs after over-proliferation.

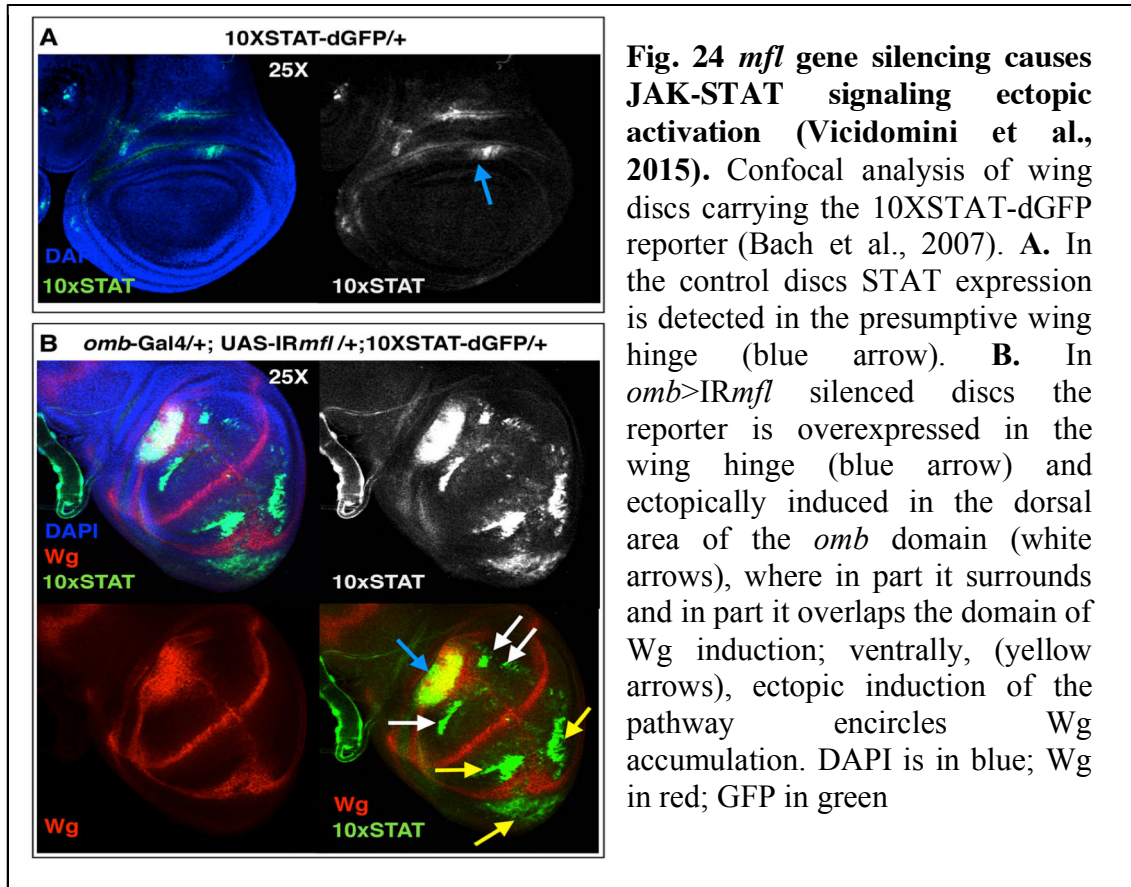


Altogether, these data indicate that *Mfl* depletion elicits opposite outcomes in diverse wing territories. While some cells (those at the A/P boundary first), activate *Cas3* and undergo apoptosis, other silenced cells undergo robust proliferation.

The “apoptosis induced proliferation” that occurs in *Mfl* depleted discs correlates with ectopic activation of the JAK/STAT pathway

The JAK/STAT pathway plays several important roles in the development of wing imaginal discs. Imaginal cells are set aside during embryogenesis and proliferate throughout larval life before differentiating and everting during pupal stages to form a large proportion of the adult fly. One of the first roles for JAK/STAT signalling in this process is its

requirement in cellular proliferation. In several years, this pathway has been associated with apoptosis induced proliferation and regeneration (Wu et al., 2010; Rodrigues et al., 2012). I thus used a 10XSTAT92E-dGFP transgenic reporter to monitor JAK/STAT pathway activity *in vivo*. This strain accurately reflects the pathway activity because it was generate by placing Stat92E binding sites derived from a Stat92E target gene (Socs36E) upstream of a destabilized GFP (Bach et al., 2007). Normally, in the third larval discs JAK/STAT is activated in the dorsal compartment and in the anterior lateral side of dorsal/ventral boundary (Fig. 24A). In *mfl* silenced discs, I found that this pathway is up-regulated at the centre of the inner ring, and ectopically activated at specific regions



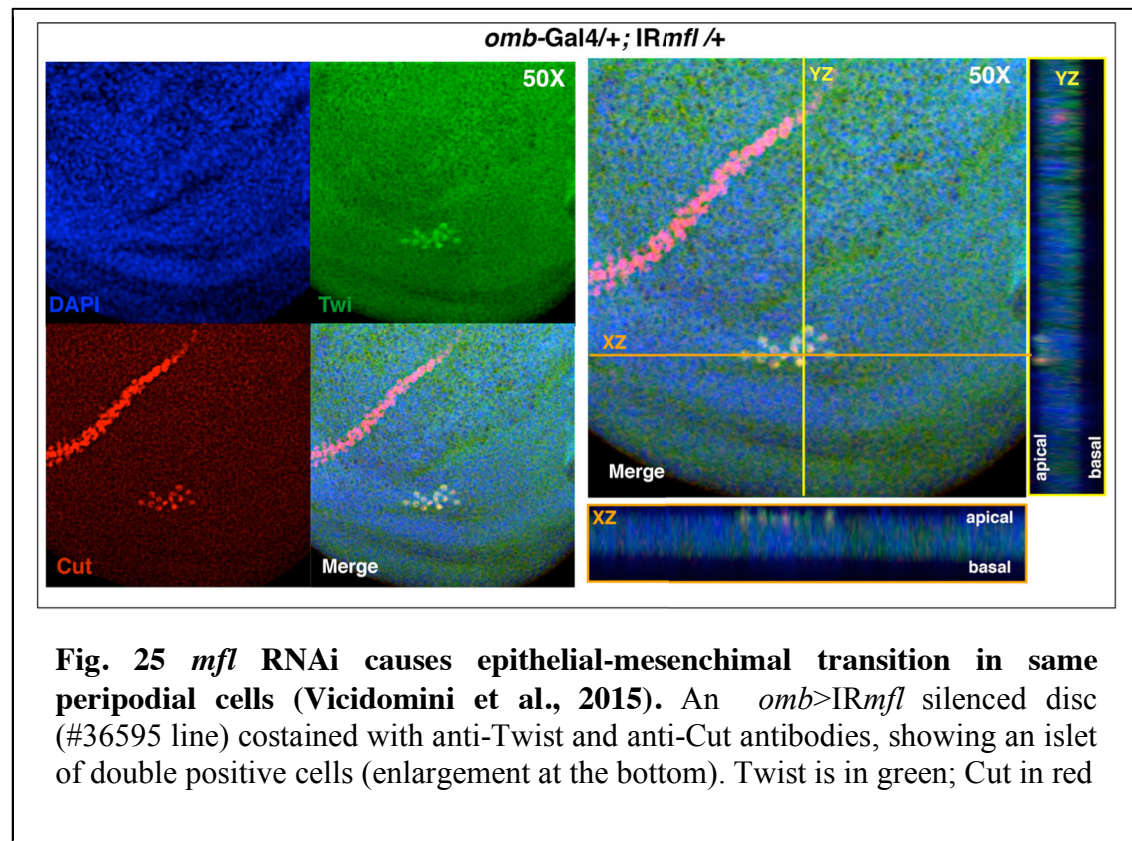
of the silenced domain. As shown in Fig. 9B, in the ventral compartment JAK/STAT activation is induced in cells surrounding those showing strong Wg accumulation, while in the dorsal compartment its activation in part surrounds and in part overlaps Wg ectopic expression (Fig. 24 B). Altogether, these data indicate that Mfl depletion induces a regenerative response mediated by Wg and JAK/STAT pathway.

Mfl depletion promotes EMT in a cell non autonomous manner

In previous experiments R. Vicidomini et al. (2015) demonstrated that Mfl depletion into the below pseudostratified epithelium induced epithelial-mesenchymal transition (EMT) in the above peripodial cells. Since it is known that high levels secretion of Wg can induce EMT (van der Velden et al., 2012), I wanted investigate this aspect in more detail.

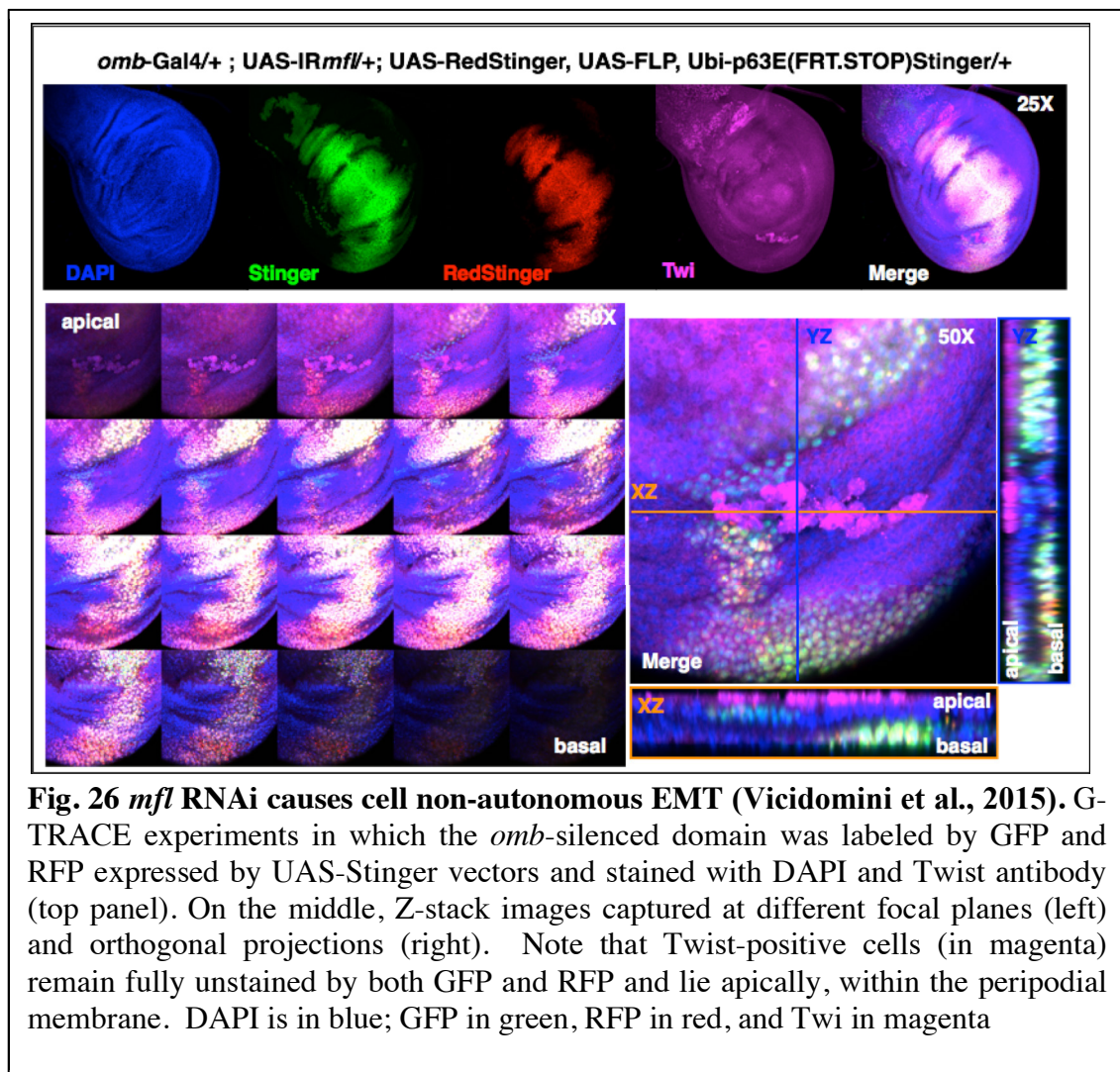
In previous experiments, the v46282 silencer transgenic line was used to knock-down the *mfl* gene. In order to define if all IR-*mfl* transgenes can induce EMT, in my experiments I used the #36595 transgenic silencer line. I thus stained the #36595 silenced discs with an antibody directed against Twist, a typical marker for mesenchymal cells (Ghazi et al., 2000; Khan et al., 2013) that is expressed in presumptive mesodermal cells and not in epithelia (Sudarsan et al., 2001). Intriguingly, patches of Twist-positive cells were detected in almost 95% of silenced discs (n = 20; Fig. 12). These cells also ectopically expressed Cut (Fig. 25), an additional

marker of myoblasts (Sudarsan et al., 2001). These results further confirmed the acquisition of mesoderm identity and the occurrence of EMT.

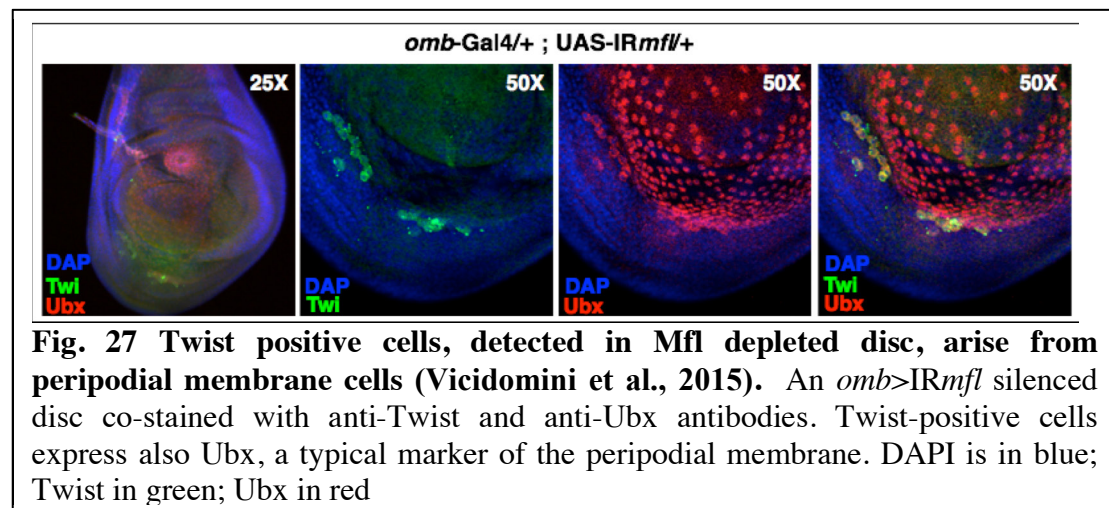


I then wondered whether the observed myoblasts originated from the underlying silenced epithelium and then migrated above or, alternatively, arose directly from the un-silenced tissue. To investigate this aspect, I performed a lineage-tracing experiments by making use of the G-TRACE system, which is based on the expression of a pair of GFP-RFP Stinger reporters (Evans et al., 2009). In this system, cells that had a previous Gal4-dependent activation of the GFP reporter, even if transient, remain

GFP-labeled; conversely, cells showing only an active real-time expression of the Stinger vector become RFP-labeled. In my experiments, Twist/Cut positive cells were never GFP or RFP-labeled, clearly indicating that they were not expressing the *omb*-Gal4 driver, nor activated it at any previous developmental stage (Fig. 26). This unexpected result definitively confirmed that these cells derive from the peripodial membrane.



To further confirm their origin, an anti-Ubx antibody that marks the majority of peripodial cells (Pallavi et al., 2005) was used. Intriguingly, the Twist/Cut positive cells faintly expressed also Ubx, indicating that they are in a state of cell fate transition (Fig. 27).

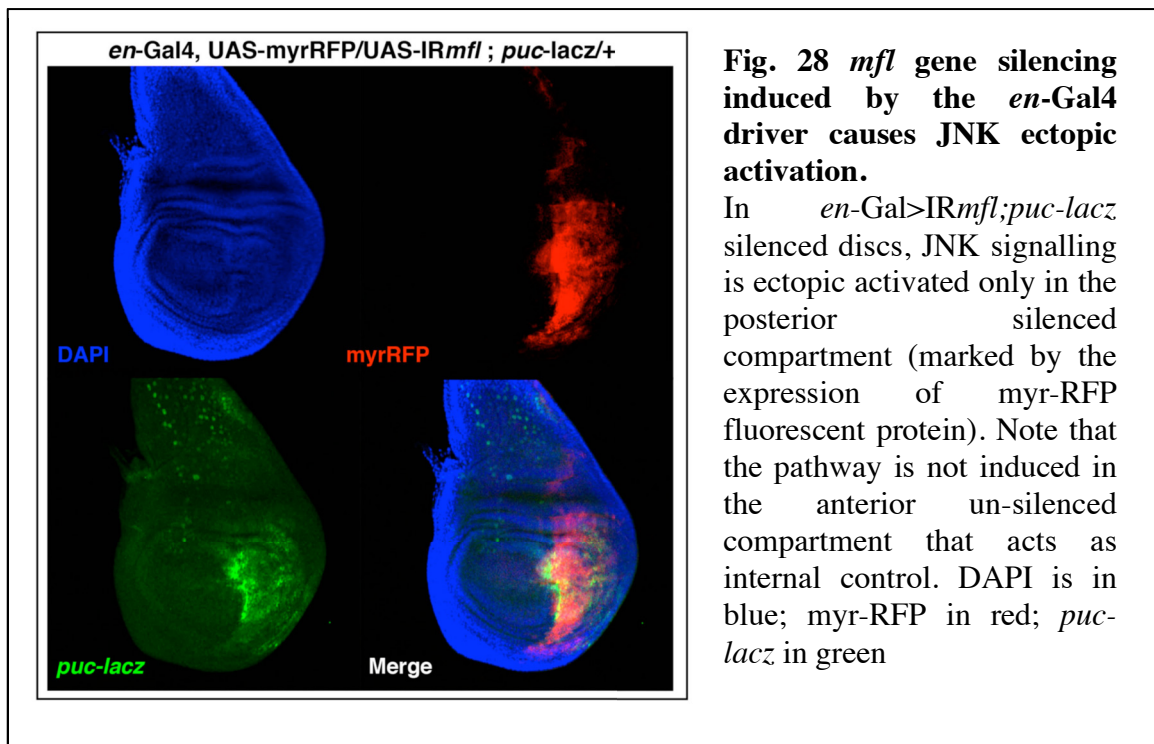


This result also ruled out the possibility that these myoblasts could derive from the ad epithelial cells abutting the wing disc in the notum region, since those myoblasts do not express Ubx (Pallavi et al., 2003). I thus concluded that Twist/Cut/Ubx positive cells originate from the unsilenced peripodial membrane upon cell fate change, and that Mfl depletion can promote cell non autonomous EMT in a contiguous tissue.

JNK activation may act to prevent overgrowth in Mfl depleted cells

Previous data indicated that *mfl* silencing induced ectopic activation of Jun-N-terminal Kinase (JNK) signaling (Vicidomini et al., 2015). JNK

pathway represents a key conserved eukaryotic signaling identified as a stress-activated protein kinase (SAPK). This signaling can be activated by various stimuli, such as UV irradiation, DNA damage, bacterial infection, cytokines, etc. JNK is also involved in several physiological developmental processes that include apoptosis, cell proliferation and regeneration (Adachi-Yamada et al., 1999; Bosch et al., 2005). In previous experiments, the pattern of JNK activation was examined by using a *puckered-lacZ* (*puc-lacZ*) strain (a JNK downstream effector) and was found strongly induced in *omb*-silenced discs. To further confirm that JNK is ectopically induced upon *mfl* silencing, I used the *en*-Gal4 driver to knock down *mfl* and the *puc-lacZ* reporter to monitor JNK activation. As shown in Fig. 28, beta-Galactosidase staining revealed that JNK is ectopically and strongly activated only in the posterior silenced

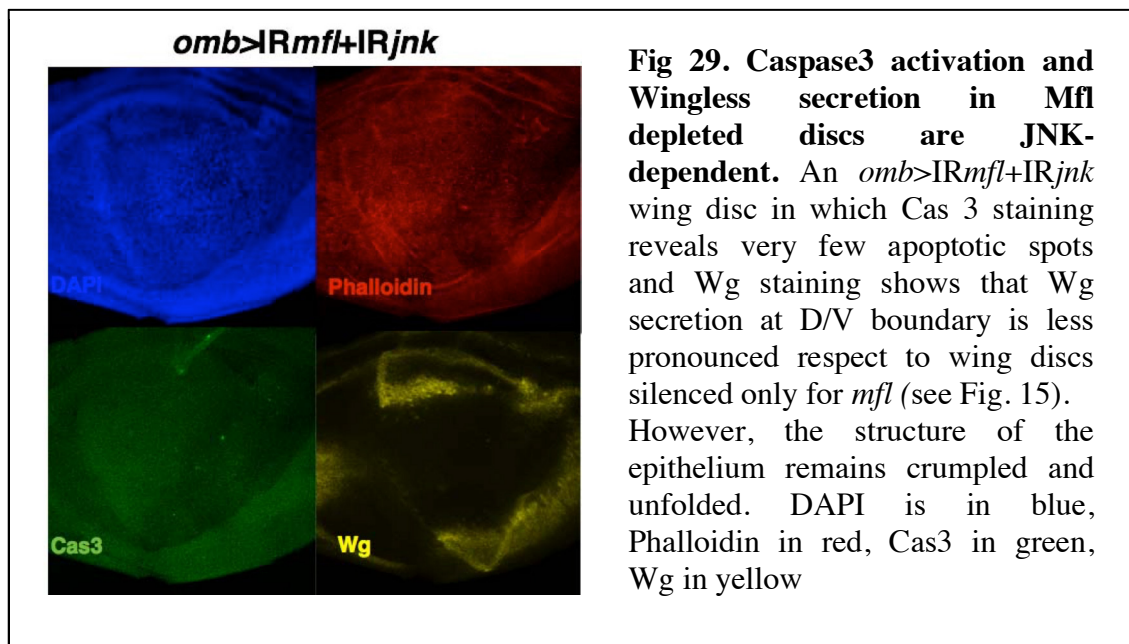


compartment of the disc (marked by the myr-RFP fluorescent protein; the anterior compartment acts as internal control).

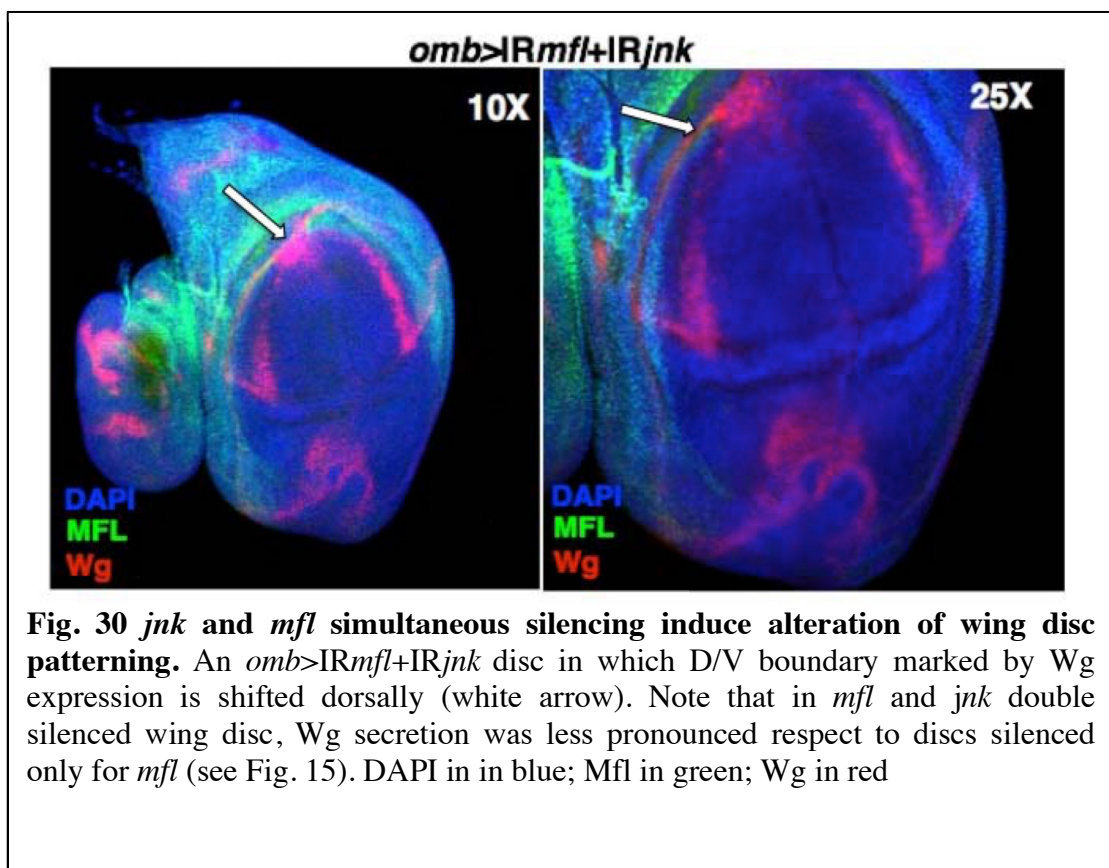
Given the role played by JNK pathway in regenerative processes, I attempted to establish whether activation of this pathway could be required to trigger the apoptosis-induced proliferation observed in *Mfl*-depleted domains.

By suitable crosses, I thus activated simultaneous silencing of *mfl* and *jnk* genes. To this purpose, I utilized a transgenic strain (#104569) able to knock down *basket* (*bsk*), the unique *Drosophila* JNK gene.

Interestingly, the expression of UAS-IR*bsk* construct in *mfl* silenced discs blocked the occurrence of apoptosis, and only a very few Cas3 apoptotic spots were detected in the double-silenced discs (Fig. 29). Furthermore,

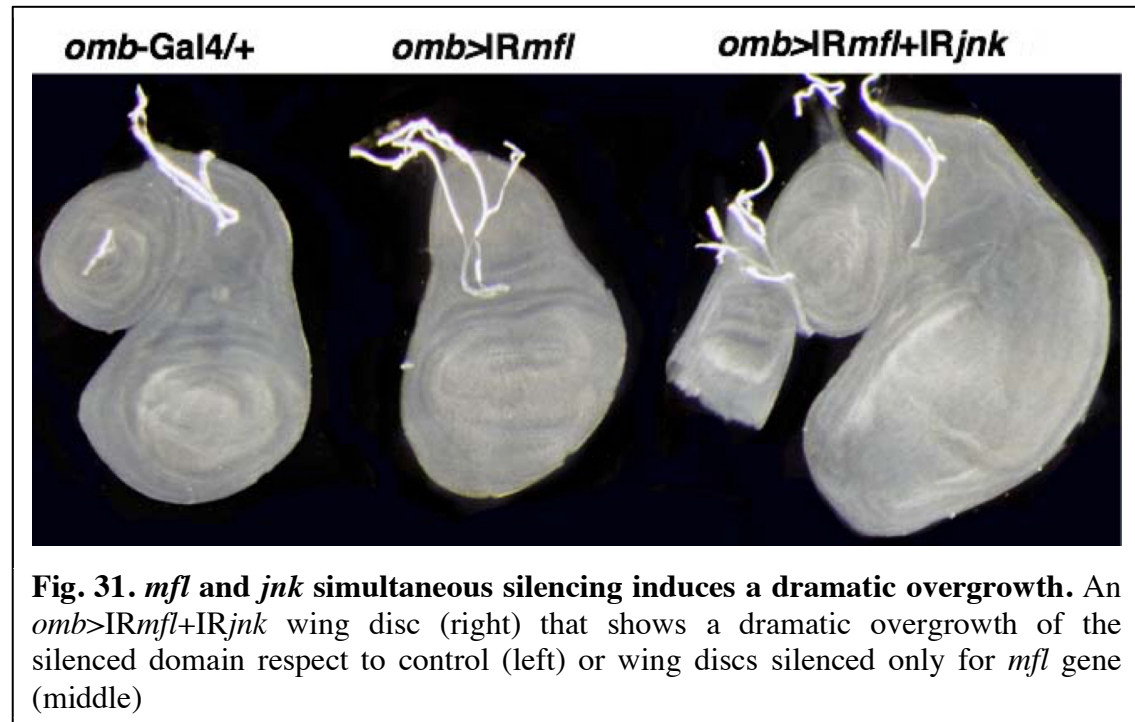


Wg secretion at D/V boundary was less pronounced (Fig.29) than in *mfl*-silenced discs (see Fig. 15), although the morphology of the epithelium (monitored by phalloidin staining) remained wrinkled and folded (Fig. 29). These results demonstrated that Cas3 activation and Wg secretion in Mfl depleted cells are JNK-dependent. Worth nothing, Wg staining in *mfl* and *jnk* double silenced discs revealed that the Dorsal/Ventral (D/V) boundary shifted dorsally (Fig. 30), indicating a strong alteration of patterning



The contemporaneous expression of UAS-*IRmfl* and UAS-*IRbsk* constructs in the *omb* domain caused in fact a pronounced overgrowth of

the silenced domain (Fig. 30,31), indicating that JNK activation in Mfl-depleted cells can suppress over-proliferation.



***mfl* acts as Tumor Suppressor Gene (TGS)**

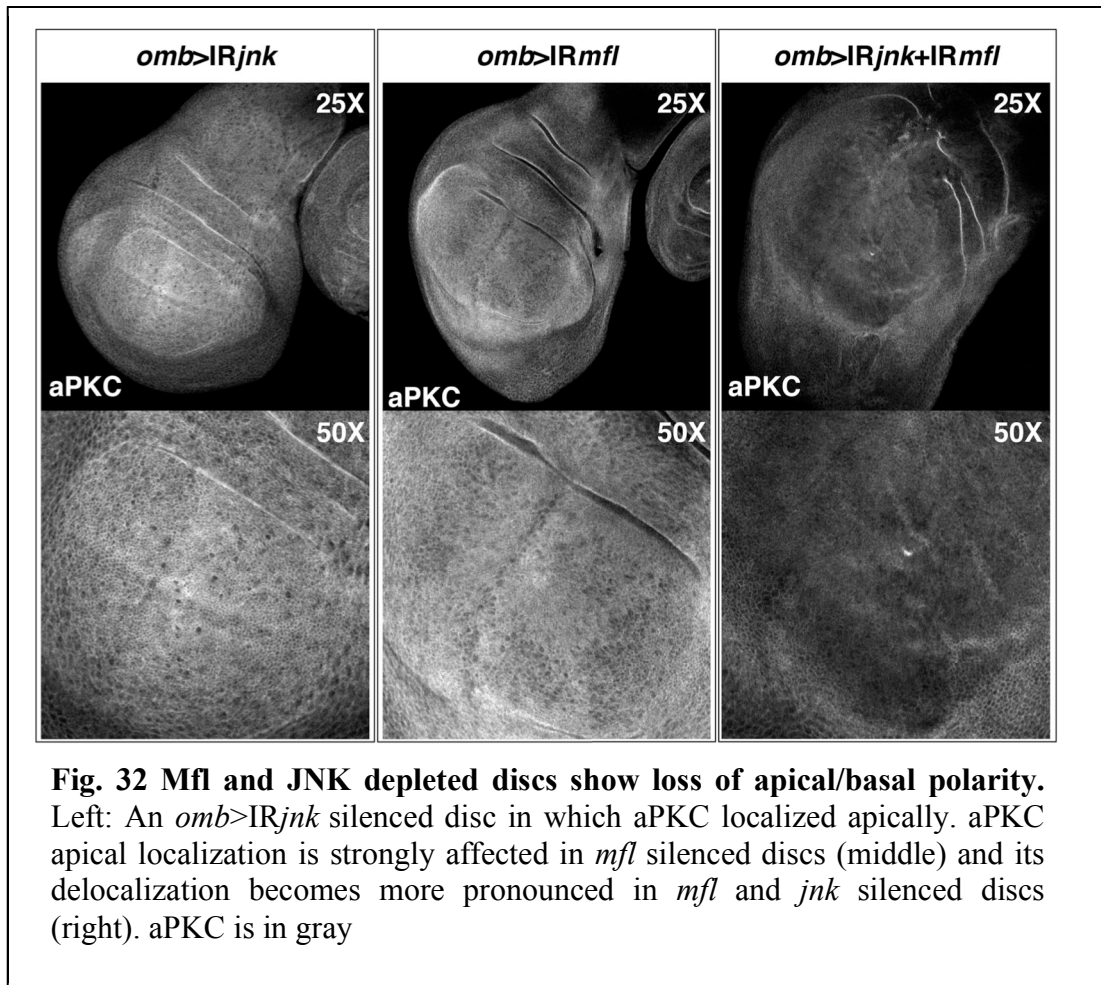
In *Drosophila*, loss-of-function mutations in tumor suppressor genes result in overgrowth of imaginal disc epithelia. Recent studies have revealed links between loss of cell polarity and proliferation, suggesting that the polarized organization of cells is necessary to regulate growth (Grzeschik et al., 2010). To check these aspects, I analyzed in more detail the localization of *Drosophila* apical/basal polarity complexes in *mfl/jnk* silenced discs.

In *Drosophila*, the maintenance of cell polarity depends on two major protein complexes localized at the apical membrane. The first complex

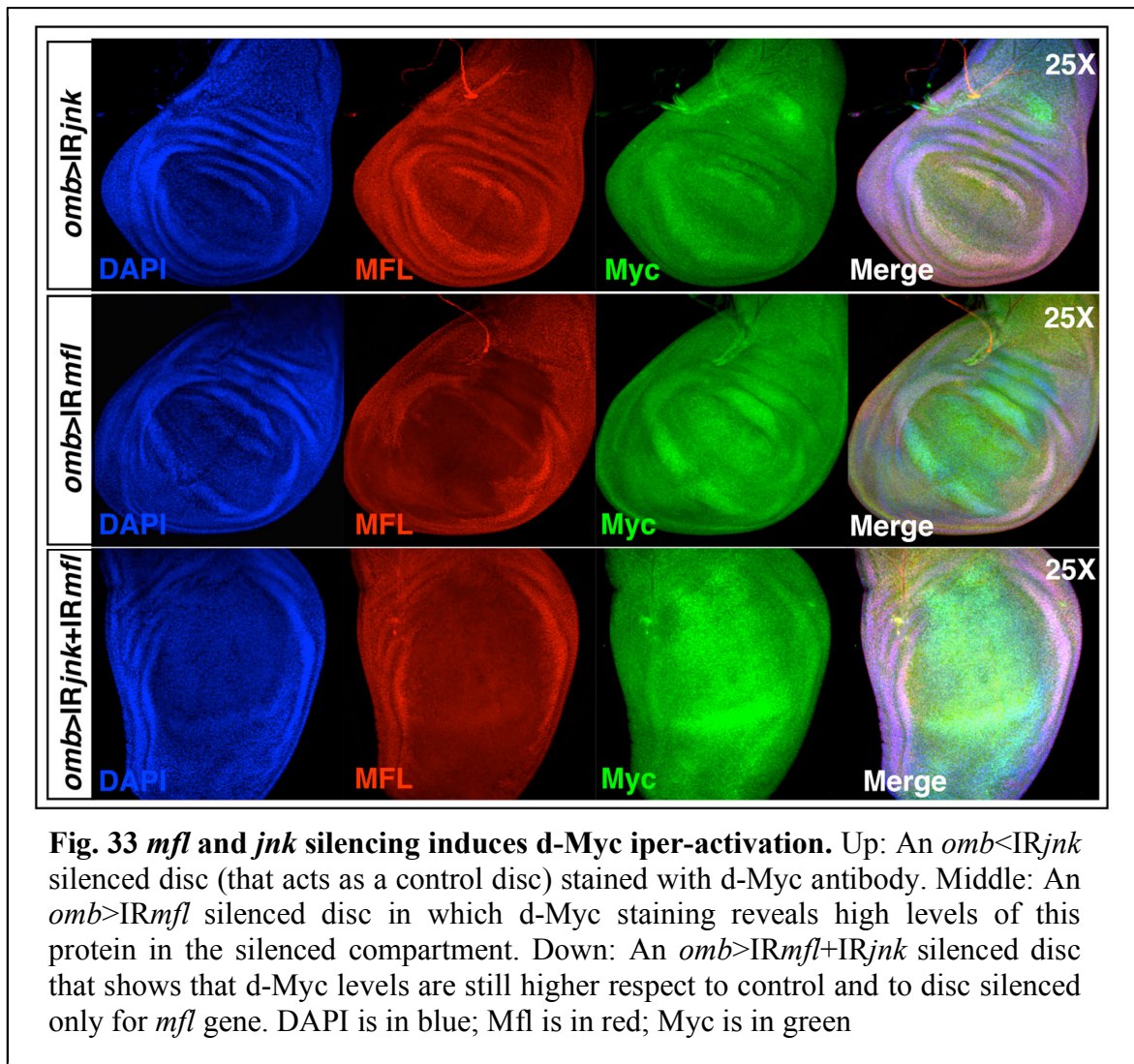
(Crumbs) is composed of the trans-membrane protein Crumbs (Cbs), the cytoplasmic scaffolding protein Discs lost (Dlt) and the Membrane-Associated Guanylate Kinase (MAGUK) Stardust. The second complex is composed of two scaffold proteins, Bazooka (Baz) and Par6, both containing PDZ domains, and the homolog of atypical Protein Kinase C. Aside from these two apical protein complexes, a lateral protein complex acts as a regulator of apical polarization. This complex is composed of the Myosin II binding protein Lethal Giant Larvae (Lgl), the multi-PDZ domain protein Discs Large (Dlg), and Scribble (Scrib; Badouel and McNeill, 2009).

In my experiments, I utilized an antibody against aPKC protein to monitor cell polarity. As shown in Fig. 32, aPKC was located apically in *jnk* silenced discs (that can act as controls); conversely, its accumulation was strongly altered in *mfl* silenced discs. Moreover, the concomitant silencing of *mfl* and *jnk* doesn't restore the aPKC correct localization, that is instead most evidently abolished in the *mfl/jnk* double-silenced discs.

Since loss-of-function mutations in tumor suppressor genes induce a strong overgrowth and loss of apico-basal cell polarity of the epithelial imaginal tissues (Badouel and McNeill, 2009), these results suggest that Mfl-depleted cells could have an intrinsic neoplastic behavior that is reinforced by JNK silencing.



To check this aspect in more detail, I used an antibody against d-Myc oncoprotein to evaluate its induction in either *mfl* and *mfl/jnk* silenced discs. As shown in Fig. 33, high-level induction of the d-Myc protein was observed in *mfl* silenced discs (*jnk* silenced discs were taken as controls), and found even more pronounced upon *jnk* silencing. Since dMyc oncoprotein promotes invasive overgrowth in larval epithelia (Froldi et al., 2010), its strong up-regulation in *mfl/jnk* silenced discs supports the hypothesis that *mfl* could act as a tumor suppressor gene.



How does Mfl depletion lead to overgrowth and dMyc up-regulation in the silenced disc tissue? Recent analysis (Grzeschik et al., 2010) has revealed that depletion of tumor suppressor genes in the eye disc leads to deregulation of the Salvador-Warts-Hippo (SWH) tumour suppressor pathway. This evolutionarily conserved signalling controls organ size and prevents hyperplastic diseases, from flies to humans, by restricting the activity of the transcriptional coactivator Yorkie (Harvey and Tapon, 2007). Since *dmyc* is a transcriptional target of the SWH pathway (Ziosi et al., 2010), I wanted to establish whether induction of this oncogene,

and the resulting overgrowth, in *mfl/jnk* silenced discs may depend on activation of the SWH pathway.

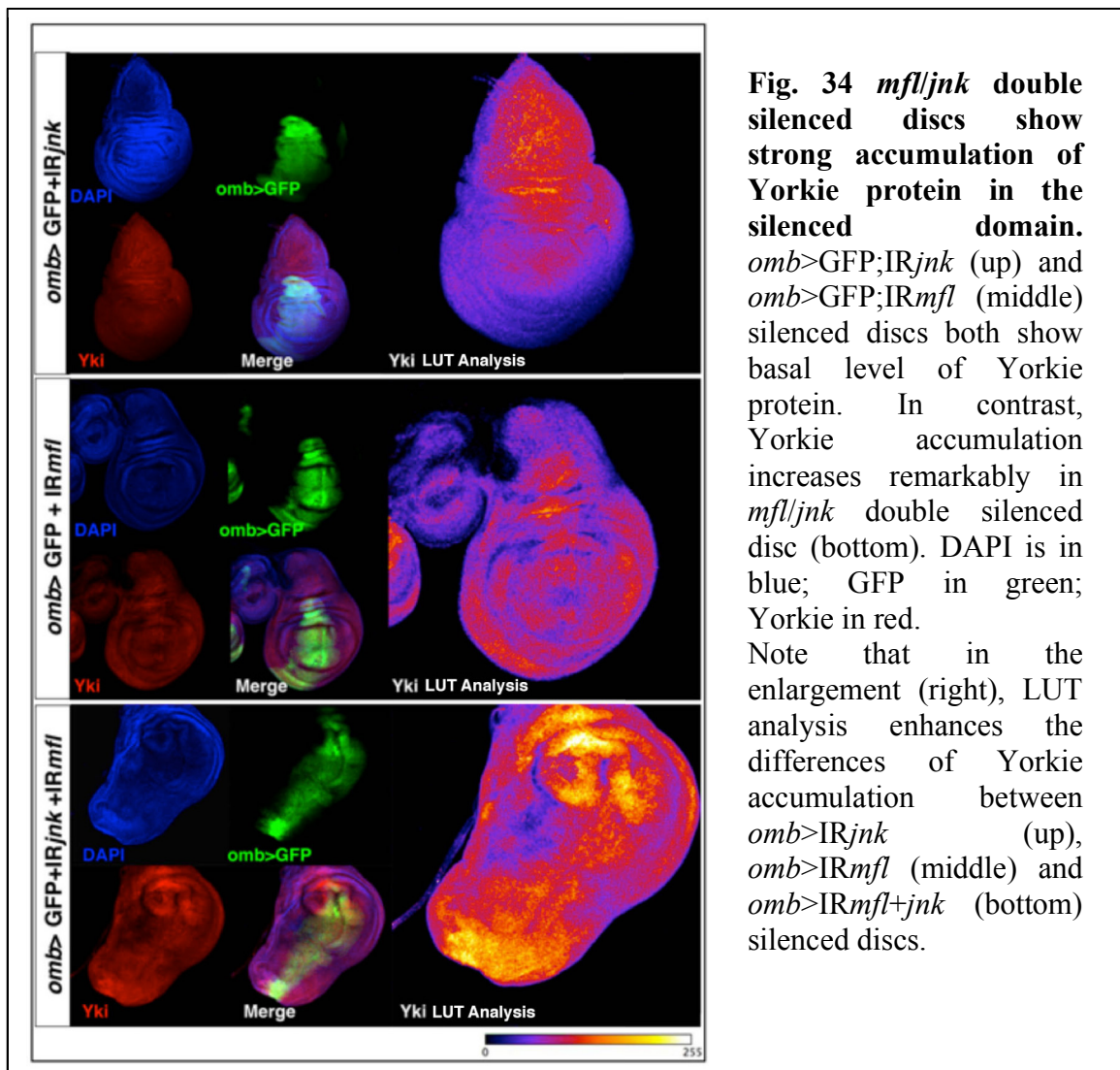
***mfl* gene silencing and its interplays with the Hippo pathway**

Recent studies have uncovered the Hippo pathway as a highly conserved tumor-suppressor pathway that plays essential roles in regulating multiple aspects of tumorigenesis, including cell growth, proliferation and survival. The four core components of Hippo pathway are the NDR family kinase Warts (Wts), the Ste20-like family kinase Hippo (Hpo), the WW-domain containing protein Salvador (Sav), and the adaptor protein Mob-as-tumor-suppressor (Mts) (reviewed by Xianjue, 2014). Hpo complexes with Sav to phosphorylate and activate Wts which, in conjunction with Mts, directly phosphorylates the transcriptional co-activator Yorkie (Yki), causing its cytoplasmic accumulation and activity inhibition (Oh and Irvine, 2008). When the Hippo pathway is activated, Yki translocates into nucleus to activate the transcription of many cell growth- and viability-regulating genes, such as *cyclin E (cycE)*, *expanded (ex)* and *Drosophila inhibitor of apoptosis protein 1 (diap1)*.

In order to establish if d-Myc induction and the strong overgrowth observed upon *mfl/jnk* silencing were depended on Hippo activation, I utilized an antibody against Yki protein to evaluate its accumulation in *jnk/mfl* double silenced discs, in *mfl* silenced discs and in control discs.

To quantify the amount of Yorkie protein, I utilized a “LUT” plugin of the ImageJ software. LUT - or lookup table - is a predefined table of gray values with matching red, green and blue values so that shadows of gray are displayed as colorized pixels. LUT assigns a pseudocolor (that is a single channel gray image) to a gray image. Thus, differences in color in the pseudo-colored image reflect differences in the intensity of the object, rather than differences in color of the specimen that has been imaged.

As shown in Fig. 34, this analysis indicated that Yorkie protein was very strongly accumulated in *omb>IRmfl/IRjnk* silenced discs. Conversely,



basal level of Yorkie protein was found in *omb>IRjnk* silenced discs (that acts as control discs) and in *omb>IRmfl* silenced discs.

Identical results were obtained by using the *en*-Gal4 driver. In these experiments, Yorkie protein strongly accumulated in the posterior compartment of *mfl/jnk* silenced discs (Fig. 35). Worth nothing, the *en>IRmfl/IRjnk* silenced discs showed morphological alterations of the posterior compartment, that is significantly larger than that of *en>IRmfl* silenced discs. Moreover, I noticed that the GFP-labeled posterior cells often penetrate into the anterior compartment. These findings suggest that *mfl/jnk* silenced cells have the intrinsic invasive behaviour that characterizes neoplastic cells. This observation points out that the specific role the *mfl/jnk/Hpo* interplay deserves further investigation. In future experiments, dysregulation of Hpo signaling will be monitored in more detail by checking the expression of Yorkie targets, such as *cyc-e*, *ex* and *diapl*. However, the preliminary data reported above represent the first link between *mfl* silencing and Hippo pathway induction.

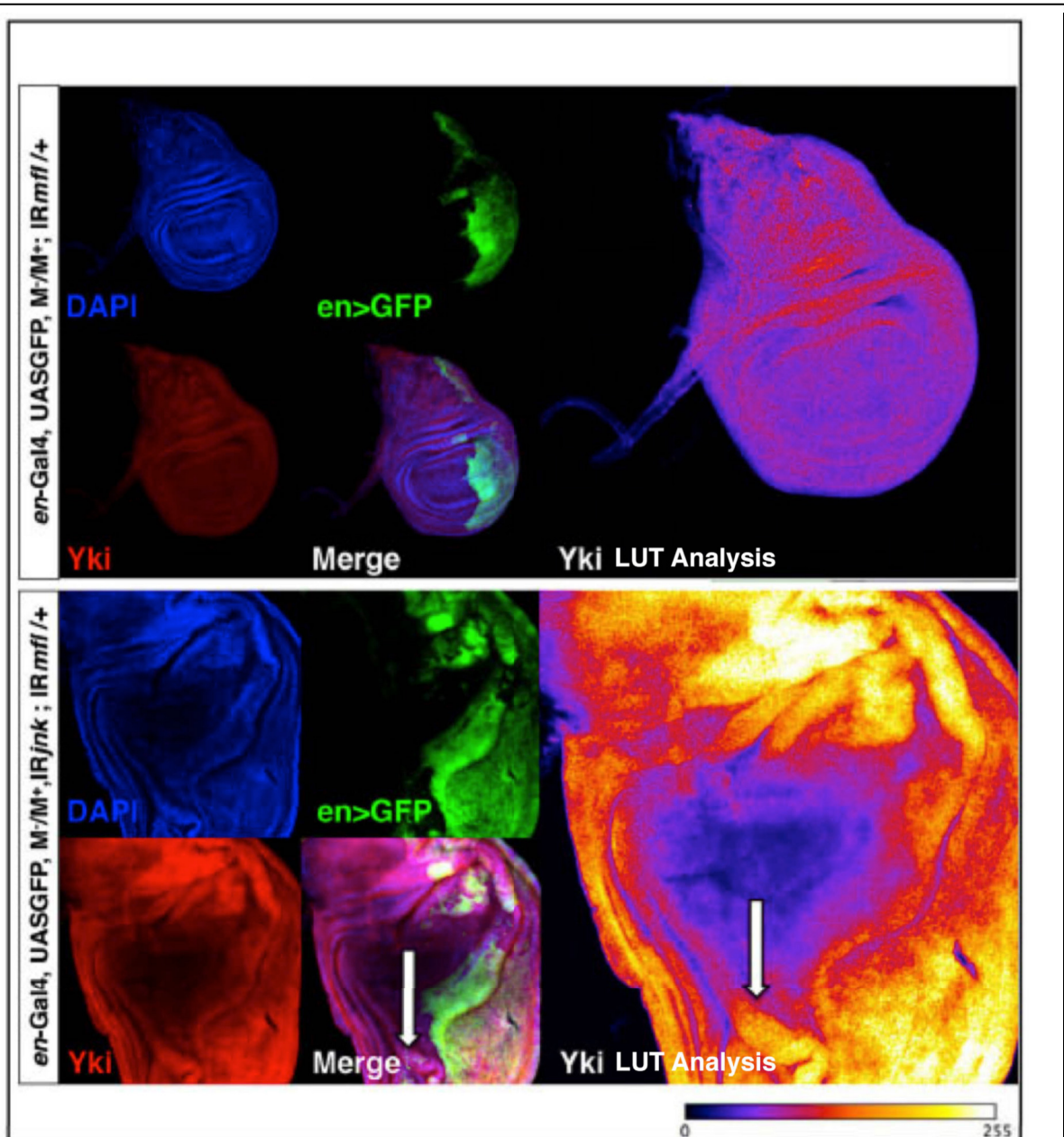


Fig. 35 *mfljnk* gene silencing induced by the *en*-Gal4 driver causes accumulation of the Yorkie protein in silenced posterior compartment. On the top: An *en*>GFP;*IRmfl* silenced disc that shows the uniform level of Yorkie protein in the anterior, unsilenced compartment (that acts as internal control) and in the posterior, silenced compartment. On the bottom: An *en*>GFP;*IRmfl*+*IRjnk* silenced disc that shows a strongly accumulation of Yorkie protein in the posterior compartment. Note that some GFP-labelled cells (white arrow) migrate in the anterior, unsilenced compartment, revealing an intrinsic neoplastic behaviour. DAPI is in blue; GFP in green; Yorkie in red. On the right: enlargement showing the LUT analysis that enhances the differences of Yorkie accumulation between *en*>*IRmfl* (up) and *en*>*IRmfl*+*jnk* (bottom) silenced discs.

DISCUSSION

The results reported in this thesis demonstrate that *in vivo* silencing of the *Drosophila* pseudouridine synthase component of H/ACA snoRNPs triggers apoptosis-induced proliferation, as typically observed during regenerative phenomena (Vicidomini et al., in press). The response of wing cells to *mfl* silencing was found to be context-dependent: some silenced cells located along the A/P boundary undergo apoptosis, while others, equally silenced, are stimulated to over-express the Wg morphogen and proliferate. Worth noting, the link between Wg over-expression and proliferation was further enhanced when execution of cell death was blocked by p35 expression, as occurs in compensative proliferation (Bergmann and Steller, 2010). In addition to reveal an unexpected and strong context-dependent effect of pseudouridine synthase depletion, the data reported here demonstrate that, although the deficiency of pseudouridine synthase was expected to limit the cell proliferative capacity, it can instead induce the production of mitogenic stimuli and promote over-proliferation.

The occurrence of proliferative events correlates with induction of the Wg and JAK-STAT mitogenic pathways, both of which were found ectopically activated in the depleted areas. The profile of Wg secretion and the ectopic activation of JAK-STAT within silenced areas suggests that dying cells can release, in response to pseudouridine synthase

depletion, long-range signals able to induce proliferation of neighboring cells. An unexpected and interesting result concerns the finding that depletion of *Drosophila* dyskerin can trigger EMT in a cell-nonautonomous manner. EMT plays important roles in many physiological developmental events, but when it is stress-induced can induce tumorigenesis and confer invasive properties (Micalizzi et al., 2010). The cell-fate change induced by pseudouridine synthase depletion in the peripodial membrane could thus help to understand the puzzling relationship that links pseudouridine synthases loss-of-function to cancer predisposition.

Worth nothing, the results I obtained also demonstrated that Cas3 and Wg induction that occur in the silenced cells are both JNK-dependent. In fact, in *mfl-jnk* double silenced discs no apoptotic spot was found, while Wg ectopic induction was evidently reduced. Despite this, *mfl-jnk* silenced disc overgrow dramatically, suggesting that JNK activity is required to counteract the hyper-proliferative potential of pseudouridine synthase depleted cells. This hyper-proliferative potential may be linked to the loss of apical-basal polarity observed in the silenced discs. Indeed, apical junctions play important roles not only in the organization of epithelia, but also in the regulation of tissue growth (Badouel and McNeill, 2009).

Noticeably, intense research over the past four years has led to the discovery and characterization of a novel signaling network, known as

the Salvador-Warts-Hippo (SWH) pathway. In *Drosophila*, this pathway is involved in the control of tissue growth by restricting the activity of the transcriptional coactivator Yorkie. The importance of SWH signaling is emphasized by its evolutionary conservation, and by the increasing evidence that its dysregulation occurs in human tumors (Harvey and Tapon, 2007). Although more detailed experiments are needed to clarify the molecular mechanisms underlying the dramatic overgrowth observed upon *mfl/jnk* silencing, Yorkie accumulation in *mfl/jnk* silenced discs may represent a first clue linking *mfl* functions to the Hippo pathway. It is worth noting that the oncogene *c-myc*, known to play essential roles in growth control, has been identified as a direct target of Yorkie (Froldi et al., 2010). The strong Myc up-regulation observed in *mfl* and *mfl/jnk* silenced discs supports and reinforces the interplay between *mfl* gene silencing and dysregulation of Hippo pathway.

Strikingly, the overall emerged picture clearly demonstrates that *mfl* can act as tumor suppressor gene, and that its loss-of-function can affect key developmental pathways, all of which are highly conserved throughout evolution. It is thus plausible to suppose that the response to pseudouridine synthase depletion could be widely evolutionarily preserved and the effects triggered in *Drosophila* can account for the tumour predisposition typical of X-linked dyskeratosis patients.

BIBLIOGRAPHY

- Adachi-Yamada T, Fujimura-Kamada K, Nishida Y and Matsumoto K. Distortion of proximodistal information causes JNK-dependent apoptosis in *Drosophila* wing. *Nature*. 1999; **400**: 166-9
- Alexander WS. Suppressors of cytokine signalling (SOCS) in the immune system. *Nat. Rev. Immunol.* 2002; **2**:410-416.
- Angrisani A, Vicidomini R, Turano M and Furia M. Human dyskerin: beyond telomeres. *Biol Chem.* 2014; **395**: 593-610
- Bach EA, Ekas LA, Ayala-Camargo A, Flaherty MS, Lee H, Perrimon N et al. GFP reporters detect the activation of the *Drosophila* JAK/STAT pathway in vivo. *Gene Expr Patterns.* 2007; **7**:323-31
- Badouel C and Mc Neill H. Apical junctions and growth control in *Drosophila*. *Biochim Biophys Acta.* 2009; **1788**:755-60
- Bate M and Martinez-Arias A. The Development of *Drosophila melanogaster* . Cold Spring Harbor Laboratory Press 1993; Volume II
- Bergmann A and Steller H. Apoptosis, stem cells and tissue regeneration. *Sci Signal.* 2010; **3**: re8
- Boncinelli E, Graziani F, Polito L, Malva C. and Ritossa F. rDNA magnification at the bobbed locus of the Y chromosome in *Drosophila melanogaster*. *Cell Differ.* 1972; **1**:133–142.
- Bosch M, Serras F, Martín-Blanco E and Bagaña J. JNK signaling pathway required for wound healing in regenerating *Drosophila* wing imaginal discs. *Dev Biol.* 2005; **280**: 73-86
- Brand AH and Perrimon N. Targeted gene expression as a means of altering cell fates and generating dominant phenotypes. *Development.* 1993; **118**: 401-15
- Brand AH and Perrimon N. Targeted gene expression as a means of altering cell fates and generating dominant phenotypes. *Development.* 1993; **118**: 401–15.
- Cadwell C, Yoon HJ, Zebajadian Y and Carbon J. The yeast nucleolar protein Cbf5p is involved in rRNA biosynthesis and interacts genetically with the RNA polymerase I transcription factor RRN3. *Mol. Cell Biol.*

1997. **17**: 6175-83.

Callus BA and Vaux DL. Caspase inhibitors: viral, cellular and chemical. *Cell Death Differ.* 2007; **14**: 73-8

Cohen SB, Graham ME, Lovrecz GO, Bache N, Robinson PJ and Reddel RR. Protein composition of catalytically active human telomerase from immortal cells *Science.* 2007; **315**:1850-1853

Dahmann C, Oates AC and Brand M. Boundary formation and maintenance in tissue development. *Nat Rev Genet.* 2011; **12**: 43-55

de Celis JF, Garcia-Bellido A and Bray SJ. Activation and function of Notch at the dorsal-ventral boundary of the wing imaginal disc. *Development.* 1996; **122**:359-69

Evans CJ, Olson JM, Ngo KT, Kim E, Lee NE, Kuoy E et al. G-TRACE: rapid Gal4-based cell lineage analysis in *Drosophila*. *Nat Methods.* 2009; **6**: 603-5

Fischer JA, Giniger E, Maniatis T and Ptashne M. GAL4 activates transcription in *Drosophila*. *Nature.* 1988; **332**:853–56.

Froldi F, Ziosi M, Garoia F, Pession A, Grzeschik NA, Bellosta P et al. The lethal giant larvae tumour suppressor mutation requires dMyc oncoprotein to promote clonal malignancy. *BMC Biol.* 2010 Apr; **8**:33

García- Bellido A, Ripoll P and Morata G. Developmental compartmentalisation of the wing disc of *Drosophila*. *Nature New Biol.* 1973; **245**: 251-53.

Garcia-Bellido A and Merriam J. R. Parameters of the wing imaginal disc development of *Drosophila melanogaster* . *Developmental Biology.*1971; **24**:61-87

Ghazi A, Anant S and Vijay Raghavan K. Apterous mediates development of direct flight muscles autonomously and indirect flight muscles through epidermal cues. *Development.* 2000; **127**: 5309-18

Giordano E, Peluso I, Senger S and Furia M. minifly, a *Drosophila* gene required for ribosome biogenesis. *J Cell Biol.* 1999; **144**: 1123–33

Gonsalves FC, DasGupta R. Function of the wingless signaling pathway in *Drosophila*. *Methods Mol Biol.* 2008; **469**:115-25

Grimm S and Pflugfelder GO. Control of the gene optomotor-blind in *Drosophila* wing development by decapentaplegic and wingless. *Science*. 1996; **271**: 1601-4

Grzeschik NA, Parsons LM, Allott ML, Harvey KF and Richardson HE. Lgl, aPKC, and Crumbs regulate the Salvador/Warts/Hippo pathway through two distinct mechanisms. *Curr Biol*. 2010; **20**:573-81

Harvey K and Tapon N. The Salvador-Warts-Hippo pathway - an emerging tumour-suppressor network. *Nat Rev Cancer*. 2007; **7**:182-91

Hay BA, Wolff T and Rubin GM. Expression of baculovirus P35 prevents cell death in *Drosophila*. *Development*. 1994; **120**: 2121-9

Heinrich PC, Behrmann I, Haan S, Hermanns H M, Muller-Newen G and Schaper F. Principles of interleukin (IL)- 6-type cytokine signalling and its regulation. *Biochemical J*. 2003; **374**:1-20.

Heiss NS, knight SW, Vulliamy TJ, Klauck SM, Wiemann S, Mason PJ et al. X-linked dyskeratosis congenita is caused by mutation in a highly conserved gene with putative nucleolar functions. *Nat Genet*. 1998; **19**: 32-8

Hombria, JC and Brown S. The fertile field of *Drosophila* Jak/STAT signalling. *Curr. Biol*. 2001; **12**:R569-75.

Irvine KD and Wieschaus E. fringe, a Boundary-specific signaling molecule, mediates interactions between dorsal and ventral cells during *Drosophila* wing development. *Cell*. 1994; **79**:595-606

Jiang W, Middleton K, Yoon HJ, Fouquet C, and Carbon J. An essential yeast protein, CBF5p, binds in vitro to centromeres and microtubules. *Mol. Cell. Biol*. 1993; **13**: 4884-93.

Kauffman T, Tran J and DiNardo S. Mutations in Nop60B, the *Drosophila* homolog of human dyskeratosis congenita 1, affect the maintenance of the germ-line stem cell lineage during spermatogenesis. *Dev. Biol*. 2003; **253**:189-199

Kay MA and Jacobs-Lorena M. Selective translational regulation of ribosomal protein gene expression during early development of *Drosophila melanogaster*. 1985; *Mol. Cell Biol*. **5**:3583–92.

Khan MA, Chen HC, Zhang D and Fu J. Twist: a molecular target in cancer therapeutics. *Tumour Biol.* 2013; **34**: 2497-506

Kim J, Irvine KD and Carroll SB. Cell recognition, signal induction, and symmetrical gene activation at the dorsal-ventral boundary of the developing *Drosophila* wing. *Cell.* 1995; **82**:795-802

Kiss T, Fayet E, Jády BE, Richard P and Weber M. Biogenesis and intranuclear trafficking of human box C/D and H/ACA RNPs. *Cold Spring Harb Symp Quant Biol.* 2006; **71**:407-17

Lafontaine DL and Tollervey D. Birth of the snoRNPs: the evolution of the modification-guide snoRNAs. *Trends Biochem.* 1998; **23**:383-88.

Martín FA, Pérez-Garijo A and Morata G. Apoptosis in *Drosophila*: compensatory proliferation and undead cells. *Int J Dev Biol.* 2009; **53**: 1341-7

McCann KL and Baserga SJ. Mysterious Ribosomopathies. *Science.* 2013; **341**: 849-5

Meier UT and Blobel G. NAP57, a mammalian nucleolar protein with a putative homolog in yeast and bacteria. *J. Cell Biol.* 1994. **127**:1505-14.

Micalizzi DS, Farabaugh SM and Ford HL. Epithelial-mesenchymal transition in cancer: parallels between normal development and tumor progression. *J Mammary Gland Biol Neoplasia.* 2010;**15**:117-34

Milán M and Cohen SM. Temporal regulation of apterous activity during development of the *Drosophila* wing. *Development.* 2000; **127**:3069-78

Oh H, Irvine KD. In vivo regulation of Yorkie phosphorylation and localization. *Development.* 2008; **135**:1081-88.

Oh SW, Kingsley T, Shin HH, Zheng Z, Chen HW, Chen X et al. A P-element insertion screen identified mutations in 455 novel essential genes in *Drosophila*. *Genetics.* 2003; **163**:195-201

Pallavi SK and Shashidhara LS. Egfr/Ras pathway mediates interactions between peripodial and disc proper cells in *Drosophila* wing discs. *Development.* 2003; **130**: 4931-41

Pallavi SK and Shashidhara LS. Signaling interactions between squamous and columnar epithelia of the *Drosophila* wing disc. *J Cell Sci.* 2005; **118**: 3363-70

Pardue ML, Rashkova S, Casacuberta E, DeBaryshe PG, George JA and Traverse KL. Two retrotransposons maintain telomeres in *Drosophila*. *Chromosome Res.* 2005; **13**: 443-53

Pardue ML, Rashkova S, Casacuberta E, DeBaryshe PG, George JA and Traverse KL. Two retrotransposons maintain telomeres in *Drosophila*. *Chromosome Res.* 2005; **13**: 443-53

Pérez-Garijo A, Martín FA and Morata G. Caspase inhibition during apoptosis causes abnormal signalling and developmental aberrations in *Drosophila*. *Development.* 2004; **131**: 5591-8

Phillips B, Billin AN, Cadwell C, Buchholz R, Erickson C, Merriam JR et al. The Nop60B gene of *Drosophila* encodes an essential nucleolar protein that functions in yeast. *Mol. Gen. Genet.* 1998; **260**:20-29

Potter CJ and Xu T. Mechanisms of size control. *Curr Opin Genet Dev.* 2001; **11**: 279-86

Procunier JD and Tartof KD. Genetic analysis of the 5S RNA genes in *Drosophila melanogaster*. *Genetics* 1975; **81**:515–523.

Rawlings JS, Rosler KM and Harrison DA. The JAK/STAT signaling pathway. *J Cell Sci.* 2004; **117**:1281-3.

Repiso A, Bergantiños C, Corominas M and Serras F. Tissue repair and regeneration in *Drosophila* imaginal discs. *Dev Growth Differ.* 2011; **53**: 177-85

Riccardo S, Tortoriello G, Giordano E, Turano M and Furia M. The coding/non-coding overlapping architecture of the gene encoding the *Drosophila* pseudouridine synthase. *BMC Mol Biol.* 2007; **8**: 15

Richard P, Darzacq X, Bertrand E, Jády BE, Verheggen C and Kiss T. A common sequence motif determines the Cajal body-specific localization of box H/ACA scaRNAs. *Embo J.* 2003; **22**:4283-93.

Rodrigues AB, Zoranovic T, Ayala-Camargo A, Grewal S, Reyes-Robles T, Krasny M et al. Activated STAT regulates growth and induces

competitive interactions independently of Myc, Yorkie, Wingless and ribosome biogenesis. *Development*. 2012; **139**: 4051-61.

Ryoo HD, Gorenc T and Steller H. Apoptotic Cells Can Induce Compensatory Cell Proliferation through the JNK and the Wingless Signaling Pathways. *Dev Cell*. 2004; **7**: 491-501

Schwartz S, Bernstein DA, Mumbach MR, Jovanovic M, Herbst RH, León-Ricardo BX et al. Transcriptome-wide Mapping Reveals Widespread Dynamic-Regulated Pseudouridylation of ncRNA and mRNA. *Cell*. 2014; **159**:148-62

Shuai K and Liu B. Regulation of JAK-STAT signalling in the immune system. *Nat Rev Immunol*. 2003; **3**:900-11.

Smith-Bolton RK, Worley MI, Kanda H and Hariharan IK. Regenerative growth in *Drosophila* imaginal discs is regulated by Wingless and Myc. *Dev Cell*. 2009; **16**: 797-809.

Sudarsan V, Anant S, Guptan P, VijayRaghavan K and Skaer H. Myoblast diversification and ectodermal signaling in *Drosophila*. *Dev Cell*. 2001; **1**: 829-39

Tabata T and Kornberg TB. Hedgehog is a signaling protein with a key role in patterning *Drosophila* imaginal discs. *Cell*. 1994; **76**:89-102

Tortoriello G, de Celis JF and Furia M. Linking pseudouridine synthases to growth, development and cell competition. *FEBS J*. 2010; **277**: 3249-63

van der Velden JL, Guala AS, Leggett SE, Sluimer J, Badura EC and Janssen-Heininger YM. Induction of a mesenchymal expression program in lung epithelial cells by wingless protein (Wnt)/ β -catenin requires the presence of c-Jun N-terminal kinase-1 (JNK1). *Am J Respir Cell Mol Biol*. 2012; **47**:306-14

Vicidomini R, Di Giovanni A, Petrizzo A, Iannucci FL, Giovanna Benvenuto G, Nagel AC et al. Loss of *Drosophila* pseudouridine synthase triggers apoptosis-induced proliferation and promotes cell-nonautonomous EMT. *Cell Death Dis*. 2015; **6**:e1705

Williams JA, Paddock SW and Carroll SB. Pattern formation in a secondary field: a hierarchy of regulatory genes subdivides the

developing *Drosophila* wing disc into discrete subregions. *Development*. 1993; **117**:571-84

Wu M, Pastor-Pareja JC and Xu T. Interaction between Ras(V12) and scribbled clones induces tumour growth and invasion. *Nature*. 2010; **463**: 545-8

Xianjue Ma. Context-dependent interplay between Hippo and JNK pathway in *Drosophila*. *AIMS Genetics*. 2014; **1**: 20-33

Zebarjadian Y, King T, Fournier, MJ, Clarke L and Carbon J. Point mutations in yeast CBF5 can abolish in vivo pseudouridylation of rRNA. *Mol. Cell Biol*. 1999. **19**:7461-7472

Zecca M, Basler K and Struhl G. Sequential organizing activities of engrailed, hedgehog and decapentaplegic in the *Drosophila* wing. *Development*. 1995; **121**:2265-78

Ziosi M, Baena-López LA, Grifoni D, Frolidi F, Pession A, Flavio Garoia et al. dMyc functions downstream of Yorkie to promote the supercompetitive behavior of hippo pathway mutant cells. *PLoS Genet*. 2010; **6**: e1001140

ORIGINAL PAPER

Loss of *Drosophila* pseudouridine synthase triggers apoptosis-induced proliferation and promotes cell-nonautonomous EMT

R Vicidomini^{1,4}, A Di Giovanni^{1,4}, A Petrizzo¹, LF Iannucci¹, G Benvenuto², AC Nagel³, A Preiss³ and M Furia^{1,4}*

Many developing tissues display regenerative capability that allows them to compensate cell loss and preserve tissue homeostasis. Because of their remarkable regenerative capability, *Drosophila* wing discs are extensively used for the study of regenerative phenomena. We thus used the developing wing to investigate the role played in tissue homeostasis by the evolutionarily conserved eukaryotic H/ACA small nucleolar ribonucleoprotein pseudouridine synthase. Here we show that localized depletion of this enzyme can act as an endogenous stimulus capable of triggering apoptosis-induced proliferation, and that context-dependent effects are elicited in different sub-populations of the silenced cells. In fact, some cells undergo apoptosis, whereas those surrounding the apoptotic foci, although identically depleted, overproliferate. This overproliferation correlates with ectopic induction of the Wg and JAK-STAT (Janus kinase-signal transducer and activator of transcription) mitogenic pathways. Expression of a p35 transgene, which blocks the complete execution of the death program and generates the so-called 'undead cells', amplifies the proliferative response. Pseudouridine synthase depletion also causes loss of apicobasal polarity, disruption of adherens cell junctions and ectopic induction of JNK (c-Jun N-terminal kinase) and Mmp1 (matrix metalloproteinase-1) activity, leading to a significant epithelial reorganization. Unexpectedly, cell-nonautonomous effects, such as epithelial mesenchymal transition in the contiguous unsilenced squamous epithelium, are also promoted. Collectively, these data point out that cell-cell communication and long-range signaling can take a relevant role in the response to pseudouridine synthase decline. Considering that all the affected pathways are highly conserved throughout evolution, it is plausible that the response to pseudouridine synthase depletion has been widely preserved. On this account, our results can add new light on the still unexplained tumor predisposition that characterizes X-linked dyskeratosis, the human disease caused by reduced pseudouridine synthase activity. *Cell Death and Disease* (2015) 6, e1705; doi:10.1038/cddis.2015.68; published online 26 March 2015

The control of cell growth and proliferation is a fundamental aspect of tissue homeostasis. To maintain homeostatic conditions, different subsets of cells are continuously required to respond coordinately to external and intrinsic stimuli, to keep the appropriate balance between death, proliferation and differentiation.

The overall capacity of the protein synthetic machinery has an obvious rate-limiting regulatory role in cell growth and division, and production of ribosomes is directly coupled with these processes. Moreover, in a growing number of cases mutations in ribosome components proved to regulate not only the overall translational capacity but also to affect specific developmental or differentiative events, revealing more specialized functions in translational regulation.^{1,2} Mutations in factors that allow synthesis, processing and modification of rRNA, assembly and nuclear export of preribosomal particles or ribosome translational efficiency also cause tissue- or cell-specific phenotypes and produce a variety of diseases,

collectively indicated as ribosomopathies.³ Eukaryotic rRNA pseudouridine synthases are among these factors. These ubiquitous nucleolar proteins are conserved from Archaea to man and associate with other conserved core proteins and H/ACA small nucleolar RNAs (snoRNAs) to compose the functional H/ACA snoRNP complexes, whose activity is known to be involved in rRNA processing and site-specific pseudouridylation of rRNA and snRNAs,⁴ as well as of mRNAs and additional classes of noncoding RNAs.⁵

Well-established, rRNA undergoes extensive modifications that influence its processing, folding and functionality. For example, reduction of rRNA pseudouridylation affects ribosome translation fidelity⁶ and modulates the efficiency of internal ribosome entry site-dependent translation,^{7–10} outlining a crucial role in the regulation of translation specificity. The high biological relevance of rRNA pseudouridine synthases is further testified by the fact that reduced levels or hypomorphic mutations in the human coding gene

¹Dipartimento di Biologia, Università di Napoli 'Federico II', via Cinthia, Naples 80126, Italy; ²Stazione Zoologica Anton Dohrn, Villa Comunale, Napoli 80121, Italy and

³Institut für Genetik, Universität Hohenheim, Garbenstrasse 30, Stuttgart 70599, Germany

*Corresponding author: M Furia, Dipartimento di Biologia, Università di Napoli 'Federico II', via Cinthia, Naples 80126, Italy. Tel. +39 081 679072; Fax +39 081 679233; E-mail: mfuria@unina.it

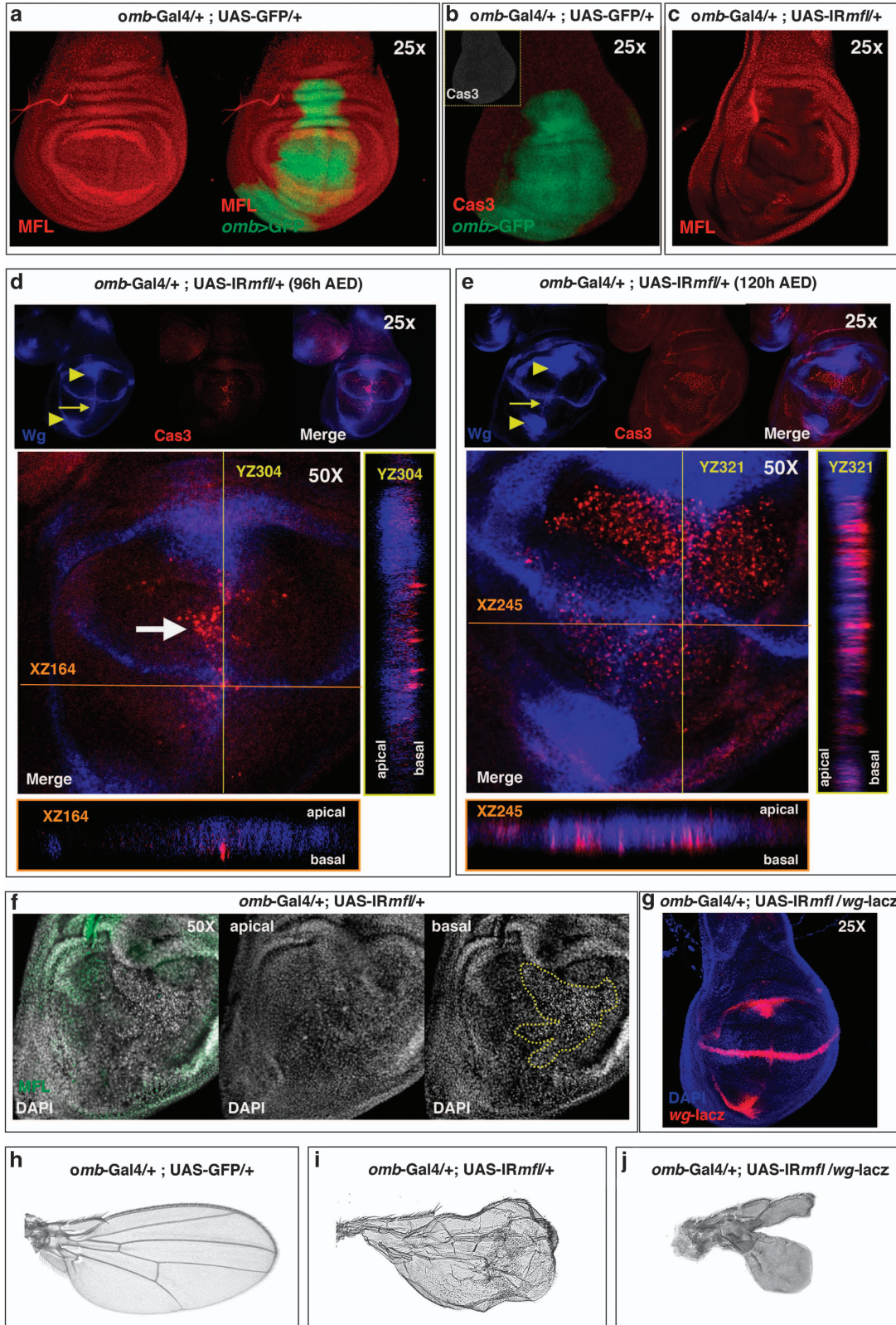
⁴These authors contributed equally to this work.

Abbreviations: H/ACA snoRNP, H/ACA box small nucleolar ribonucleoprotein; snoRNA, small nucleolar RNA; X-DC, X-linked dyskeratosis congenita; Omb, optomotor blind; En, engrailed; Dpp, decapentaplegic; Wg, Wingless; Arm, Armadillo/ β -catenin; Cas3, caspase-3; pH3, phosphohistone H3; EdU, 5-ethynyl-2'-deoxyuridine; JAK-STAT, Janus kinase-Signal Transducer and Activator of Transcription; JNK, c-Jun N-terminal kinase; Puc, puckered; Mmp1, matrix metalloproteinase-1; Ubx, ultrabithorax; EMT, epithelial–mesenchymal transition

Received 20.10.14; revised 11.2.15; accepted 12.2.15; Edited by N Tavernarakis

cause the human X-linked dyskeratosis (X-DC) multisystemic disorder.¹¹ Beside H/ACA snoRNPs, the human pseudo uridine synthase, called dyskerin, is also a component of the

active telomerase complex; this dual role makes it difficult to distinguish between the effects related to loss of snoRNP functions and those caused by telomere attrition. As a



consequence, whether X-DC must be regarded primarily as a ribosomopathy or as a telomere disease is still being debated. Considering the availability of sophisticated genetic tools, *Drosophila melanogaster* can represent an advantageous model organism to dissect the multiple roles played by pseudouridine synthases. *Drosophila dyskerin* is 66% identical and 79% similar to human dyskerin, and is equally involved in rRNA processing and pseudouridylation;¹² however, it has no established role in the maintenance of telomere integrity, as fly telomeres are maintained by insertion of specific retrotransposons at chromosome ends.¹³ This divergent procedure of telomere maintenance makes *Drosophila* an ideal organism to delineate the range of biological effects specifically triggered by loss of H/ACA snoRNP activity, especially focusing at the interface among cell growth, proliferation and differentiation. Because of their striking capacity of undergoing regenerative growth,¹⁴ the imaginal wing disc provides an ideal system in which to investigate how growth, proliferation and differentiation are coordinated in the context of a developing organ. In fact, cell proliferation is essentially uniform across the whole disc¹⁵ and is controlled by the same morphogens that govern wing patterning. Gradients of two morphogens, decapentaplegic (Dpp), a member of the transforming growth factor- β family, and wingless (Wg), a member of the Wnt family, establish a tight link between cell proliferation and developmental programs. During disc development, a gradient of Dpp determines the anterior/posterior (A/P) axis, whereas a gradient of Wg subsequently defines the dorsal/ventral (D/V) axis, giving rise to the A/P and D/V compartments.¹⁶ We previously showed that localized depletion of *Drosophila dyskerin* in the wing discs not only caused cell death but also additionally triggered a variety of developmental defects.¹⁷ Here, we further investigated the role of *Drosophila dyskerin* in wing disc homeostasis and demonstrate that its loss can induce regenerative growth and extensive tissue remodeling, as well as stimulate cell-nonautonomous events of cell fate changes that result in epithelial–mesenchymal transition (EMT).

Results

Effect of *mfl* silencing on wing growth and patterning.

Drosophila dyskerin, called Mfl, is encoded by the *Nop60B/minify* (*mfl*) gene.^{12,18,19} To define in more detail how Mfl loss can affect growth and development, we silenced Mfl activity in

the area of the wing disc that flanks the A/P border and includes the main organization center of patterning. Gene silencing made use of the Gal4/UAS system²⁰ and was directed by the *omb* (optomotor blind)-Gal4 driver line, which is expressed in the wing central domain from between presumptive veins 1 and 2 in the A compartment to presumptive veins 4 and 5 in the P compartment.²¹ Two different UAS-*IRmfl* target lines were used (v46282 and no. 36595); both lines had no predicted off-targets and gave identical results. The v46282 line already proved to knock down efficiently all *mfl* mRNAs.¹⁷ The effects of *mfl* silencing were then carefully followed within the *omb* domain of silenced discs (Figures 1a–c). Discs were collected at two developmental times during the third larval instar, that is, at 96 and 120 h after egg deposition (AED), and costained with anti-caspase-3 (Cas3) to follow cell death and with anti-Wingless (Wg) to monitor wing patterning and growth. Control discs at 96 h AED did not show any significant Cas3 staining (Figure 1b), whereas clusters of Cas3-positive cells arised along the A/P boundary in the silenced discs (Figure 1d), confirming that cell death is a major consequence of *mfl* downregulation.¹⁷ However, in the same discs Wg was strongly upregulated at the center of the inner ring, in both D and V compartments, and ectopically expressed along the A/P boundary (Figure 1d). At the later developmental time (120 h AED), the number of Cas3 spots further increased, massively spreading from A/P border throughout the wing pouch. In parallel, Wg accumulation at the inner ring became more conspicuous (Figure 1e). As shown by confocal Z-stack analysis, Wg staining at the D/V border flanked the Cas3 apoptotic signals, most of which were located more basally (Figures 1d and e). The presence of dying cells was further confirmed by a large number of pyknotic nuclei detected basally in the pseudostratified epithelium (Figure 1f). To mark precisely the cells that were actively producing the Wg proliferative signal, we followed the expression of the *wg-lacZ* transcriptional reporter. Activity of the reporter increased in the silenced background, and stained the same areas previously marked by Wg accumulation (Figure 1g). This observation confirmed that the silenced cells surrounding the apoptotic foci were actively producing high level of Wg. Ectopic secretion of Wg at the edge of the dying tissue has been reported by several authors,^{22–24} and in some cases has been described to be essential for regenerative growth.²⁴ Consistent with this view, we noticed that most of the silenced larvae carrying the *wg-lacZ* reporter died at the pupal stage,

Figure 1 Mfl depletion induces both Cas3 and Wg activation in the wing discs. (a–g) Confocal analysis of control and *omb > IRmfl* silenced wing discs (v46282 line). (a) Ubiquitous expression of Mfl protein (in red) in an *omb > GFP* control disc, in which GFP (green) marks the *omb* expression domain. (b) Cas3-positive spots are not present in the *omb > GFP* controls. GFP in green and Cas3 in red (gray in the inset). (c) An *omb > IRmfl* silenced disc showing efficient and localized Mfl depletion within the *omb* domain (Mfl in red). (d and e) *omb > IRmfl* discs collected at 96 h (d) and 120 h AED (e). At 96 h AED, clusters of Cas3-positive spots mark the A/P boundary (white arrow), flanked by Wg ectopic induction (see yellow arrow at the top); Wg accumulates also at the middle of the inner ring (see yellow arrowheads on the top). At 120 h AED, the number of Cas3-positive spots increased, concomitantly with Wg ectopic induction along the A/P border (see yellow arrow at the top) and Wg upregulation at the inner ring (see yellow arrowheads at the top). Z-stack confocal analysis showed that most Cas3 signals lie basally and do not overlap Wg staining (see XZ and YZ projections). Cas3 in red and Wg in blue. (f) DAPI (4',6-diamidino-2-phenylindole) staining of an *omb > IRmfl* disc shows basal clusters of pyknotic nuclei within the silenced domain (area encircled by the yellow line); DAPI is in gray and Mfl in green. (g) Expression of *wg-lacZ* reporter in *omb > IRmfl* silenced discs confirms that *wg* expression is transcriptionally upregulated compared with controls (see Figure 4d) and marks the same areas where Wg protein accumulates (DAPI in blue and β -gal in red). (h–j) Comparison of an *omb > GFP* adult wing, taken as control (h), with an *omb > IRmfl* silenced wing, whose blade appears crumpled and highly disorganized (i), and an *omb > IRmfl;wg-lacZ* wing (j), in which Wg haploinsufficiency strongly enhances the growth defects (see also Supplementary Figure 1)

whereas rare adult escapers all display underdeveloped/deformed wings that miss the central *omb* domain (Figures 1h–j and Supplementary Figure 1). As the *wg-lacZ* allele is mutant owing to the *lacZ* insertion,²⁵ silenced larvae carrying this allele have only one active copy of the *wg* gene. With respect to *mfl* silencing alone, which led to disturbed wing morphology with detachment of the two epithelial layers and blistering, the heterozygous *wg* background markedly worsened the silenced phenotype (Figures 1h–j and Supplementary Figure 1). This enhancement is consistent with a dose effect, and suggests that the level of *wg* activation in these silenced flies is inadequate to counteract the developmental defects caused by Mfl depletion.

Finally, we analyzed by phalloidin staining the structure of the silenced disc. As shown in Figure 2, the tissue appeared wrinkled, folded and fractured along the A/P border, where clusters of Cas3-positive cells were observed. These local fractures were strongly enhanced in the presence of an UAS transgene that expresses the baculovirus p35 protein, known to inhibit the function of Cas3 but not its activation.^{26,27} UAS-p35 expression has no effect on the epithelium structure in a wild-type background (Figure 2a), whereas in the silenced discs it generates along the A/P margin patches of large ‘undead cells’ that, as typical,²⁸ secrete high levels of Wg (Figures 2b and c). The alignment of undead cells along the A/P boundary indicated that these margin cells exhibit a particular sensitivity to Mfl depletion, and first undergo apoptosis. This susceptibility may be an indirect consequence of abnormal formation of the A/P border, possibly due to defects in cell adhesion and/or cell communication.

***mfl* Silencing elicits context-dependent effects and apoptosis-induced proliferation.** A proliferative role has generally been attributed to Wg in regenerative phenomena.²⁹ Indeed, we noticed that at both 96 and 120 h AED the silenced discs exhibited morphological alterations in shape, including an evident bending of the A/P boundary that was indicative of localized overgrowth (see Figure 1 and Supplementary Video 1).

In previous experiments, we triggered *mfl* silencing by the *en-Gal4* (engrailed-Gal4) driver, whose expression specifically marks the P compartment. Despite the induction of apoptosis, no reduction in the number of phosphohistone H3 (pH3)-positive mitotic cells was noted in the silenced domain.¹⁷ To further check this aspect, we stained the *en-Gal4* silenced discs by EdU (5-ethynyl-2'-deoxyuridine) incorporation, to mark with higher sensitivity DNA synthesis and label S-phase cells. This approach highlighted a significant enhancement of the proliferative activity in the silenced P compartment (Figure 3a). According to the previous data,¹⁷ the A/P boundary was discontinuous and deformed and, upon p35 expression, undead cells that overexpress Wg were detected close to this irregular border (Figure 3b). Note that these cells are located basally, whereas Wg upregulation at the A/P margin is detected only apically.

Enhanced proliferative activity was similarly observed in the *omb* silenced domain. In fact, despite the massive apoptosis (see Figure 1), the overall proliferation rate was not reduced. pH3-positive dividing cells were visualized inside and around Wg-secreting regions, and their number markedly augmented upon p35 expression (Supplementary Figure 2). Consistent with this observation, EdU labeling of S-phase cells was markedly enhanced with respect to controls, and even further by p35 expression (Figures 4a and c; note that in the silenced discs the *omb* domain is expanded and bent). Reliably, upon UAS-p35 expression the rare adult escapers develop wings typified by epithelial refolding, as it occurs upon excessive and hyperplastic overgrowth (Supplementary Figure 3).

Proliferation of the silenced cells also correlated with upregulation and ectopic induction of JAK-STAT, another proliferative pathway associated with apoptosis-induced proliferation and regeneration.^{30,31} As shown in Figure 5, this pathway is upregulated at the center of the inner ring, and ectopically activated at specific regions of the silenced domain. In the V compartment, its induction surrounded the areas showing Wg accumulation, whereas in the dorsal part it encircled and in part overlapped Wg ectopic expression. Altogether, these data indicate that Mfl depletion induces a regenerative response,

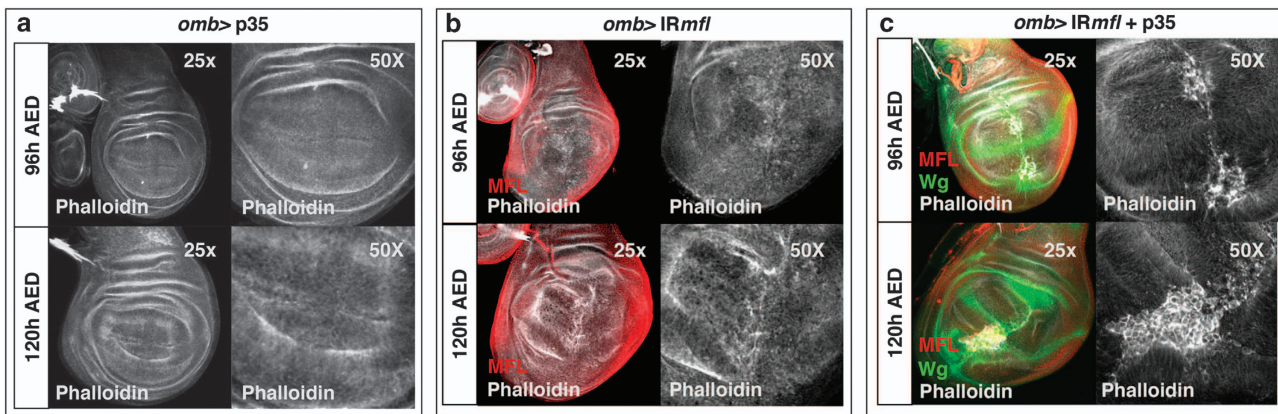


Figure 2 Epithelial remodeling and formation of p35-induced undead cells in the *omb* silenced domain. Confocal analysis of wing discs at 96 and 120 h AED upon phalloidin staining. (a) An *omb* > p35 control disc. Phalloidin is in gray. (b) An *omb* > *IRmfl* silenced disc (no. 36595 line) exhibiting a strong tissue disorganization. Phalloidin is in gray and Mfl in red. (c) Expression of p35 in the silenced discs causes formation of big patches of large undead cells that secrete high level of Wg (in green) and cluster along the A/P border

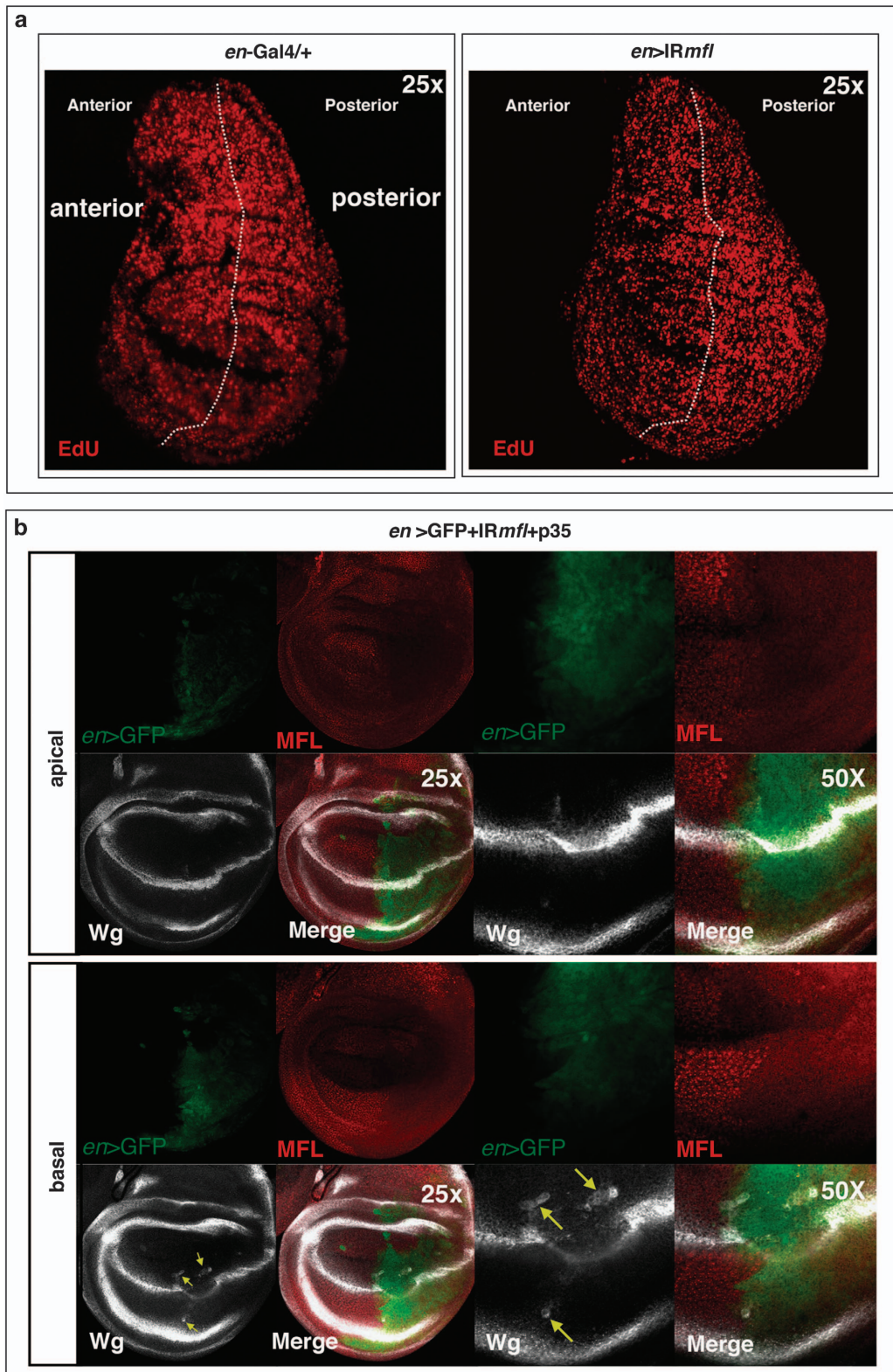


Figure 3 Enhanced proliferation and formation of p35-induced undead cells in the silenced P compartment. Confocal analysis of wing discs at 96 h AED. (a) On the left, an *en/+* control disc, in which EdU labeling marks S-phase cells; on the right, an *en > IRmfl* silenced discs (v46282 line) in which EdU labeling stains more intensely the P silenced compartment, indicating that the silenced cells overproliferate. The A compartment serves as internal control. (b) Expression of p35 causes formation of undead cells that secrete high level of Wg (in gray) and are dispersed along the irregular A/P border. Note that Wg accumulation at the D/V boundary is detected apically, whereas deformation of the A/P margin is more evident basally, in keeping with previous data¹⁷

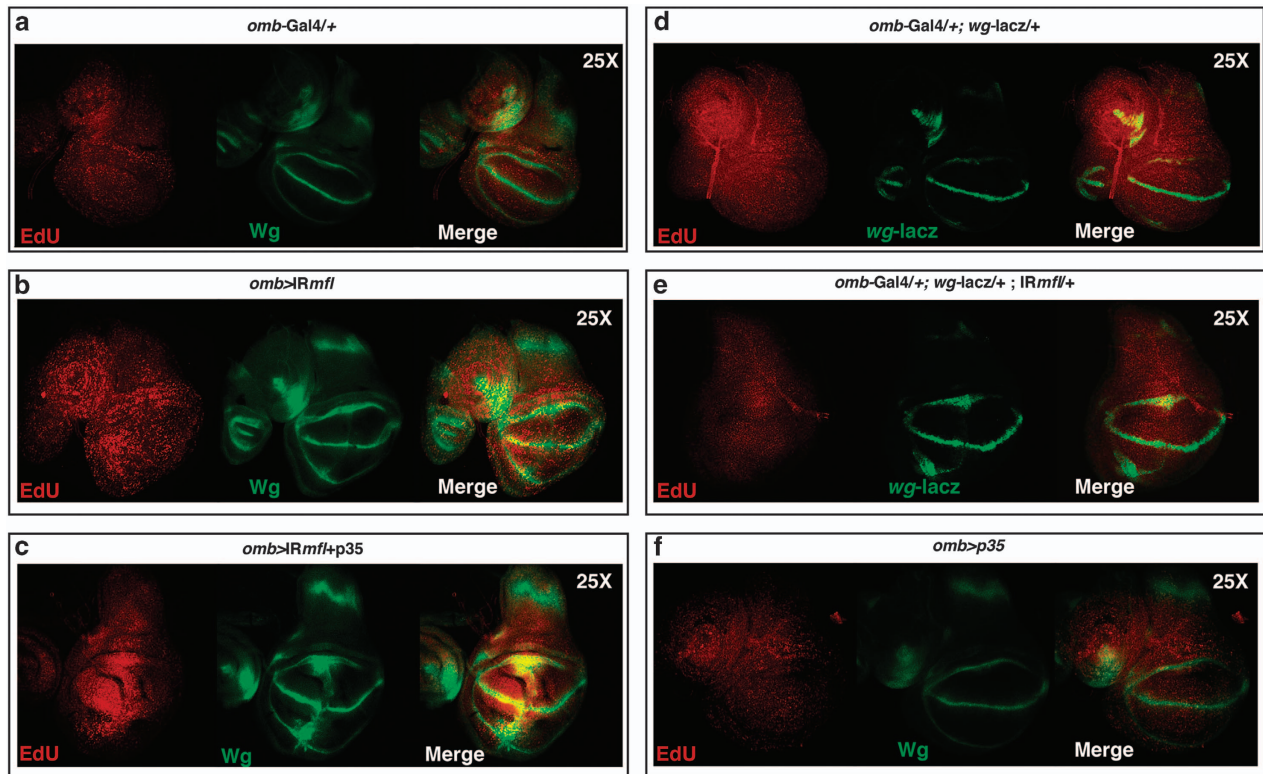


Figure 4 *mfl* Silencing causes apoptosis-induced proliferation. Confocal analysis of wing discs at 96 h AED. (a) An *omb*^{-/-} control disc labeled by EdU incorporation to mark specifically DNA synthesis and label S-phase cells. (b) An *omb* > *IRmfl* silenced disc (no. 36595 line) showing a significant increase of proliferating cells. (c) P35 expression further boosts proliferation and elicits a more pronounced hyperplastic overgrowth. EdU is in red and Wg in green. (d and e) EdU labeling of *omb*^{-/-}, *wg-lacZ* (d) and *omb* > *IRmfl*, *wg-lacZ* discs (e), both carrying a single active copy of the *wg* gene (β -gal is in green). Note that in the *wg-lacZ* background the proliferative activity of the silenced domain is significantly reduced compared with that of *omb* > *IRmfl* discs (b). (f) Expression of p35 in unsilenced discs has no effect on the proliferation rate (Wg in green)

which, as observed in other cases,³² in the presence of p35 results in a pronounced hyperplastic phenotype.

Intriguingly, the emerged scenario pointed out that Mfl depletion elicits opposite outcomes in diverse wing territories. Although some cells (those at the A/P boundary first) activate Cas3 and undergo apoptosis, other silenced cells undergo robust proliferation.

The silenced discs show extensive epithelial remodeling and JNK and Mmp1 ectopic activation. As shown above, the silenced discs appeared crumpled and folded (Figure 1 and Supplementary Video 1), indicating the occurrence of extensive tissue reorganization and remodeling. As regenerative processes require widespread tissue restoration, we followed in detail the expression of two typical markers of epithelial restructuring: the apicobasal distribution of the *Drosophila* β -catenin/Armadillo (Arm) and the levels of polymerized F-actin. Within the wing discs, Arm and F-actin are ubiquitously expressed, but they are both strongly stabilized in two stripes surrounding the D/V boundary.^{33,34}

The Arm protein is a known effector of Wg signaling and has a dual role: as a component of the cell adherens junctions on the one hand and as a nuclear transcription factor transducing Wg signal on the other hand.³⁵ Within the wing disc, Arm concentrates apically, in which it binds transmembrane cadherins to build up the adherens junctions that connect actin filaments across polarized epithelial cells³⁶

(see Figure 6a). Interestingly, upon *mfl* silencing directed by *en*-Gal4, Arm accumulation was strongly reduced in the whole silenced area, and most evidently at the D/V boundary. Moreover, confocal Z-stack analysis revealed a reduction of apical Arm accumulation, so that cells had lost their polarity (Figure 6b). Identical results were obtained when silencing was directed by the *omb*-Gal4 driver (Supplementary Figure 4). Reduction of apical Arm is consistent with the observation that Wg overexpression in the wing discs induces a transient reduction of membrane-associated Arm, this way allowing an immediate decline of cell adhesion that facilitates structural reorganization of the cytoskeleton.³⁷ Similarly to Arm, F-actin accumulation was also heavily reduced, and accumulation at the D/V boundary disrupted (Figures 6c and d and Supplementary Videos 2 and 3). Hence, the concomitant induction of cell death and proliferation is accompanied by extensive cytoskeletal remodeling. The involvement of pseudouridine synthase activity in cytoskeletal dynamics and cell adhesion is worth noting, and it has previously been described also in human cells.³⁸

Given that the JNK pathway is known to be involved in cytoskeletal remodeling during both apoptotic^{39,40} and regenerative processes,^{41–45} we checked whether it was specifically induced upon Mfl depletion. We then followed the expression of *puckered* (*puc*), a JNK downstream effector,⁴⁶ taking advantage of the widely used *puc-lacZ* reporter. As described,⁴⁷ *puc-lacZ* expression in wild-type discs is

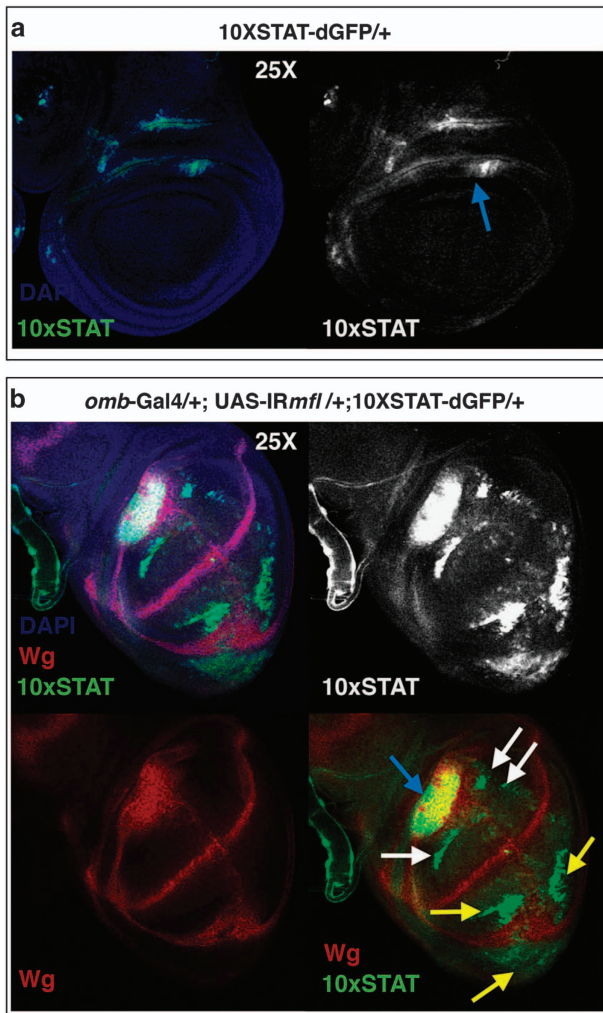


Figure 5 Mfl depletion triggers ectopic activation of JAK-STAT signaling. Confocal analysis of wing discs collected at 120 h AED carrying the 10XSTAT-dGFP reporter (the use of destabilized dGFP⁶⁹ allows to visualize real-time activation of the reporter). (a) No activity of the reporter was detectable in the wing pouch of control discs, whereas JAK-STAT expression is detected in the presumptive wing hinge (blue arrow). (b) In *omb > IRmfl* silenced discs (v46282 line in the picture), the reporter was overexpressed in the wing hinge (blue arrow) and ectopically induced in the dorsal area of the *omb* domain (white arrows), where it, in part, surrounded and overlapped the domain of Wg induction. In the ventral region (yellow arrows), JAK-STAT ectopic induction encircled Wg accumulation. DAPI (4',6-diamidino-2-phenylindole) is in blue, Wg in red and GFP in green

restricted to the stalk region, where wing discs are connected to the larval epidermis (Figure 7a). In contrast, expression of this reporter was found strongly induced within the silenced discs (Figure 7b). Along the A/P border, JNK ectopic induction matched the local clusters of pyknotic nuclei, suggesting that it resulted in a local cell death. However, in the ventral regions it overlapped the areas of Wg accumulation, suggesting that in these regions JNK activity could instead promote proliferation, in keeping with the dual role recently suggested for this pathway.⁴⁵ JNK also has a well conserved role in the induction of Mmps that degrade the extracellular matrix and are strongly expressed during regeneration.^{48,49} Specifically, *Drosophila* Mmp1 is directly involved in re-epithelialization after wound healing, remodeling of the basement membrane and

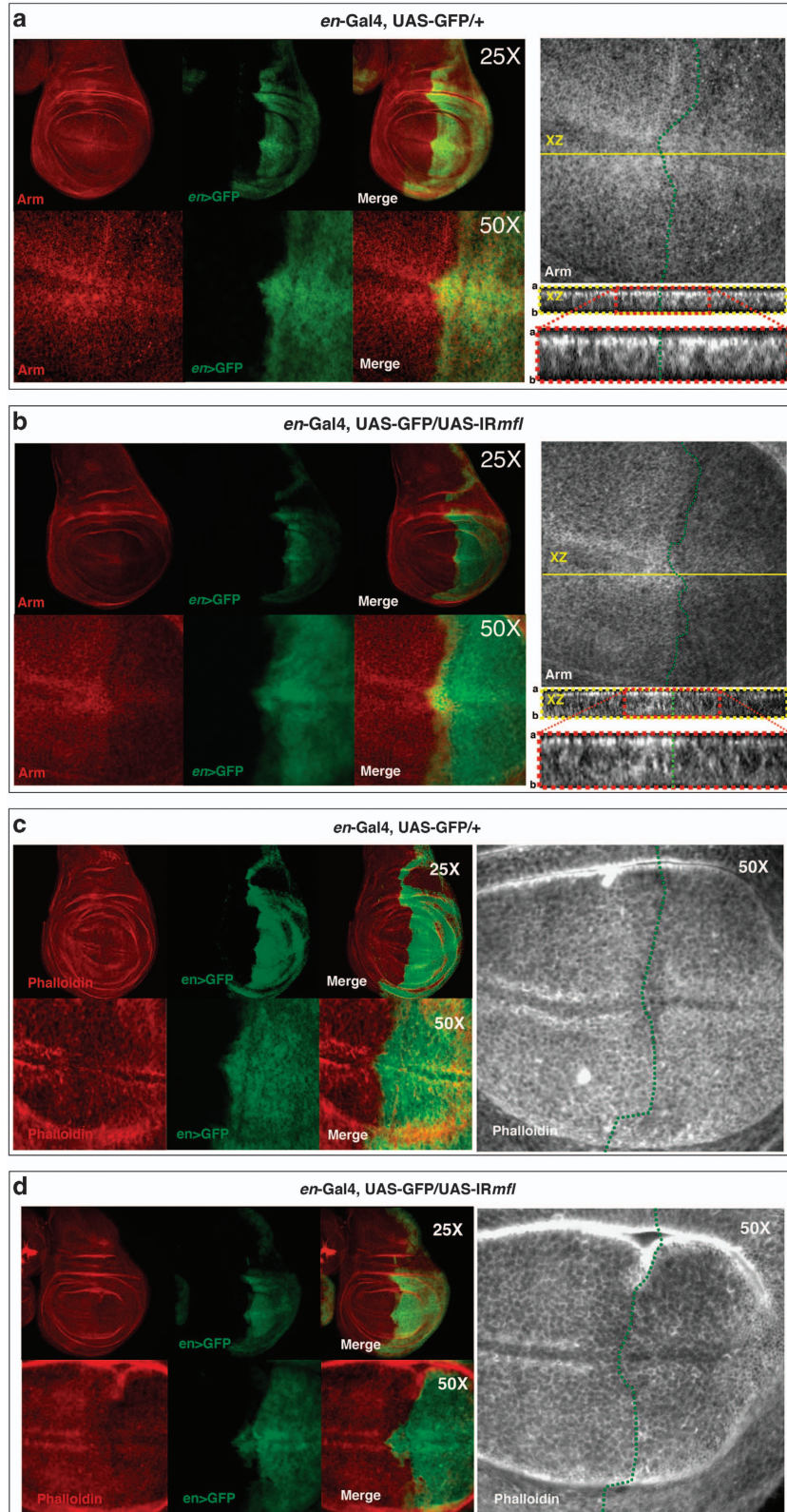
cytoskeletal reorganization.^{50,51} Not surprisingly, Mmp1 was strongly induced along the A/P border and ventrally, where it matched the area of Wg overexpression at the middle of the inner ring (Figures 7c and d).

Mfl depletion promotes EMT in a cell-nonautonomous manner. The concomitant occurrence of Wg overexpression, reduction of adherens junctions, loss of apicobasal polarity, JNK and Mmp1 induction raised the intriguing possibility that Mfl depletion could also trigger changes in cell fate, and possibly give rise to EMT. EMT occurs in many developmental events but, if induced by pathological conditions, can lead to tumourigenesis.⁵² As X-DC is characterized by a still unexplained susceptibility to malignancy, the possibility that pseudouridine synthase depletion could trigger EMT was of great interest. We thus stained the silenced discs with an antibody directed against Twist, a typical marker for mesenchymal cells known to be involved in EMT.^{53,54} Twist is expressed in presumptive mesodermal cells and not in epithelia,⁵⁵ and thus no disc cell was expected to be positively stained. Intriguingly, patches of Twist-positive cells were instead detected in about 95% of the silenced discs (Figure 8a). These cells also ectopically expressed Cut, an additional marker of myoblasts,^{55,56} further confirming the acquisition of mesoderm identity and the occurrence of EMT. Surprisingly, Z-stack confocal analysis lead to locate these myoblasts within the peripodial membrane, that is, the overlying squamous epithelium that lies outside the *omb* expression domain and thus was not silenced (Figure 8b). Note that, as awaited, Cut-positive cells are never present in the peripodial membrane of control discs (Supplementary Figure 5). We then wondered whether the observed myoblasts originated from the underlying silenced epithelium and then migrated above or, alternatively, directly arose from the unsilenced tissue. To investigate this aspect, we performed a lineage-tracing experiments by using the G-TRACE system, which is based on the expression of a pair of GFP-RFP Stinger reporters.⁵⁷ In this system, cells that had a previous Gal4-dependent activation of the GFP reporter, even if transient, remain GFP-labeled; conversely, cells showing only an active real-time expression of the Stinger vector become RFP-labeled. In our experiments, Twist/Cut-positive cells were never GFP- or RFP-labeled, clearly indicating that they were not expressing the *omb*-Gal4 driver nor activated it at any previous developmental stage (Figure 8c). This result confirmed that these cells derive from the peripodial membrane. To learn more, we used an anti-Ubx antibody that marks the majority of peripodial cells.^{58,59} Intriguingly, the Twist/Cut-positive cells faintly expressed also Ubx, indicating that they are in a state of cell fate transition (Figure 8d). This result ruled out also the possibility that these myoblasts could derive from the adepithelial cells abutting the wing disc in the notum region, as those myoblasts do not express Ubx.⁵⁸ EMT in the peripodial membrane was identically induced in a different *mfl* silencing line (no. 36595; Supplementary Figure 6), confirming the occurrence of cell-nonautonomous fate changes.

Discussion

In *Drosophila* wing discs, cell death provoked by a variety of approaches, including disc transplantation, exogenous

injuries or localized induction of proapoptotic genes, can induce regenerative growth.⁶⁰ In response to death, neighboring cells are stimulated to proliferate and reconstitute tissue loss,



a process defined as apoptosis-induced proliferation.^{28,61,62} Here we show that the level of expression of pseudouridine synthase is crucial for tissue homeostasis and that its local reduction triggers apoptosis-induced proliferation, as typically observed during regeneration.⁶³ This regenerative stimulus is enhanced by blocking the execution of death by p35 expression, which, as occurring after several different types

of tissue injuries, elicits hyperplastic overgrowth.⁶⁴ As both apoptotic and proliferating cells are identically Mfl-depleted, our results outlined an unexpected context-dependent effect of pseudouridine synthase level. Possibly, as a consequence of their differentiation status, different cell sub-populations respond in a reverse manner to lessening of this enzyme: those more susceptible undergo apoptosis, whereas others

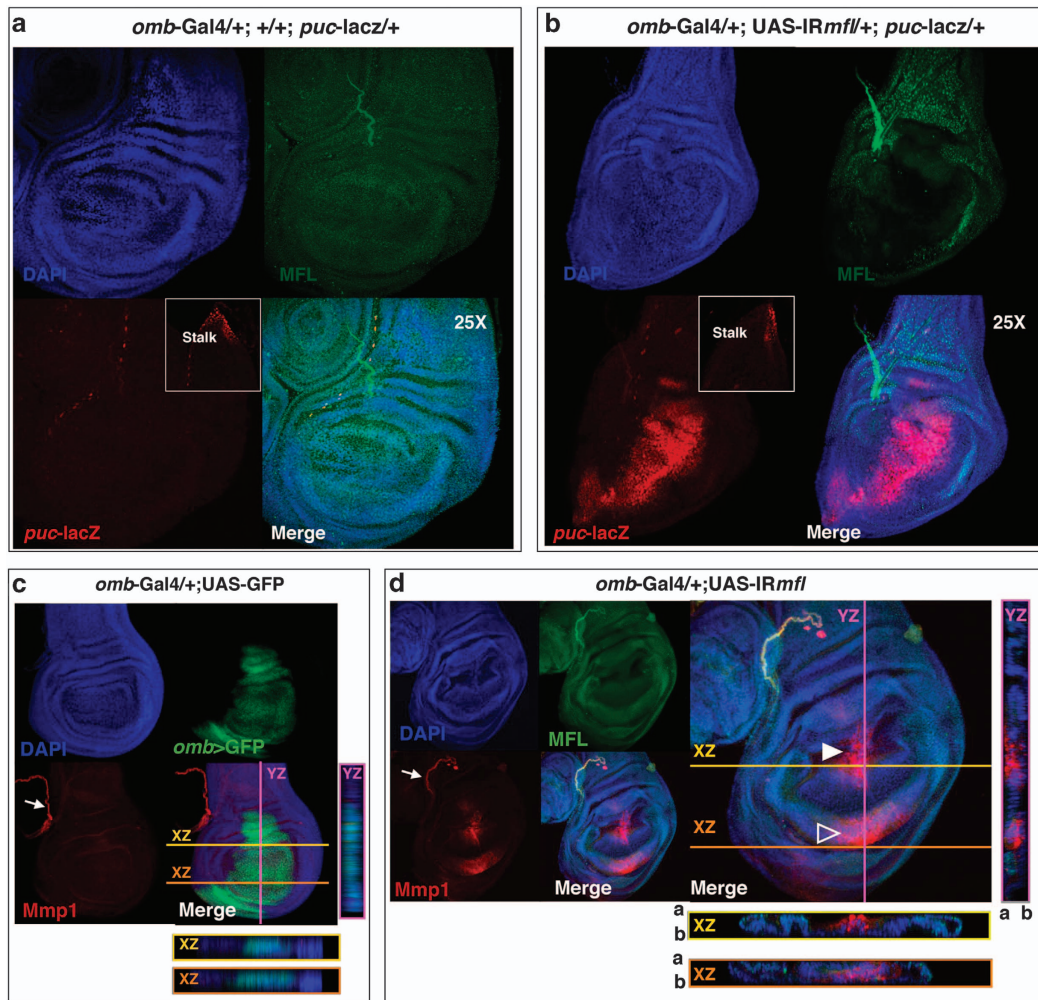
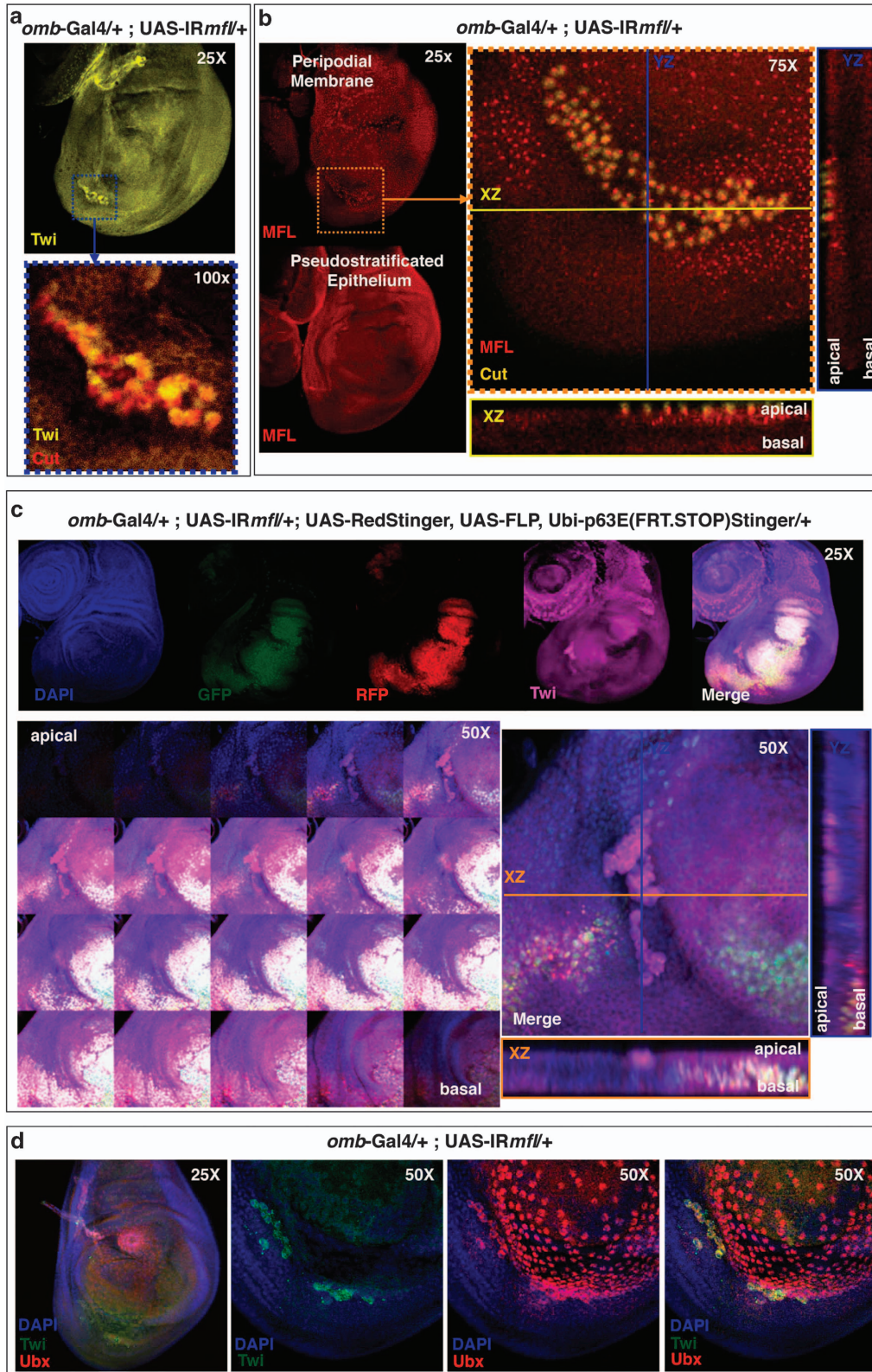


Figure 7 Mfl depletion induces JNK and Mmp1 ectopic activation. Confocal analysis of wing discs collected at 120 h AED. (a) In *omb> puc-lacZ* control discs, activation of the JNK pathway, marked by the *puc-lacZ* reporter, is restricted to the stalk cells (inset) and to some dispersed cells.⁴⁷ (b) In *omb> IRmfl; puc-lacZ* silenced discs (v46282 line in the picture), JNK is ectopically and strongly activated. In (a and b), DAPI (4',6-diamidino-2-phenylindole) is in blue, Mfl in green and β -gal in red. (c) Mmp1 expression in *omb> GFP* control discs marks the trachea (arrow) and the stalk cells (not in frame), where it overlaps *puc-lacZ* expression. Z-stack analysis (see XZ and YZ projections) confirms Mmp1 absence in the *omb* domain. (d) In *omb> IRmfl* silenced discs (v46282 line in the picture), Mmp1 is strongly and ectopically induced in the MFL-depleted domain; in the D compartment, Mmp1 enrichment flanks the A/P border (closed arrowhead) within the area of JNK activation (compared with b), whereas in the V compartment, Mmp1 concentrates in a small domain (open arrowhead) overlapping the Wg-expressing inner ring. In both areas, Z-stack analysis (see XZ and YZ projections) confirms Mmp1 active secretion within the silenced domain. DAPI is in blue; GFP (c) and Mfl (d) in green and Mmp1 in red. a, Apical; b, basal

Figure 6 Loss of Arm/ β -catenin apical localization and reduced F-actin accumulation in the silenced discs. Confocal analysis of wing discs collected at 120 h AED and stained with Arm antibody (in red or gray) or phalloidin (red or gray). (a) Localization of Arm protein in *en> GFP* control discs, in which GFP (green) marks the *en* posterior domain. Note that Arm is strongly concentrated in two stripes of cells adjacent to the D/V boundary, and Z-stack analysis (right panels) shows its uniform apical localization in both A/P compartments. (b) Localization of Arm in an *en> IRmfl* silenced disc (v46282 line). *mfl* silencing causes a strong reduction of Arm protein, with Z-stack analysis (right panels) demonstrating loss of apical localization (right panel). In a and b, green dots mark the boundary between the A and P compartments within the enlargements; red dots mark XZ projection enlargements. (c and d) Confocal analysis of wing discs stained with phalloidin. (c) In *en> GFP* control discs, F-actin concentrates in two stripes of cells adjacent to the D/V boundary. (d) In *en> GFP; en> IRmfl* silenced discs (v46282 line in the picture), F-actin accumulation is strongly reduced within the whole silenced domain, and particularly at the D/V margin. GFP is in green and phalloidin in red or gray. Green dots mark the A/P boundary. a, Apical; b, basal



hyperproliferate, acting as a blastema.²⁹ This dual effect also establishes for the first time that pseudouridine synthase depletion *per se* does not hamper proliferation, as generally considered; on the contrary, under mitogenic stimuli the

depleted cells are able to overproliferate vigorously. This finding further supports the view that this enzyme has a more specialized than a general effect on ribosome functionality.

Figure 8 Mfl depletion promotes EMT in the contiguous peripodial membrane. Confocal analysis of wing discs collected at 120 h AED. (a) An *omb* > *IRmfl* silenced disc (v46282 line) costained with anti-Twist (on the top) and anti-Cut antibodies, showing an islet of double positive cells (enlargement at the bottom; Twist is in yellow and Cut in red). (b) Z-stack images captured at different planes show that the Twist-Cut-positive islet lies apically, in the peripodial membrane. As this membrane is not included in the *omb* silenced domain, these cells were actively accumulating the Mfl protein within their nucleoli; conversely, cells of the underlying silenced pseudostratified epithelium are efficiently depleted (Mfl in red and Cut in yellow). (c) G-TRACE experiments in which the *omb* silenced domain was labeled by GFP and RFP expressed by UAS-Stinger vectors and stained with DAPI (4',6-diamidino-2-phenylindole) and Twist antibody (top panel). In the middle, Z-stack images captured at different focal planes (left) and orthogonal projections (right). Note that Twist-positive cells (in magenta) remain fully unstained by both GFP and RFP and lie apically, within the peripodial membrane. DAPI is in blue, GFP in green, RFP in red and Twist in magenta. (d) Twist-positive cells faintly express also Ubx, a typical marker of the peripodial membrane, indicating that they are in a state of fate transition. DAPI is in blue, Twist in green and Ubx in red. Twi, Twist

As described in regenerative processes, massive epithelial remodeling occurs in the silenced tissue. Loss of Arm apical localization, reduction of F-actin polymerization and JNK and Mmp1 ectopic activation, altogether converged to underscoring cytoskeletal rearrangement dynamics and massive epithelium reorganization. In our experiments, the sustainment of the proliferative activity correlates with the activation of Wg and JAK-STAT mitogenic pathways, both of which are found ectopically induced in the depleted areas. However, the Wg signal was actively produced not only by the apoptotic but also by surrounding cells, where it partially overlapped with JAK-STAT ectopic induction. These features suggest the involvement of long-range intercellular signaling in response to pseudouridine synthase depletion. Indeed, an interesting conclusion that can be drawn by our experiments is that cell-cell communication is likely to have a key role in the pseudouridine synthase loss-of-function phenotype. This conclusion is further supported by the striking discovery that depletion of *Drosophila* dyskerin can trigger cell fate changes in a cell-nonautonomous manner. Unexpectedly, in response to Mfl silencing, EMT occurs in the adjacent unsilenced peripodial membrane, where groups of cells exhibited ectopic expression of myoblast markers. Considering the pivotal role played by EMT in development, regeneration and stem cell behavior,⁶⁵ this result is of utmost importance. Moreover, it emphasizes the important role of dyskerin, which is also reflected by extensive consequences of its depletion on many processes during fly development.¹⁷ Indeed, the regenerative growth described here is likely to reflect a general intrinsic homeostatic mechanism occurring in the context of physiological metabolic perturbation. In developing tissues, a local decrease in the amount of pseudouridine synthase, or in its activity, can occur stochastically or be caused by developmentally or metabolically regulated processes. Our results show that such variations can act not only as an apoptotic trigger but also as a regenerative stimulus, and thus nicely fit with the general observation that a tight control of the level of this enzyme is crucial in human cultured cells⁶⁶ and developing organisms as well.^{4,17}

Collectively, the effects observed upon Mfl depletion all converge to make the tumor predisposition observed in the X-DC patients⁶⁷ much easier to understand. Indeed, considering the high degree of conservation of all the pathways affected by Mfl reduction, we foresee that the core wiring diagram of pseudouridine synthase tasks might be conserved between flies and mammals. We surmise that *in vivo* experimental approaches in this animal model may help to better define the wide range of biological processes that interlace with these multifunctional proteins, and that perturbation of cell-cell

interactions, so far largely ignored in the studies of X-DC pathogenesis, may represent a relevant aspect of the disease.

Materials and Methods

Fly stocks. Flies were raised on standard *Drosophila* medium at 25 °C. The *en-Gal4*, *omb-Gal4/FM7*, UAS-GFP/CyO, 10XSTAT92E-dGFP/TM6C, *puc-lacZ/TM3Sb*, UAS-2XEGFP, UAS-RedStinger, UAS-FLP, Ubi-p63E(FRT.STOP)Stinger and UAS-*IRmfl* (no. 36595) strains were obtained from the Bloomington *Drosophila* Stock Center at Indiana University (BDSC, Bloomington, IN, USA); UAS-*IRmfl* RNAi (v46282) was obtained from the Vienna *Drosophila* RNAi Center (VDRC, Vienna, Austria). *wg-lacZ/CyO* and UAS-*p35/TM3Sb* stocks were kindly provided by L Johnston (Columbia University, New York, NY, USA).

Mounting adult wings. Wings were removed from adult flies, dehydrated in 100% ethanol for 5 min and placed on a microscope slide to allow ethanol to evaporate. A small drop of Euparal Mounting Medium (Roth, Karlsruhe, Germany) was dropped onto the wing and a glass coverslip placed on top. Images were captured with a Spot digital camera and a Nikon E1000 microscope (Nikon Instruments Europe, Tokyo, Japan).

Immunofluorescence stainings. Wing discs were dissected, fixed and immunostained as described in Tortoriello *et al.*¹⁷ Antibodies used were as follows: customer rabbit polyclonal antibody against Mfl (Sigma-Aldrich Inc., St. Louis, MO, USA; dilution 1:100); mouse monoclonal antibodies against Wingless, Cut, Arm, Mmp1, β -galactosidase, ultrabithorax (Ubx; Hybridoma Bank, University of Iowa, Iowa City, IA, USA; dilution 1:50 anti-Wg, 1:100 anti-Cut, 1:50 anti-Arm, 1:50 anti-Mmp1 mixture of 5H7B11, 3B8D12 and 3A6B4, 1:250 anti- β -Gal and 1:50 anti-Ubx); rabbit polyclonal antibody against Twist (Yin *et al.*,⁶⁸ dilution 1:50; gift from M Frasch); rabbit polyclonal antibodies against pH3 and cleaved Cas3 (Cell Signaling Technology, Danvers, MA, USA; dilutions 1:100 anti-pH3 and 1:500 anti-Cas3). Fluorescent secondary antibodies were from Jackson ImmunoResearch (Dianova, Hamburg, Germany) and used at a final dilution of 1:200. Rhodamine phalloidin conjugate for actin cytoskeleton staining were obtained from Molecular Probes (Eugene, OR, USA; dilution 1:250). Confocal images were obtained with a Bio-Rad MRC1024 (Bio-Rad, Munich, Germany) or Zeiss LSM510 (Carl Zeiss, Jena, Germany) confocal microscope.

Labeling of S-phase cells. For EdU immunohistochemistry, the Click-iT EdU Imaging Kit (Invitrogen, Carlsbad, CA, USA) was used. Discs were dissected and incubated in 10 μ M EdU in Ringer's for 20 min or 2 h and, following EdU labeling, fixed and immunostained as described in Tortoriello *et al.*¹⁷ Afterwards, they were incubated in 1x Click-iT reaction cocktail for 30 min, washed thoroughly in PBS and mounted.

Z-stack analysis. All captured pictures (in RAW format) have been analyzed and processed with ImageJ v1.440 software (National Institutes of Health, Bethesda, MD, USA). Z-stack analysis was performed by using STACK > ZProjection and STACK > Orthogonal views ImageJ plug-in.

Conflict of Interest

The authors declare no conflict of interest.

Acknowledgements. This work was supported by University Federico II of Naples and by POR Campania FSE 2007-2013 Project CREMe CUP B25B0900050007, which funded Rosario Vicidomini, Arianna Petrizzo and Liliana

Felicia Iannucci with research fellowships. A Di Giovanni PhD fellowship was supported by POR Campania FSE 2007-2013 Project 'Dottorato in Azienda' c/o Microtech srl.

- Kondrashov N, Pusic A, Stumpf CR, Shimizu K, Hsieh AC, Xue S *et al*. Ribosome-mediated specificity in Hox mRNA translation and vertebrate tissue patterning. *Cell* 2011; **145**: 383–397.
- McGowan KA, Li JZ, Park CY, Beaudry V, Tabor HK, Sabnis AJ *et al*. Ribosomal mutations cause p53-mediated dark skin and pleiotropic effects. *Nat Genet* 2008; **40**: 963–970.
- McCann KL, Baserga SJ. Mysterious ribosomopathies. *Science* 2013; **341**: 849–5.
- Angrisani A, Vicidomini R, Turano M, Furia M. Human dyskerin: beyond telomeres. *Biol Chem* 2014; **395**: 593–610.
- Schwartz S, Bernstein DA, Mumbach MR, Jovanovic M, Herbst RH, León-Ricardo BX *et al*. Transcriptome-wide mapping reveals widespread dynamic-regulated pseudouridylation of ncRNA and mRNA. *Cell* 2014; **159**: 148–162.
- Jack K, Bellodi C, Landry DM, Niederer RO, Meskauskas A, Musalgaonkar S *et al*. rRNA pseudouridylation defects affect ribosomal ligand binding and translational fidelity from yeast to human cells. *Mol Cell* 2011; **44**: 660–666.
- Yoon A, Peng G, Brandenburg Y, Zollo O, Xu W, Rego E *et al*. Impaired control of IRES-mediated translation in X-linked dyskeratosis congenita. *Science* 2006; **312**: 902–906.
- Bellodi C, Krasnykh O, Haynes N, Theodoropoulou M, Peng G, Montanaro L *et al*. Loss of function of the tumor suppressor DKC1 perturbs p27 translation control and contributes to pituitary tumorigenesis. *Cancer Res* 2010; **70**: 6026–6035.
- Montanaro L, Calienni M, Bertoni S, Rocchi L, Sansone P, Storci G *et al*. Novel dyskerin-mediated mechanism of p53 inactivation through defective mRNA translation. *Cancer Res* 2010; **70**: 4767–4777.
- Rocchi L, Pacilli A, Sethi R, Penzo M, Schneider RJ, Treré D *et al*. Dyskerin depletion increases VEGF mRNA internal ribosome entry site-mediated translation. *Nucleic Acids Res* 2013; **41**: 8308–8318.
- Heiss NS, Knight SW, Vulliamy TJ, Klauk SM, Wiemann S, Mason PJ *et al*. X-linked dyskeratosis congenita is caused by mutations in a highly conserved gene with putative nucleolar functions. *Nat Genet* 1998; **19**: 32–38.
- Giordano E, Peluso I, Senger S, Furia M. Minifly, a *Drosophila* gene required for ribosome biogenesis. *J Cell Biol* 1999; **144**: 1123–1133.
- Pardue ML, Rashkova S, Casacuberta E, DeBaryshe PG, George JA, Traverse KL. Two retrotransposons maintain telomeres in *Drosophila*. *Chromosome Res* 2005; **13**: 443–453.
- Ryoo HD, Bergmann A. The role of apoptosis-induced proliferation for regeneration and cancer. *Cold Spring Harb Perspect Biol* 2012; **4**: a008797.
- Potter CJ, Xu T. Mechanisms of size control. *Curr Opin Genet Dev* 2001; **11**: 279–286.
- Dahmann C, Oates AC, Brand M. Boundary formation and maintenance in tissue development. *Nat Rev Genet* 2011; **12**: 43–55.
- Tortoriello G, de Celis JF, Furia M. Linking pseudouridine synthases to growth, development and cell competition. *FEBS J* 2010; **277**: 3249–3263.
- Phillips B, Billin AN, Cadwell C, Buchholz R, Erickson C, Merriam JR *et al*. The Nop60B gene of *Drosophila* encodes an essential nucleolar protein that functions in yeast. *Mol Gen Genet* 1998; **260**: 20–29.
- Riccardo S, Tortoriello G, Giordano E, Turano M, Furia M. The coding/non-coding overlapping architecture of the gene encoding the *Drosophila* pseudouridine synthase. *BMC Mol Biol* 2007; **8**: 15.
- Brand AH, Perrimon N. Targeted gene expression as a means of altering cell fates and generating dominant phenotypes. *Development* 1993; **118**: 401–415.
- Grimm S, Pflugfelder GO. Control of the gene optomotor-blind in *Drosophila* wing development by decapentaplegic and wingless. *Science* 1996; **271**: 1601–1604.
- Pérez-Garijo A, Martín FA, Morata G. Caspase inhibition during apoptosis causes abnormal signalling and developmental aberrations in *Drosophila*. *Development* 2004; **131**: 5591–5598.
- Ryoo HD, Gorenc T, Steller H. Apoptotic cells can induce compensatory cell proliferation through the JNK and the wingless signaling pathways. *Dev Cell* 2004; **7**: 491–501.
- Smith-Bolton RK, Worley MI, Kanda H, Hariharan IK. Regenerative growth in *Drosophila* imaginal discs is regulated by Wingless and Myc. *Dev Cell* 2009; **16**: 797–809.
- Oh SW, Kingsley T, Shin HH, Zheng Z, Chen HW, Chen X *et al*. A P-element insertion screen identified mutations in 455 novel essential genes in *Drosophila*. *Genetics* 2003; **163**: 195–201.
- Hay BA, Wolff T, Rubin GM. Expression of baculovirus P35 prevents cell death in *Drosophila*. *Development* 1994; **120**: 2121–2129.
- Callus BA, Vaux DL. Caspase inhibitors: viral, cellular and chemical. *Cell Death Differ* 2007; **14**: 73–78.
- Martín FA, Pérez-Garijo A, Morata G. Apoptosis in *Drosophila*: compensatory proliferation and undead cells. *Int J Dev Biol* 2009; **53**: 1341–1347.
- Sun G, Irvine KD. Control of growth during regeneration. *Curr Top Dev Biol* 2014; **108**: 95–120.
- Wu M, Pastor-Pareja JC, Xu T. Interaction between Ras(V12) and scribbled clones induces tumour growth and invasion. *Nature* 2010; **463**: 545–548.
- Rodríguez AB, Zoranovic T, Ayala-Camargo A, Grewal S, Reyes-Robles T, Krasny M *et al*. Activated STAT regulates growth and induces competitive interactions independently of Myc, Yorkie, Wingless and ribosome biogenesis. *Development* 2012; **139**: 4051–4061.
- Pérez-Garijo A, Shlevkov E, Morata G. The role of DPP and Wg in compensatory proliferation and in the formation of hyperplastic overgrowths caused by apoptotic cells in the *Drosophila* wing disc. *Development* 2009; **136**: 1169–1177.
- Couso JP, Bishop SA, Martínez Arias A. The wingless signalling pathway and the patterning of the wing margin in *Drosophila*. *Development* 1994; **120**: 621–636.
- Major RJ, Irvine KD. Influence of Notch on dorsoventral compartmentalization and actin organization in the *Drosophila* wing. *Development* 2005; **132**: 3823–3833.
- Valenta T, Hausmann G, Basler K. The many faces and functions of β -catenin. *EMBO J* 2012; **31**: 2714–2736.
- Somorjai IM, Martínez-Arias A. Wingless signalling alters the levels, subcellular distribution and dynamic of Armadillo and E-cadherin in third instar larval wing imaginal discs. *PLoS One* 2008; **3**: e2893.
- Wodarz A, Stewart DB, Nelson WJ, Nusse R. Wingless signaling modulates cadherin-mediated cell adhesion in *Drosophila* imaginal disc cells. *J Cell Sci* 2006; **119**: 2425–2434.
- Angrisani A, Turano M, Paparo L, Di Mauro C, Furia M. A new human dyskerin isoform with cytoplasmic localization. *Biochim Biophys Acta* 2011; **1810**: 1361–1368.
- Adachi-Yamada T, Fujimura-Kamada K, Nishida Y, Matsumoto K. Distortion of proximodistal information causes JNK-dependent apoptosis in *Drosophila* wing. *Nature* 1999; **400**: 166–169.
- McEwen DG, Peifer M. Puckered, a *Drosophila* MAPK phosphatase, ensures cell viability by antagonizing JNK-induced apoptosis. *Development* 2005; **132**: 3935–3946.
- Bosch M, Serras F, Martín-Blanco E, Baguña J. JNK signaling pathway required for wound healing in regenerating *Drosophila* wing imaginal discs. *Dev Biol* 2005; **280**: 73–86.
- Bosch M, Baguña J, Serras F. Origin and proliferation of blastema cells during regeneration of *Drosophila* wing imaginal discs. *Int J Dev Biol* 2008; **52**: 1043–1050.
- Mattila J, Omelyanchuk L, Kytälä S, Turunen H, Norkkala S. Role of Jun N-terminal Kinase (JNK) signaling in the wound healing and regeneration of a *Drosophila melanogaster* wing imaginal disc. *Int J Dev Biol* 2005; **49**: 391–399.
- Bergantiños C, Corominas M, Serras F. Cell death-induced regeneration in wing imaginal discs requires JNK signalling. *Development* 2010; **137**: 1169–1179.
- Rudrapatna VA, Bangi E, Cagan RL. Caspase signalling in the absence of apoptosis drives Jnk-dependent invasion. *EMBO Rep* 2013; **14**: 172–177.
- Ring JM, Martínez Arias A. Puckered, a gene involved in position-specific cell differentiation in the dorsal epidermis of the *Drosophila* larva. *Dev Suppl* 1993; **121**: 251–259.
- Agnès F, Suzanne M, Noselli S. The *Drosophila* JNK pathway controls the morphogenesis of imaginal discs during metamorphosis. *Development* 1999; **126**: 5453–5462.
- Reuben PM, Cheung HS. Regulation of matrix metalloproteinase (MMP) gene expression by protein kinases. *Front Biosci* 2006; **11**: 1199–1215.
- Fanjul-Fernández M, Folgueras AR, Cabrera S, López-Otín C. Matrix metalloproteinases: evolution, gene regulation and functional analysis in mouse models. *Biochim Biophys Acta* 2010; **1803**: 3–19.
- Stevens LJ, Page-McCaw A. A secreted MMP is required for reepithelialization during wound healing. *Mol Biol Cell* 2012; **23**: 1068–1079.
- Uhlirova M, Bohmann D. JNK- and Fos-regulated Mmp1 expression cooperates with Ras to induce invasive tumors in *Drosophila*. *EMBO J* 2006; **25**: 5294–5304.
- Radisky ES, Radisky DC. Matrix metalloproteinase-induced epithelial–mesenchymal transition in breast cancer. *J Mammary Gland Biol Neoplasia* 2010; **15**: 201–212.
- Ghazi A, Anant S, Vijay Raghavan K. Apterous mediates development of direct flight muscles autonomously and indirect flight muscles through epidermal cues. *Development* 2000; **127**: 5309–5318.
- Khan MA, Chen HC, Zhang D, Fu J. Twist: a molecular target in cancer therapeutics. *Tumour Biol* 2013; **34**: 2497–2506.
- Sudarsan V, Anant S, Guptan P, Vijay Raghavan K, Skaer H. Myoblast diversification and ectodermal signaling in *Drosophila*. *Dev Cell* 2001; **1**: 829–839.
- Roy S, Vijay Raghavan K. Muscle pattern diversification in *Drosophila*: the story of imaginal myogenesis. *BioEssays* 1999; **21**: 486–498.
- Evans CJ, Olson JM, Ngo KT, Kim E, Lee NE, Kuoy E *et al*. G-TRACE: rapid Gal4-based cell lineage analysis in *Drosophila*. *Nat Methods* 2009; **6**: 603–605.
- Pallavi SK, Shashidhara LS. Egr/Ras pathway mediates interactions between peripodial and disc proper cells in *Drosophila* wing discs. *Development* 2003; **130**: 4931–4941.
- Pallavi SK, Shashidhara LS. Signaling interactions between squamous and columnar epithelia of the *Drosophila* wing disc. *J Cell Sci* 2005; **118**: 3363–3370.
- Worley MI, Setiawan L, Hariharan IK. Regeneration and transdetermination in *Drosophila* imaginal discs. *Annu Rev Genet* 2012; **46**: 289–310.
- Mollereau B, Pérez-Garijo A, Bergmann A, Miura M, Gerlitz O, Ryoo HD *et al*. Compensatory proliferation and apoptosis-induced proliferation: a need for clarification. *Cell Death Differ* 2013; **20**: 181.
- Sun G, Irvine KD. Regulation of Hippo signaling by Jun kinase signaling during compensatory cell proliferation and regeneration, and in neoplastic tumors. *Dev Biol* 2011; **350**: 139–151.
- Repiso A, Bergantiños C, Corominas M, Serras F. Tissue repair and regeneration in *Drosophila* imaginal discs. *Dev Growth Differ* 2011; **53**: 177–185.
- Bergmann A, Steller H. Apoptosis, stem cells and tissue regeneration. *Sci Signal* 2010; **3**: re8.

65. Lamouille S, Xu J, Derynck R. Molecular mechanisms of epithelial–mesenchymal transition. *Nat Rev Mol Cell Biol* 2014; **15**: 178–196.
66. Parry EM, Alder JK, Lee SS, Phillips JA III, Loyd JE, Duggal P *et al*. Decreased dyskerin levels as a mechanism of telomere shortening in X-linked dyskeratosis congenita. *J Med Genet* 2011; **48**: 327–333.
67. Alter BP, Giri N, Savage SA, Rosenberg PS. Cancer in dyskeratosis congenita. *Blood* 2009; **113**: 6549–6557.
68. Yin Z, Xu XL, Frasch M. Regulation of the twist target gene tinman by modular cis-regulatory elements during early mesoderm development. *Development* 1997; **124**: 4971–4982.
69. Bach EA, Ekas LA, Ayala-Camargo A, Flaherty MS, Lee H, Perrimon N *et al*. GFP reporters detect the activation of the *Drosophila* JAK/STAT pathway *in vivo*. *Gene Expr Patterns* 2007; **7**: 323–331.



Cell Death and Disease is an open-access journal published by **Nature Publishing Group**. This work is licensed under a **Creative Commons Attribution 4.0 International License**. The images or other third party material in this article are included in the article's Creative Commons license, unless indicated otherwise in the credit line; if the material is not included under the Creative Commons license, users will need to obtain permission from the license holder to reproduce the material. To view a copy of this license, visit <http://creativecommons.org/licenses/by/4.0/>

Supplementary Information accompanies this paper on Cell Death and Disease website (<http://www.nature.com/cddis>)